

ESD ACCESSION LIST

TRI Call No.

74198

Copy No.

of

cys.

ESD RECORD COPY

RETURN TO

SCIENTIFIC & TECHNICAL INFORMATION DIVISION

(TRI), Building 1210

Technical Note

1971-15

Final Report:
Development of a 10^7 Bit
Magnetic Film Memory

J. I. Raffel
A. H. Anderson
R. Berger
T. S. Crowther
T. O. Herndon
M. L. Naiman
C. E. Woodward

10 June 1971

Prepared under Electronic Systems Division Contract F19628-70-C-0230 by

Lincoln Laboratory

MASSACHUSETTS INSTITUTE OF TECHNOLOGY

Lexington, Massachusetts



AD727768

MASSACHUSETTS INSTITUTE OF TECHNOLOGY
LINCOLN LABORATORY

FINAL REPORT: DEVELOPMENT
OF A 10^7 BIT MAGNETIC FILM MEMORY

J. I. RAFFEL
A. H. ANDERSON
R. BERGER
T. S. CROWTHER
T. O. HERNDON
M. L. NAIMAN
C. E. WOODWARD

Group 23

TECHNICAL NOTE 1971-15

10 JUNE 1971

Approved for public release; distribution unlimited.

The work reported in this document was performed at Lincoln Laboratory, a center for research operated by Massachusetts Institute of Technology, with the support of the Department of the Air Force under Contract F19628-70-C-0230.

This report may be reproduced to satisfy needs of U.S. Government agencies.

Abstract

Batch fabrication techniques for making 200,000 bit substrates with word lines integral with a closed magnetic film structure and keepered digit lines on large area substrates are described. A sense amplifier was designed which does not require a transformer for impedance matching to the digit lines. Cross-section-stack tests proved the feasibility of a 10 million bit memory with 1.0 μ sec cycle time. All fabrication processes are consistent with the goal of low memory construction costs.

Accepted for the Air Force
Joseph R. Waterman, Lt. Col., USAF
Chief, Lincoln Laboratory Project Office

CONTENTS

I.	Design Principles and Previous Experience	1
II.	Cell Design	3
III.	Word Substrate	9
IV.	Digit Substrate	18
V.	System Noise	27
VI.	Sense System	34
VII.	Cross-Section-Stack Experiments	62
VIII.	Word Selection Matrix	84
IX.	Further Development	87
X.	A Feasible 10^7 Bit Memory	88
XI.	Conclusions	89
	REFERENCES	90
	APPENDICES	
A.	Word Line Fabrication	91
B.	Electroless Plating of Magnetic Films	95
C.	Digit Substrate Fabrication	117
D.	Capacitive Imbalance Tester	126
E.	The Effect of a Differentiator on Signal-to-Random-Noise Ratio	127

I. Design Principles and Previous Experience

The progressive development of magnetic film memories has required new techniques for achieving higher bit densities, simplified interconnections and circuits, and the servicing of more storage bits per access circuit. The principal design problem relative to these objectives is the attendant reduction in signal and increase in parasitic and random noise associated with smaller storage bits and longer word and digit lines. Solutions to these problems are at the heart of achieving high speed and low cost simultaneously.¹ The approach described in this report is to batch fabricate integral structures large enough so that connections are required only at the stack periphery. To accomplish this, word and digit lines are placed on separate rectangular substrates, at the same time eliminating the need for thin pinhole-free insulating layers. Provision is made for substituting spare word lines for defective ones to circumvent the otherwise prohibitive yield probabilities of a 200,000 bit substrate. The memory is organized for read-out of long words so that the data rate of fast computers can be matched to the moderate circuit speeds and delays of relatively long digit lines. The expected applications are as main memory for a one-microsecond-cycle machine or back up memory to a fast semiconductor cache memory.

In 1968, a million bit memory (LCM I) designed and built at Lincoln Laboratory, was described in detail and since July of that year has been operating on the TX-2 computer as part of the main storage system.^{2,3} It has 3200 words of 32 bytes each (eight TX-2 words); was tested at 1.2 μ sec cycle time and is operating at a computer-limited cycle time of 1.6 μ sec as main memory. Following the substitution of spare lines for those having bits with marginal signal-to-random noise ratio because of word-noise reduced signal amplitudes, the memory has exhibited excellent reliability, running

error-free for periods of months. Those errors which do occur have been traced to occasional circuit failure or to contact-resistance change in digit line connectors which received a good deal of wear during early experimentation.

The experience in designing and testing this memory led to the following conclusions regarding future developments:

1. Increasing the word density from the 250 per inch of LCM I was both desirable and possible using the techniques of scribing previously developed.
2. An increase in digit line length over the existing 10" was desirable to minimize digit circuit cost/bit. A factor of 5 seemed reasonable from fabrication and electrical delay considerations.
3. The increased digit line length would significantly increase susceptibility to word and group noise due to capacitive imbalance; therefore capacitive imbalance had to be substantially reduced below LCM I levels where extensive substitution of spare lines was required on noisy bits which were otherwise magnetically acceptable.
4. Signal-to-random noise ratio at the sense amplifier could not be below LCM I levels, therefore, because of the greater loss and delay of the longer digit lines the signal at the bit would have to be about twice the LCM I amplitude.
5. The complicated front end of the LCM I sense amplifier requiring a network of input chokes and matching transformer had to be simplified and made more amenable to integration.

Work over the past two years has concentrated on developing a partially populated experimental stack based on the above conclusions.

LCM II utilizes a word density of 500 lines/inch with word conductors which have flux closure in the hard direction to reduce required word current. Signal levels are actually higher than in LCM I at half bit size because the use of a digit keeper allows a thicker film by reducing demagnetizing and increases the coupling of the storage film flux to the digit line. While digit line density is the same as in LCM I, (digit hairpins on 20 mil centers) the digit line length is approximately 50 inches providing a factor of 10 increase in the number of bits per digit circuit. Each digit hairpin on both sides of the stack covers 16,000 bits excluding spares, giving 32,000 bits per digit circuit. Both word and digit lines are mechanically scribed on an automatic ruling machine. Rigid digit substrates substantially reduce capacitive imbalance problems and simplify scribing. The use of large area input transistors having relatively low input impedance has eliminated the need for an input transformer. Operating cycle time has been demonstrated at less than $1\mu\text{sec}$, with 500 nsec access time to the full 300 bit word.

II. Cell Design

A design goal was to operate with drive currents about the same as in LCM I, i.e. word current of 500 ma and digit current in each line of 200 ma. The LCM I film thickness was 1200 Å. (Throughout this report the thicknesses of magnetic films will be expressed as the equivalent thickness of permalloy ($B_s = 10^4$ gauss) for the same total magnetic flux.) In order to obtain twice the signal of LCM I it was necessary to increase storage-film thickness and use a digit keeper. Figure 1 shows cross-section views of the closed-magnetic-film word lines and keepered digit lines.

The advantage of using a digit keeper in flat magnetic film memories has been adequately demonstrated.^{4,5,6} Three distinct effects of a digit

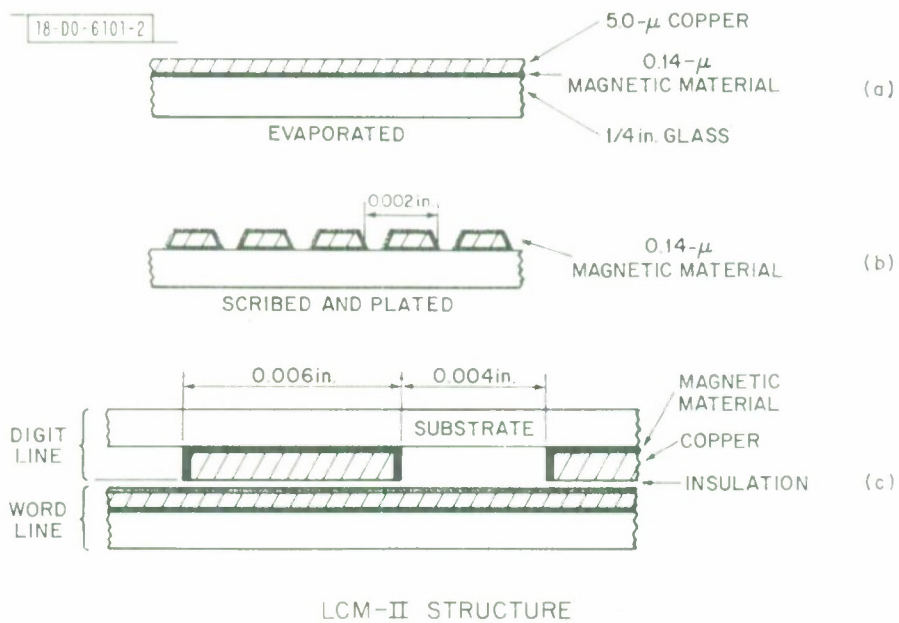


Fig. 1. Word and digit lines for LCM II. (a) Word substrate after evaporation of magnetic film and copper; (b) after scribing and top plating of word lines; (c) side view of word lines and edge view of keptered digit lines.

keeper are 1) Stray Field Reduction - a decrease in easy-direction stray magnetic fields, both the self-demagnetizing field of a particular storage element and the stray field from neighboring elements; 2) Digit Field Enhancement - an increase in magnetic field strength at the storage film per unit of current in the digit-sense conductor; 3) Signal Enhancement - an increase in the fraction of the stored flux that links the digit-sense conductor.

A simplified magnetic circuit model is useful in understanding the interaction of these three effects. In Figure 2, magnetic flux is assumed to enter and leave the film at the end regions. P_k is the permeance of the flux path between the end regions that lies above the film and includes the keeper. P_s is the permeance of the shunt path below the film (usually not ferromagnetic). The magnetic fluxes in these paths are ϕ_k and ϕ_s , respectively. The magnetic film in Figure 2 is a single storage element that extends only one word-line width normal to the plane of the figure. Other storage films on neighboring word lines along the digit-sense conductor will act as sources of magnetic flux, some of which passes through the region around the film in Figure 2 and is labeled ϕ_n . The characteristics of the magnetic film material enter the circuit model by specifying the relation between m , the mmf across the magnetic film, and ϕ_f , the magnetic flux through the film. The effect of a current I in the digit-sense conductor is represented by an mmf numerically equal to I in the circuit model.

Solution of the circuit model for the digit current needed to produce the state of the film specified by ϕ_f and m is

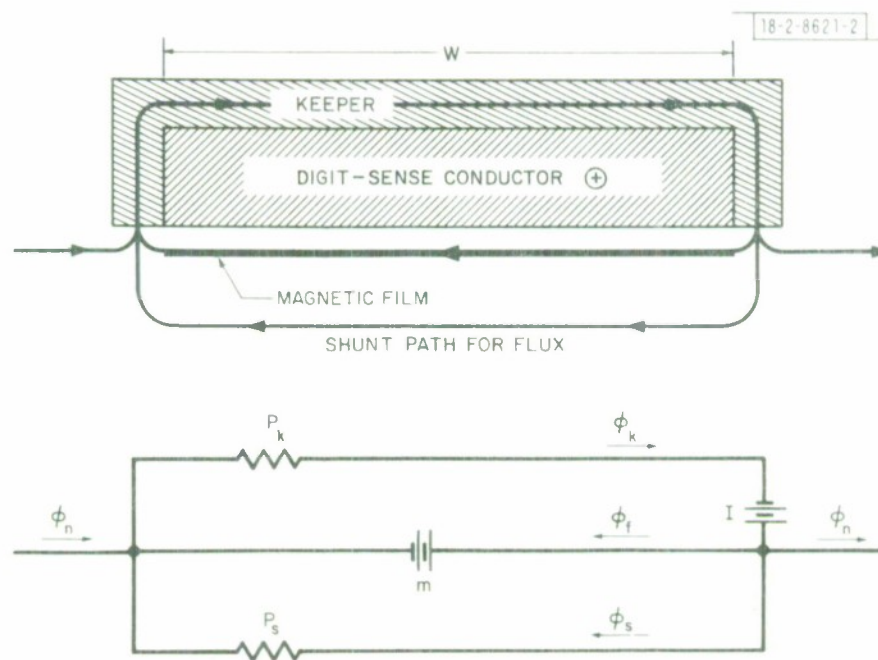


Fig. 2. Cross-section of digit-keeper and magnetic storage film and an electric circuit analogy.

$$\frac{I}{2w} = \left[(H_f + H_n) \frac{2P_s}{P_s + P_k} + H_{net} \right] \frac{P_s + P_k}{2P_k} \quad (1)$$

where $H_f \equiv \phi_f / 2P_s W$ and $H_n \equiv \phi_n / 2P_s W$ are the average (over the film) of the stray fields from the film element in Figure 2 and its neighboring film elements, respectively. $H_{net} \equiv m/W$ is the average net magnetic field at the film.

Compared to the case of no keeper ($P_k = P_s$), the stray fields, H_f and H_n , are reduced by the factor $(P_s + P_k) / 2P_s$, while the digit field per unit current is increased by the factor $2P_k / (P_k + P_s)$. One can also calculate from the model that the remanent flux linking the digit-sense conductor is increased by a factor $2P_k / (P_k + P_s)$. For $P_k \gg P_s$, the digit field enhancement and signal enhancement factors both approach 2.

While the digit keeper circuit model is far from exact, it has proved very useful in calculating the benefits of proposed keeper configurations. An example is the calculation of the increase in signal to be expected through the use of a digit keeper. Even with no change in the magnetic film the keeper can increase the sensed flux up to a factor of 2. Further, reduction in stray field due to the keeper will permit a further increase in signal through an increase in film thickness. In particular, we wished to maintain the bit current ratio, R , above a minimum acceptable value where:

$$R = \frac{\text{minimum digit current for disturbing}}{\text{maximum digit current for writing}} = \frac{H_c - H_d}{H_k \alpha_{90} + H_d} \quad (2)$$

H_c is the wall coercive force, H_d is the worst-case demagnetizing field from the bit itself and neighboring bits, and α_{90} is the angular dispersion in the absence of demagnetizing fields. Equation 2 determines the maximum film thickness, because H_d is proportional to thickness.

If t is the maximum film thickness with no keeper, then the maximum thickness, t' , with a keeper can be found by applying (1) to (2) and noting that the demagnetizing field is the worst-case sum of H_n and H_f , each of which scales with thickness.

$$R' = \frac{H'_c - KH_d}{H'_k \alpha'_{90} + KH_d} \quad \text{where} \quad K = \frac{t'}{t} \cdot \frac{2P_s}{P_s + P_k} \quad (3)$$

and H'_c and H'_k are values for the film of thickness t' . For $R' = R$, the following solution for t'/t is obtained assuming that $\alpha'_{90} = \alpha_{90}$ and $H'_c/H'_k = H_c/H_k$.

$$\frac{t'}{t} = \frac{H'_c}{H_c} \cdot \frac{P_s + P_k}{2P_s} \quad (4)$$

The change in digit current is given by:

digit current for keptered film of maximum thickness t'
digit current for unkeptered film of maximum thickness t

$$= \frac{H'_c}{H_c} \cdot \frac{P_s + P_k}{2P_k} \quad (5)$$

For equal digit currents, equations (4) and (5) together give $t'/t = P_k/P_s$. Since the signal enhancement is $2P_k/(P_k + P_s)$ the total signal increase due to the keeper is $2(P_k/P_s)^2/(1 + P_k/P_s)$.

The digit keeper circuit model has as its only parameter of keeper quality the permeance ratio, P_k/P_s . Once a keeper structure is built, this is easy to measure by means of the crossover current, i.e. that digit current needed to write the selected bit to a null against the worst-case stray field

from neighboring bits. Referring to equation (1), such a null occurs when $H_{\text{net}} = 0$, which means $I_{\text{crossover}}/2W = (H_f + H_n) (P_s/P_k)$. Therefore the ratio of crossover currents with and without a keeper is the inverse of the permeance ratio for that keeper.

For the optimistic value of $P_k/P_s = 4$ (see Section IV) the total signal increase due to the keeper achievable by increasing film thickness while maintaining equal digit current amplitude and margin would be 6.4 for equal width word lines, or 3.2 with word lines one half as wide.

With the same $P_k/P_s = 4$ the digit field at the center of the bit for $W = 6$ mils, word-to-digit spacing = 0.4 mils and digit current of 200 ma is calculated to be 12 Oe. For $R = 2$ as used in LCM I and for $H'_k \propto'_{90}$ small compared to KH_d , the value of H_c should be twice the drive field or 24 Oe.

For LCM I the optimum film thickness was 1200 Å so $t' = (P_k/P_s)t = 4800$ Å, or 2400 Å for each layer of two layer word film. Because H_c decreases so fast with thickness in electroless films, however, it was impossible to increase thickness beyond 1500 Å and still maintain $H_c \geq 25$ Oe, at least in single-layer electroless deposition.

H_k is made as low as possible for the required H_c . As will be seen in the next section, the word current is determined by hard axis demagnetizing fields since the magnetic closure is not perfect.

III. Word Substrate

A. Evaporated Materials

The first magnetic layer and the copper on the word substrate were deposited from an rf induction heated melt in a vacuum using a substrate changing apparatus so that twelve substrates could be coated in one run.⁷

An alloy evaporated from a melt of 50 Co 47 Ni 3 Fe (LCM I composition) required a 200° C substrate to satisfy the new magnetic requirements. This substrate temperature left the film in a high state of stress and over a period of a month the glass under the edge of a line would fracture to a depth of about one mil. This was avoided by using a melt alloy of 90 Co 10 Fe which gave the desired magnetic properties at a substrate temperature of 320° C where the stress has been reported to go through zero for NiFe.⁸

Table 1 give specifications and typical values for the evaporated magnetic films.

Copper was evaporated in two layers to eliminate through-pinholes and at a rate of 0.2 μ / min. or less to avoid copper spatter from the melt.

B. Word Line Fabrication

One mil lines on two mil centers were fabricated with excellent line edge definition and very few defects by scribing through the copper with a diamond tool. The fabrication details are described in Appendix A.

C. Word Line Closure Plating

After scribing, the word lines were coated on the top and sides with a magnetic film using an electroless plating technique. Electroless plating produced a uniform coating on top and sides, something which could not be done by evaporation or electroplating. The magnetic characteristics are given in Table 1. Coercive force of the films was very sensitive to copper surface conditions and adequate H_C control had not been achieved at the end of the project. Full details on the plating technique, magnetic characteristics, and annealing experiments are given in Appendix B.

TABLE 1

Specifications and Typical Values for Magnetic Films on Word Line

		Specification	Evaporated 90 Co 10 Fe	Electroless CoNi
H_c	(Oe)	≥ 25	30	25
H_k	(Oe)	≤ 35	18	30
α_{50}	(Degrees)	< 10	6	1-2
t	(Permalloy equivalent Å)	1500	1500	1500

TABLE 2

Film Properties on Substrates T334-3 and T334-7

		Film T334-3		Film T334-7	
		<u>Evaporated</u>	<u>Plated</u>	<u>Evaporated</u>	<u>Plated</u>
Thickness	Å	1700	1400	1600	1800
H_c	Oe	27	28	27	30
H_k	Oe	16	25	19	41

D. Word-Line Test Results

Word substrates were tested using a glass digit substrate with permalloy and carbonyl-iron keeper (type E of Figure 8). All word lines were electronically accessible and 10 adjacent digit lines were driven simultaneously with mechanical movement of the digit substrate used for complete coverage of the word substrate. Information storage was by conventional word and digit pulse coincidence. The worst-case test pattern included an adverse prewrite of the test word, setup of two adjacent words on each side for maximum adverse demagnetizing field and the same polarity digit pulse on adjacent digit lines. Figure 3 shows the test pattern used for writing followed by disturbing by opposite polarity writing on adjacent words. Disturbing by digit pulses alone was done by removing the word pulses in the disturb sequence. The tester automatically sequenced through write and disturb patterns of both polarities. Two variable-amplitude digit pulses were electronically selectable so that writing and disturbing could be done at different current levels, but only one variable-amplitude word pulse was available. By sweeping digit pulse amplitude while sampling signal amplitude, curves of signal vs. writing or disturbing digit current were automatically traced.

Figure 4 shows the effect on signal and word current of the plated closure layer for two substrates. Peak-to-peak signal amplitude is plotted vs. word current (same amplitude for writing and reading) with a digit current of 270 ma. The before (open) and after (closed) data were taken on the same word line at the same position (± 50 mils). The evaporated films tested were almost identical while the plated layers differed significantly in H_k and thickness as shown in Table 2.

The increase in signal and decrease in word current, with closure, is apparent for both films. Maximum signals greater than 7.6 at currents of

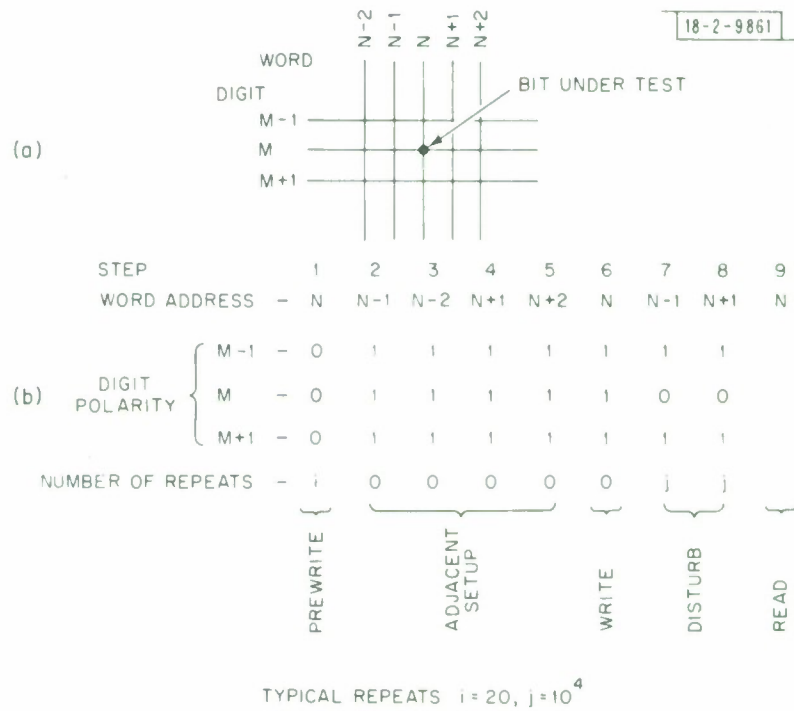


Fig. 3. Worst-case test. (a) Labeling of word and digit lines; (b) time sequence of drive pulses.

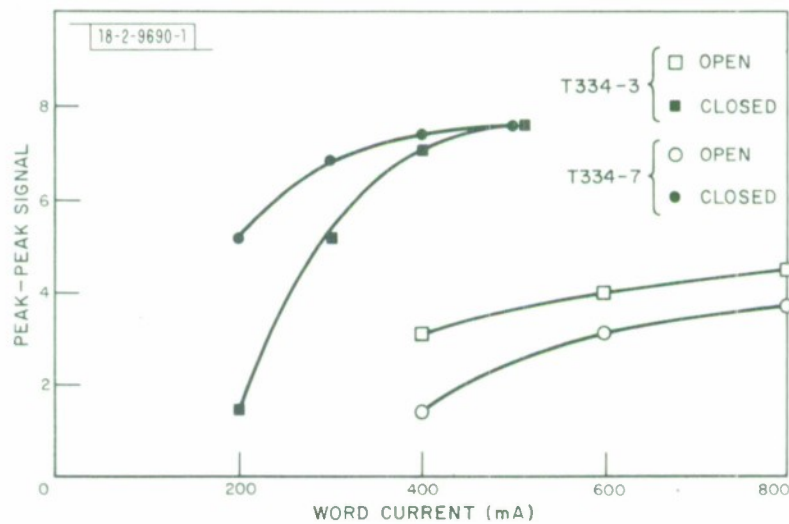


Fig. 4. Peak-to-peak signal vs word current on two substrates before and after plating of a closure layer.

500 ma were achieved with closure while signals of approximately 4 units at current of 800 ma resulted for the open film.

Word lines are typically 1.2 mils wide at the bottom and the peripheral distance along the top and two edges is 1.4 mils providing a ratio of magnetic cross-sections, for equal thickness, of about 2.2 for the closed structure vs. the open. However, because of high demagnetizing fields at the edge of an open structure, less than total switching occurs; therefore, with perfect closure the signal increase should be larger than the cross-section ratios. From Figure 4 the ratio of closed-structure signal at 500 ma to open structure signal at 800 ma was 2.1 and 1.7 for Film #7 and #3 respectively. Correcting for the unequal film thickness these ratios would be 1.9 for both substrates. less than 2.2, the value of cross-section ratio. It is clear therefore, that the closure is not perfect. This is confirmed by the curves of Figure 4 since the field for 300 ma in a 1.2 mil wide line is approximately 60 Oe and the highest H_k for these films is only 41 Oe. Also the large difference between the curves for the two closed structures indicates that Film #7 had better closure than Film #3. The known causes of imperfect closure are unequal film thicknesses and a gap due to etch undercut of the evaporated layer. In addition no way has been found to measure the thickness and characteristics of the plated film on the relatively rough line edges. The closure, however, was much better than with a structure that had top but no edge coverage. One substrate of this type fabricated by evaporating a magnetic layer onto the copper and then scribing was measured before and after etching away the top magnetic layer. The top film was 5/7 as wide as the bottom one due to the slanted edges of the scribed copper. Figure 5 shows curves of signal vs. word current for the single and double layer and a curve of 12/7 times the single layer amplitude. Below 300 ma the effects of closure can be seen

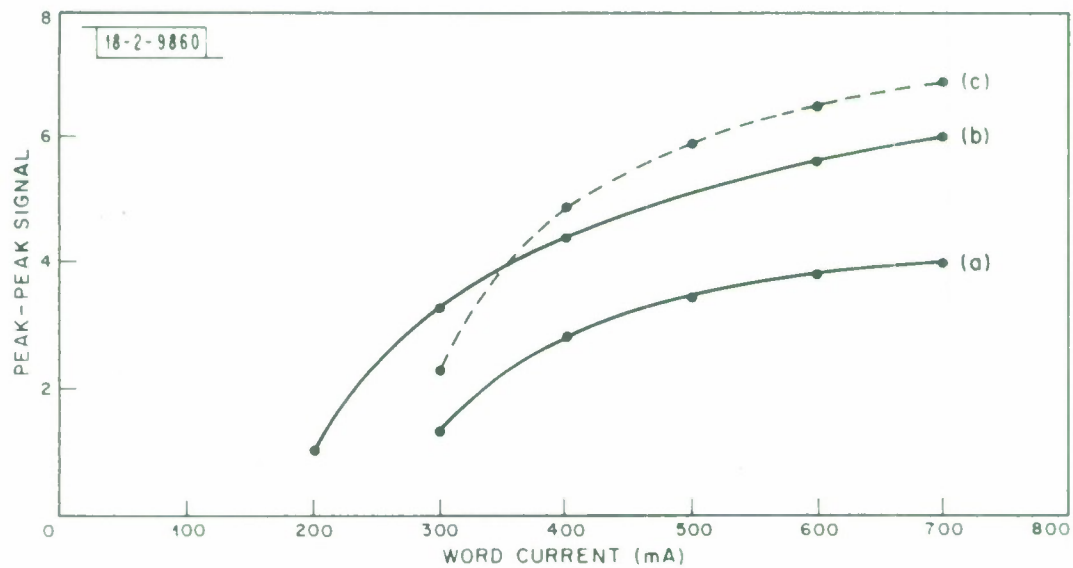


Fig. 5. Peak-to-peak signal vs word current for (a) a single layer, open structure word line, (b) a "closed" structure with film on top of the word line but not on the edges and (c) $12/7$ times the curve in a.

but at higher currents there is no evidence of demagnetizing field reduction by closure and in fact the total signal is less than expected. Clearly, an edge magnetic film is essential to achieving a useful reduction in demagnetizing field.

Figure 6 shows curves of signal vs. digit writing current for three word-line configurations. Preset of the test bit and writing of adjacent words was done at constant digit current of 270 ma. The first curve is of an LCM I substrate with 1150 Å magnetic film and was measured with an un-keepered digit line as used in that memory. The required writing currents were about 600 ma word and 225 ma digit. The other two curves are for one of the LCM II substrates used in Figure 4 with a single layer and with a closure layer and were made with a keepered digit line. The reverse-polarity signals at zero digit current are primarily due to the demagnetizing fields from the written surrounding bits and to a lesser degree the prewrite of the test bit. The larger saturation writing field for the closed film is attributable to the added demagnetizing fields from the second layer. Because of the good closure, this substrate could be written with 400 ma word current. An adequate digit writing current would be about 225 ma which was typical of substrates with good plating. The peak-peak signals for these three configurations at the word currents of Figure 6 and 225 ma digit current were 2.5, 2.8, and 7.1 units respectively. The LCM II signal was 2.8 times the LCM I signal.

The evaporated films alone did not disturb under either digit disturb or adjacent word disturb when written at 270 ma and disturbed at 360 ma digit current. The best plated films, such as on Film #7, also did not disturb under these conditions. Although no substrate was 100% tested, visual inspection indicated that with proper scribing and adhesion control,

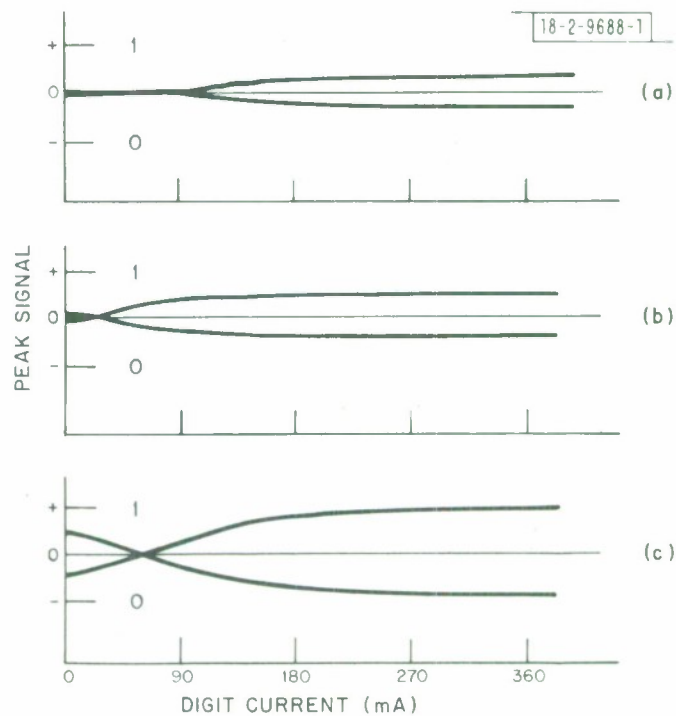


Fig. 6. Signal amplitude vs digit current for (a) LCM I configuration at 600 ma word current, (b) LCM II open word line (T334-7) at 800 ma word current with a keptered digit line, and (c) LCM II closed word line (T334-7) at 400 ma word current with a keptered digit line.

pinholes and mechanical defects in the evaporated layers were largely eliminated. LCM I experience had demonstrated that these were the only significant sources of failures in evaporated films. In addition, tests failed to reveal any local variation from bit to bit in the plated films due to poor closure or thickness or H_c variation. The principal limitation on yields was the variation in H_c in plated films over distances large compared to bit dimensions. This problem is discussed more fully in Appendix B.

IV. Digit Substrate

A. Keeper Materials

Small element dimensions require that the digit keeper be in contact with the digit conductor. This requirement and that for rigid substrates, as explained in Section V, led to the use of an oriented permalloy film as the keeper behind the digit line. This was originally made by evaporating Cr and then 75% Ni - 25%Fe from tungsten filaments onto the glass substrate followed by films of evaporated and plated copper. Poor adhesion and spatter from the evaporation source were problems with this method. A more successful technique involved electroplating permalloy onto copper foil which was then laminated onto the substrate. This technique is described in Appendix C. In either case the permalloy film was about 1μ thick, magnetically oriented along the length of the digit line and had low H_k (< 4 Oe). When the word line film is in the remanent storage state the closure direction is along the hard axis of the keeper film. In this direction permeability is determined by shape anisotropy and, to first order, is $2 \times 10^3 \mu_0$. Due to the magnetic anisotropy of the film material itself however, there are significant second order effects. At read and write time the digit keeper is subject to word fields several times

as large as the digit fields. Experimentally, it was found that the signal was smaller with the keeper magnetized antiparallel to the direction of word field at the keeper. A discussion of these results appears in Section IV C.

Since the direction of word current alternated with every second word group, and since the minimum length of a stable easy-axis domain in the permalloy keeper film is much longer than this distance, it is not feasible to pre-magnetize the keeper so that the word field at the keeper is always parallel to the keeper magnetization. Therefore one must accept the degradation of the keeper susceptibility by the word field. This means that there is a limit beyond which the increasing of keeper permeance will not improve keeper performance appreciably.

Several different linear isotropic materials were used between the digit lines. Indiana General T-1 ferrite was ground to 10μ particle size and mixed with about 20% by volume of Scotch-Weld No. 2216 B1A epoxy as a binder. Carbonyl iron powder (General Aniline and Film Corp. GS-6) which has smaller particle size was also used, but under some preparation conditions it caused shorts between lines. Low frequency permeability was $7.0 \pm 1 \mu_0$ for both materials when cured. Emerson & Cumming, Inc. Eccosorb CR-117 with $\mu = 5\mu_0$ which casts to a smooth finish was also successfully used.

B. Digit Keeper Experimental Results

Keeper Comparisons on a Flexible Substrate

One series of keeper configuration experiments is summarized in Figure 7. These lines were made from a sheet of 0.7 mil copper on 0.7 mil Kapton on which had been plated one micron of isotropic permalloy. Since the permalloy was on top of the copper the lines were placed with the Kapton against the word substrate so the spacing of digit to word lines was controlled by the Kapton thickness. Edge permalloy was electroplated after copper

DIGIT LINE KEEPER STRUCTURES
(0.006 in. lines on 0.010 in. centers, insulation 0.0007 in.)












Keeper Structure	Reduced Crossover Current	Relative Signal Amplitude	Figure of Merit
 A	1.0	1.0	1.0
 B	1.0	1.1	1.1
 C	1.6	1.1	1.8
 D	1.8	1.3	2.4
 E	2.5	1.7	4.2
 F	3.1	1.7	5.1
 G	3.3	1.8	6.0
 H	3.3	1.8	6.1
 I	3.3	1.9	6.2
 carbonyl Fe 0.004 in. thick, $\mu = 7 \mu_o$  plated NiFe 10,000 Å thick, $\mu = 2 \times 10^3 \mu_o$			

Fig. 7. Comparison of digit line keeper configurations on a flexible substrate.

etching and was, presumably, anisotropic. All nine configurations were prepared on one 10" piece of digit lines and were tested with an LCM I word substrate.

Reduced crossover current is the ratio of crossover current with no keeper to that with the given keeper and in theory is P_k/P_s as given in Section II. Relative signal amplitude is the ratio of signal with the keeper to that without the keeper. Figure of merit is the product of these two ratios and represents the possible signal increase through use of a keeper. The data show that the figure of merit increases with increasing amounts of keeper material and that permalloy alone is better than carbonyl iron alone. The improvement with carbonyl iron and permalloy over permalloy alone is explained by the distributed nature of the domain tips in the word film; experiments have shown that the domain edges are a zig-zag wall extending over the 4 mil space between digit lines. Since, theoretically, a figure of merit of 4 should be sufficient for our specifications, any configuration listed in Figure 7 from E on should be adequate.

Keeper Comparisons on a Glass Substrate

With a glass or metal substrate it was not feasible to have carbonyl iron behind the digit line so further consideration was not given to those configurations. (Some substrates were made using the lamination technique with a ferrite-epoxy mixture as the adhesive but it was difficult to remove all bubbles in the stiff adhesive and adhesion was not as good as with epoxy alone.)

Figure 8 shows test results for several keeper configurations made by laminating copper with electroplated permalloy onto glass. The data are from two 10" digit substrates fabricated as one piece so the permalloy was the same thickness on each. An LCM II word substrate without closure plating










Keeper Structure		Reduced Crossover Current Ratio	Relative Signal Amplitude	Figure of Merit
A		1.0	1.0	1.0
B		2.0	1.4	2.8
C		2.3	1.5	3.5
D		2.2	1.7	3.7
E		3.1	1.8	5.6
F		3.2	2.0	6.4
G		4.0	1.8	7.2
H		4.1	2.3	9.4
				

Fig. 8. Comparison of digit line keeper configurations on a glass substrate. Full width copper or permalloy is 6 mils wide. Permalloy extends beyond the copper 0.6 mil on C and F and 1.1 mil on D and H.

was used for testing and the digit keeper was saturated in the same direction for all data points. The results are probably not better than $\pm 10\%$ accurate. The so-called "T" configurations of C, D, F, and H were made by selective etching of copper as described in Appendix C. The carbonyl iron extended behind the permalloy since in scribing the tool cut into the epoxy layer between permalloy and glass. Where direct comparisons can be made the figure of merit of Figure 8 is higher than on Figure 7. Possible explanations are the closer word-digit spacing used for Figure 8 and possibly a better permalloy keeper.

It is likely that it is energetically favorable for some flux to come out of the surface of the permalloy keeper rather than all out of the edge of the film. Thus with carbonyl iron, it is reasonable that the "T" configuration of H was better than E since a lower reluctance path exists for the surface magnetic poles also. If there were no gap between back and edge permalloy, the "T" shape might be inferior with plated edges. The data show the "T" shape, F, to have larger signal but a smaller reduced crossover current than G. The advantage of the "T" shape without an edge keeper, C or D vs. B, is more difficult to explain. If with a full width copper line the domain walls between bits extended under the copper, flux lines going through the copper would not couple with full efficiency to the digit line so that narrowing the line might increase coupling efficiency. A similar explanation can be used to explain the signal increase of more than a factor of 2. With no keeper, besides losing all of the signal flux on one side of the word lines, there may be flux passing through the space between word and digit lines or through the copper which with a keeper will become coupled to the sense line.

Configurations with both permalloy and ferrite (or carbonyl iron) on line edges were not tested on glass. Unless necessary it would seem

advisable not to complicate fabrication by using both materials. It is seen that permalloy on the back alone is not adequate for the required factor of four in the figure of merit although, for convenience, it was used in the stack experiments of Section VII. Since any of the configurations with edge keeper are adequate the choice would depend upon "noise" and fabrication considerations.

"Noise" in this context refers to coupling from word to digit line due to inhomogeneities in the keeper, such as pinholes and voids, which causes asymmetric signals or essentially reduces the signal amplitude. Very little data were taken on this; only impressions can be reported. On one substrate with ferrite-epoxy behind the lines, large "noise" was traced to voids in the keeper. On a "T" configuration without edge keeper on which the copper had been over-etched so that it had very irregular edges the noise was small. On similar lines without the permalloy keeper the noise was large so the straight-edge keeper was determining the coupling. With the different configurations of Figure 8 the signal asymmetry, i.e., "noise," was more noticeable than with no keeper but only on the order of 10% of signal amplitude. Since a figure of merit of more than four can be obtained, some level of keeper "noise" will be acceptable. Complete testing of keptered substrates for both efficiency and "noise" would be a necessary next step.

Effect of Digit Keeper Magnetization Direction

Figure 9 illustrates the effect of digit keeper magnetization direction. The curve is a writing curve of signal vs. digit writing current with a worst case pattern for a closed LCM II word substrate and a digit line with the keeper configuration H of Figure 8 but with a smaller etchback of the copper (1/4 mil). For the curves labeled \perp , the digit keeper was saturated with a magnet (> 100 Oe) along its easy axis opposite to the direction of the field from the word line at the keeper. For the curves labeled \parallel the magnetization



Fig. 9. Signal vs digit current with two saturation directions of the digit keeper film.

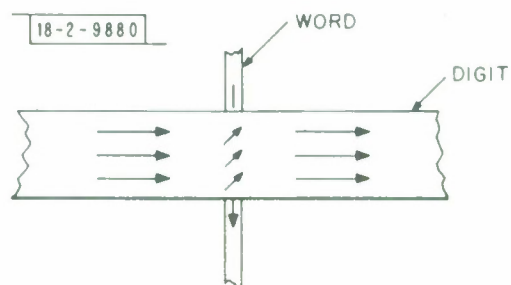


Fig. 10. Idealized representation of magnetic orientation in digit keeper film.

direction was the same as the word field. Figure 10 shows one bit of word and digit line with an idealized representation of the magnetic orientation in the keeper film. At read time the word film magnetization rotates into the easy direction of the keeper (but is probably poorly coupled to the digit keeper due to the dimensions and the word line closure). If the word field at the keeper is in the same direction as the keeper magnetization, it will aid the keeper rotation into the easy direction (along the digit line); but if the word field is antiparallel it may prevent complete rotation of the keeper flux into the easy direction and therefore reduce the signal amplitude. There was some evidence that this effect was slightly larger with an "open" word line where the demagnetizing field of the word film added to the word current field at the keeper.

The data of Figure 8 were taken with the adverse antiparallel magnetization.

Keeper Disturb on Aluminum Substrate

When a keepered digit line was laminated onto an anodized aluminum substrate a severe disturb effect was observed. One such sample (with perm-alloy keeper on back only), when used in the stack with an LCM I word substrate and at 500 ma word and 150 ma digit, disturbed to 1/3 signal amplitude with one digit disturb pulse. On a similar digit line on glass there was about 30% disturbing. At those current levels even the 30% was suprising which raised some unresolved questions about the keeper material on those substrates. With the test digit substrates the disturb was less severe but it was determined that the aluminum substrate was responsible for the disturb. The signal was restored to full amplitude with one digit pulse of opposite polarity and nearly completely restored when a word pulse was applied to a word line adjacent to the one under test. No switching voltage could be

detected on the digit line terminals at the time of the digit-disturb pulse so the entire line did not seem to be switching. The disturb level was not dramatically sensitive to spacing of the keepered line to the substrate over the range of 0.2 to 30 mils. The amount of disturbing was essentially linear with disturb current, i.e. there was no evidence of a threshold. A digit line keepered only with carbonyl iron when placed on an aluminum substrate did not show the disturb effect.

Project termination prevented further examination of this disturb and no explanations can be offered. Obviously, if not solved, it prevents use of aluminum digit substrates.

Word-to-Digit Spacing

Table 3 shows the effects of word-digit spacing on signal and digit crossover for a closed LCM II word substrate and a digit line similar to H of Figure 8 (1/4 mil etchback).

V. System Noise

A. Types of System Noise

Memory performance is limited by three types of non-random interference: "word noise," "group-select noise," and "digit-recovery transient." Word noise is a sense-system transient at read time caused by capacitive and/or inductive coupling from word drive. Because it subtracts directly from one signal polarity, it is critical for memory reliability. Group-select noise is the sense-system transient caused by the level change for the selection of one word group, at the start of the memory cycle, and is the primary limiting factor on memory access time. Finally, the digit-recovery transient is a consequence of some of the digit drive being coupled into the

TABLE 3

Signal and Digit Current Crossover vs Spacing Between Word and Digit Lines
With A Keeped Digit Line

<u>Spacing-mil</u>	<u>Relative Signal</u>	<u>Relative Digit Crossover</u>
0.2	1.00	1.00
0.5	.86	1.28
1.0	.65	1.72

sense system, a problem particularly serious in systems, such as LCM II, using a common line for digit and sense. Because its decay sets the minimum time between a write operation and the following read, it is the fundamental limit on memory cycle time in read-rewrite cycles. Since digit-recovery transient is primarily a sense-system problem it will be treated in Section VI.

B. Effect of Random Noise on Tolerance to System Noise

In the system under study here bit size has been reduced to the point where random noise is not negligible, and it is therefore necessary that systematic noise be always small enough so that when it is subtracted from film signal the net signal have a signal-to-random noise ratio consistent with a required Mean-Time-Between-Failure for the entire system. To calculate the required signal to noise consider a memory in which M bits are read out simultaneously at cycle time T, with a signal-to-random-noise ratio A/σ uniform over all bits. The mean time between failure is

$$MTBF = \frac{2T}{M (1 - \text{erf } A/\sigma\sqrt{2})} \quad 9$$

An asymptotic expression valid for all A/σ large enough to be practical is*

$$MTBF = \sqrt{2\pi} \frac{T}{M} \frac{A}{\sigma} \exp \frac{1}{2} (A/\sigma)^2$$

For a MTBF of 1 year, a 400-digit 1- μ sec memory must have $A/\sigma = 8.2$.

*Dwight, Herbert B., Table of Integrals and Other Mathematical Data 3rd ed., 591, MacMillan, N. Y., (1957).

In a practical memory most bits will be well above a critical A/σ threshold, with only a few bits that are a potential source of errors. Consider the extreme case of a memory with only a single questionable bit where systematic noise has reduced the amplitude of one signal polarity. Assuming random accesses to all words and random information patterns the above memory would require $A/\sigma = 5.9$ at the bad bit for 1-year MTBF.

A practical memory of LCM II dimensions, then, must have a minimum A/σ between 6 and 8. A developmental LCM II sense amplifier had a nominal $A/\sigma \sim 20$; the sum of systematic noise could therefore conceivably reach 60 to 70% of signal amplitude without an excessive failure rate. Some allowance must be made for signal amplitudes below nominal, strobe offsets, etc. Still, systematic noise up to almost half signal amplitude should be tolerable on a few bits.

C. Sources of Group Noise

At group-select time the selected group has a voltage transient of 27 volts which is capacitively coupled to the digit lines. The array of digit lines in parallel constitutes a low-impedance low-loss transmission line for common-mode transients. The digit-line common-mode pulse excited by the group-voltage transient may experience multiple reflections from the array ends depending upon the common-mode termination of the digit lines. At least three different sources of group-select noise can be categorized. First, there is simple imperfect rejection by the sense system of common-mode voltage on the digit lines. Second, there is the conversion of that voltage to difference mode due to unequal capacitance between word lines and the two sides of the digit hairpin. A third source of noise appears if one considers the capacitive charging currents flowing on all of the neighboring mutually coupled digit conductors. In the center of a uniform digit array there can be no net coupling

into a digit hairpin by these charging currents, but any perturbation on array symmetry such as nearness of a stack edge, some irregularity in line geometry, or variation in word-to-digit spacing, will result in a net induced signal into a digit line.

Considerations of capacitive imbalance between word and digit lines led to a change from the flexible digit substrates in LCM I to rigid substrates. It is convenient to think of two different modes of imbalance due to short and long range spacing variation. Figure 11 shows two cross sections along the selected word line group where there is a piece of dust between the word and digit lines. In Figure 11a the digit substrate is flexible so that it can bend around the particle. Since the spacing of lines a and b to the word lines are different they will have different common mode voltages and a difference voltage between them. A difference-voltage pulse equal in length to the group-pulse rise time will travel in both directions from the excitation point with the same polarity; at the shorted end, one pulse will be reflected with reversed polarity. When the delay time of the digit line is much less than the group voltage rise time as it was in LCM I, the shorted sense line will attenuate the noise pulse. Even so, the principal source of group (and word) noise in LCM I was short-range capacitive imbalance due to small dust particles between the rigid word and flexible digit substrates. (Calculation and experiments have shown that an air spacing difference of only 20 microinches ($1/2$ micron) can be significant.)

Figure 11b shows the situation where both substrates are rigid. A small particle causes a long wedge shaped space between word and digit lines. The capacitance difference between two adjacent lines is small and so there will be a small difference voltage. Over a larger number of lines the difference in voltage will be the same as in Figure 11a and, depending upon the mutual coupling, there may be noise due to surge current imbalance.

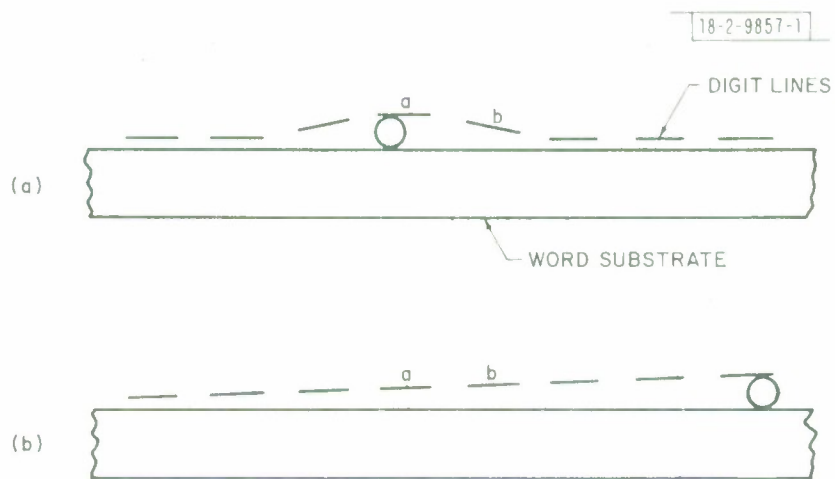


Fig. 11. Effect of a foreign particle on word-digit spacing with a rigid word substrate and (a) a flexible digit substrate, (b) a rigid digit substrate.

Another possible solution is to fill in the air spaces created by dust particles with a high-dielectric-constant material to reduce the difference in capacitance. Tests of the effectiveness of two high-dielectric-constant (K) fillers with a flexible substrate were made using the tester described in Appendix D. As in LCM I the flexible-substrate digit piece was 5 mil thick fiberglass-epoxy with 0.7 mil thick Cu backed by a 20 mil thick piece of expanded vinyl and pressed by a metal plate against the glass word substrate. The two fillers were Dow Corning 510 and FS1265 fluids with dielectric constants of 2.77 and 6.90 respectively. At one position with a known spacing variation, the oils reduced the imbalance voltage by factors of 3 and 4 1/2 respectively. Tests of all 7740 word-digit intersections were made for a number of dry and wet assemblies. Since no two assemblies were the same with respect to spacing variations, the results are statistical but in terms of number of noisy positions with a given insulating thickness on the word substrate, the comparison between dry and wet assemblies was unambiguous. With one insulating coating, a dry assembly had 250 positions with noise above a certain threshold and a wet assembly with 510 oil 126 noisy positions at the same threshold. With another coating (probably thicker) but the same threshold, a dry assembly had 71 noisy positions and a wet assembly with FS 1265 oil no noisy positions and 39 noisy positions at half the noise threshold. No long-range-imbalance inductive coupled noise was observed with flexible digit lines, except at edges, in either the tester or memories.

Using the same tester, no short-range-imbalance noise was observed with digit lines on 40 mil and 1/4 inch glass substrates. Some long-range-imbalance noise was observed due to relatively large spacing variation. Since the noise performance of rigid digit substrates was superior to that of either dry or wet flexible substrates and they were better adapted to fabrication of keepered digit lines the cross-section stack was built with glass and metal substrates.

C. Word Noise

At word-current-rise time there are three sources of voltage which will be capacitively coupled to the digit lines: the voltage drop on the selected word line itself, the voltage drop across the selected group switch which is coupled to digit lines through the entire group, and voltages inductively coupled onto adjacent word lines. Word noise will be generated by these voltages by the capacitive imbalances discussed above.

Since the word and digit lines are orthogonal and long there should be no inductive coupling between them except through the storage film. Inductive coupling occurs due to discontinuities such as ends of lines or discontinuous ground planes and defects such as nicks in lines or voids in keeper material. A defect in the edge of either a word or digit line will be a source of inductive coupling. Such defects may be caused by pinholes in the copper or etch defects. The relation between noise and defect size is quite sensitive to defect shape and relative positioning of word-to-digit line. In LCM I a typical circular-shaped nick extending $1/2$ mil into the 2-mil word line generated a noise voltage $1/4$ as large as peak signal amplitude.

VI. Sense System

A. Introduction

The sense system of a thin-magnetic-film memory must amplify the fractional-millivolt film signal to logic amplitudes while rejecting common-mode digit-line voltages orders of magnitude larger, make a correct decision as to signal polarity despite random noise, and be able to perform the sensing operation as quickly as possible after the large transient caused by digit current from a previous writing operation. A block diagram of a developmental sense system for LCM II is shown in Figure 12. The system starts with a

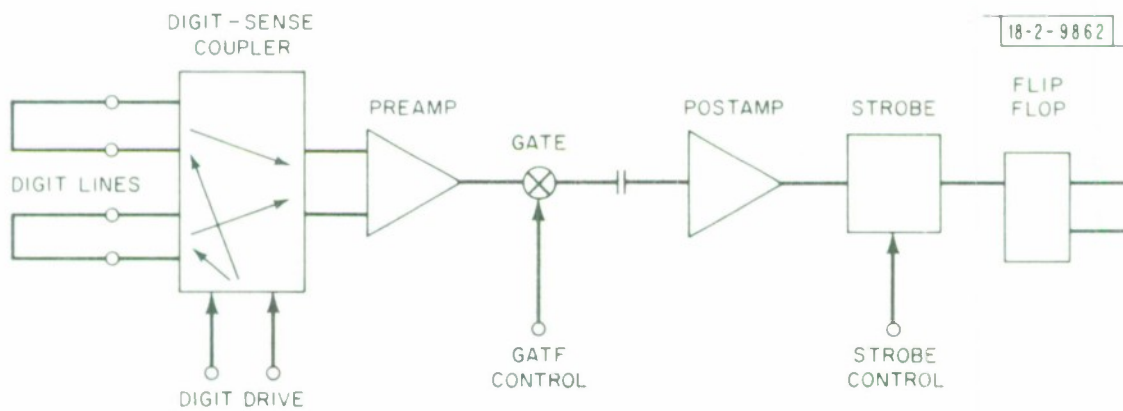


Fig. 12. Sense-system block diagram.

digit-sense coupler arranged to couple a preamplifier to a pair of digit lines for film signal, but to isolate it, at least to first order, for digit drive. The preamplifier is followed by a switch or gate that keeps residual digit transient off subsequent coupling and filter capacitors. The switch is followed by a post-amplifier, with filtering for an optimum frequency response, and a strobe or comparator element with associated storage.

B. Preamplifier

Multi-transformer digit-sense coupler--In LCM I, input-circuit requirements were met with a multi-transformer digit-sense coupler shown in Figure 13. Common-mode rejection was provided by filters CMC_1-L_1 and CMC_2-L_2 , each consisting of a series common-mode choke and a shunt, center-tapped inductor. The signal was transformer coupled to the sense amplifier in a bridge arrangement that provided first-order isolation of the amplifier from digit drive. This digit-sense coupler had many shortcomings: it was complicated and difficult to fabricate; it required an adjustment potentiometer to balance the isolation bridge; and the inductive elements provided energy-storage locations that slowed recovery from the digit transient.

"Double-differential" amplifier--An alternative input arrangement that eliminates almost all inductive components is the "double-differential" input stage of Figure 14. Each digit line of the pair is connected to a transistor differential amplifier; amplifier outputs are in parallel. Diode couplers attached to each input are open circuits for signal amplitudes, but connect digit drive to the digit lines in such a fashion that, for matched amplifier halves, there is no net output. The separate amplifier inputs provide common-mode rejection. However, common-mode chokes are still necessary in digit-line leads to reduce charging currents on the lines themselves.

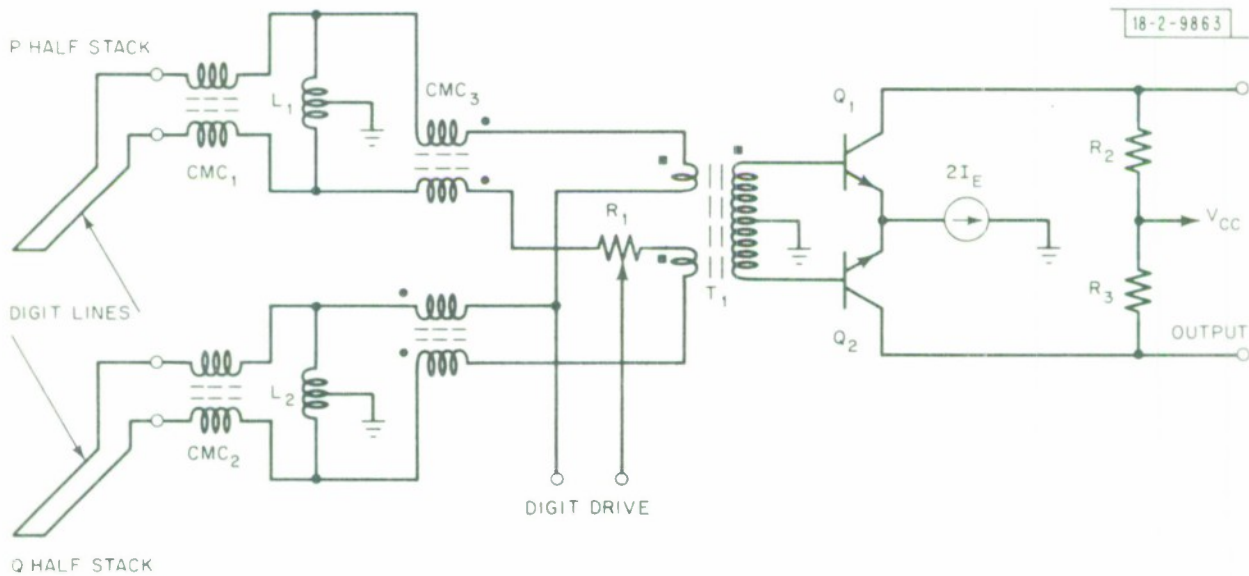


Fig. 13. LCM I sense-system input with multi-transformer digit-sense coupler.

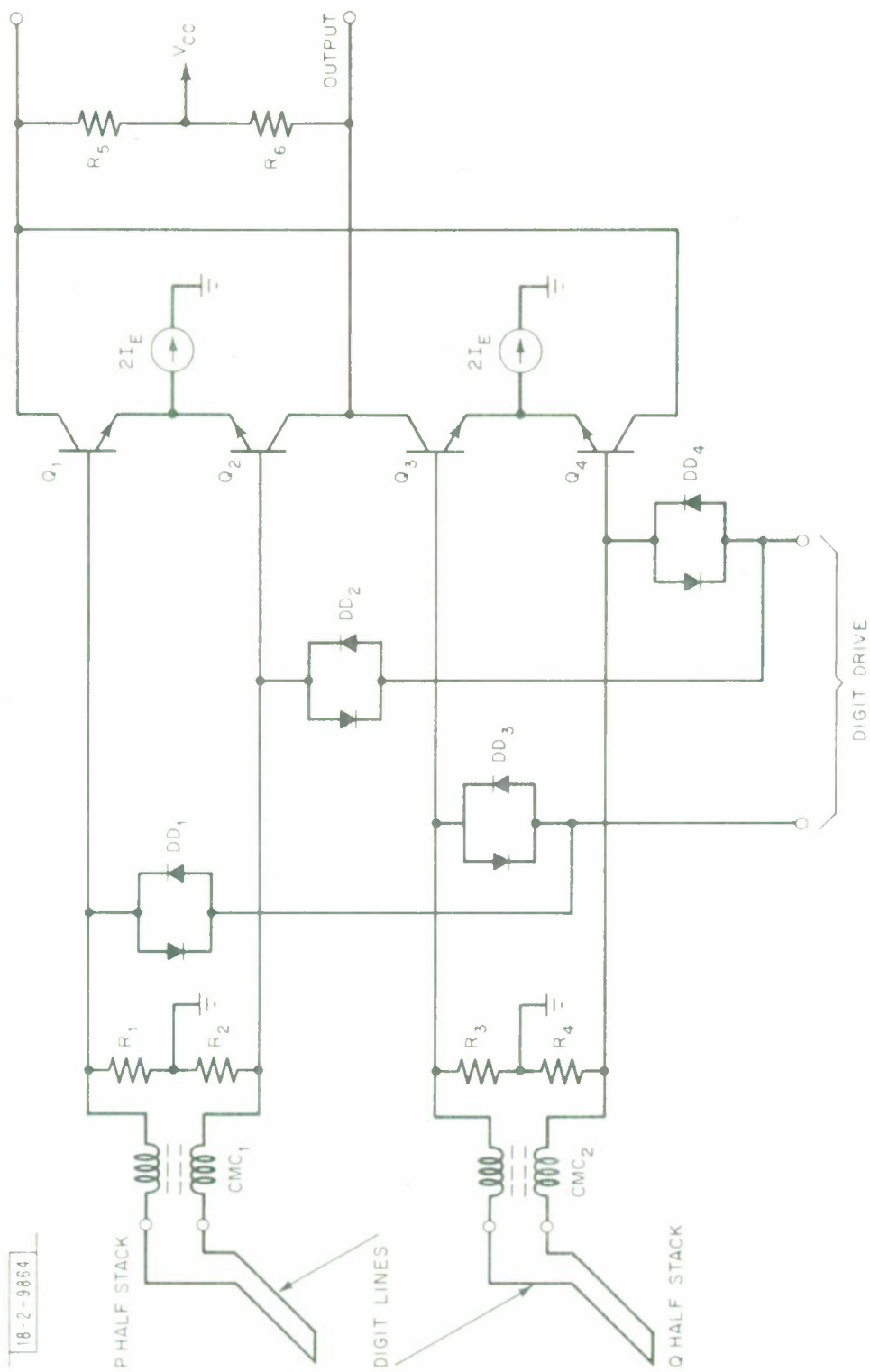


Fig. 14. "Double-differential" sense-system input stage.

Several factors indicate that the "double-differential" input stage should be fabricated as a monolithic integrated circuit: the complexity of the amplifier, in terms of number of semiconductor components used; the need for good match between input transistors of a pair; and the need for good match between transistor pairs, their emitter-current sources, and the coupling diodes. Because design and fabrication of such a circuit was outside the scope of the project, the "double-differential" input stage was not investigated in depth; only a relatively few experiments were performed with it, primarily with such commercially available matched-transistor arrays as the Signetics NE511B and RCA CA3026, which have too much random noise to be considered for a practical amplifier design. Indications are that performance should be about as good as with the more thoroughly investigated "single-differential" amplifier. However, the amplifier does have a couple of limiting peculiarities. First of all, each input pair sees in difference mode the full digit-drive voltage across its associated line; this can run as high as 8 volts. Second, for reasons that will be explained in the section on noise, it is to be expected that optimum signal-to-random-noise performance will require input transistors of larger area operated at substantially higher emitter currents than in the "single-differential" amplifier.

"Single-differential" amplifier--A third input arrangement is the "single-differential" amplifier of Figure 15. The two digit lines are connected in series to the differential input of the amplifier. Digit drive is applied to the lines in parallel through diode couplers. If the lines and coupling diodes are matched, no differential sense-amplifier input results from digit drive.

A common-mode choke and center-tapped shunt resistor provide common-mode rejection for each input. Notice that, if the amplifier input bases were connected directly to the outputs of these filters, there would be

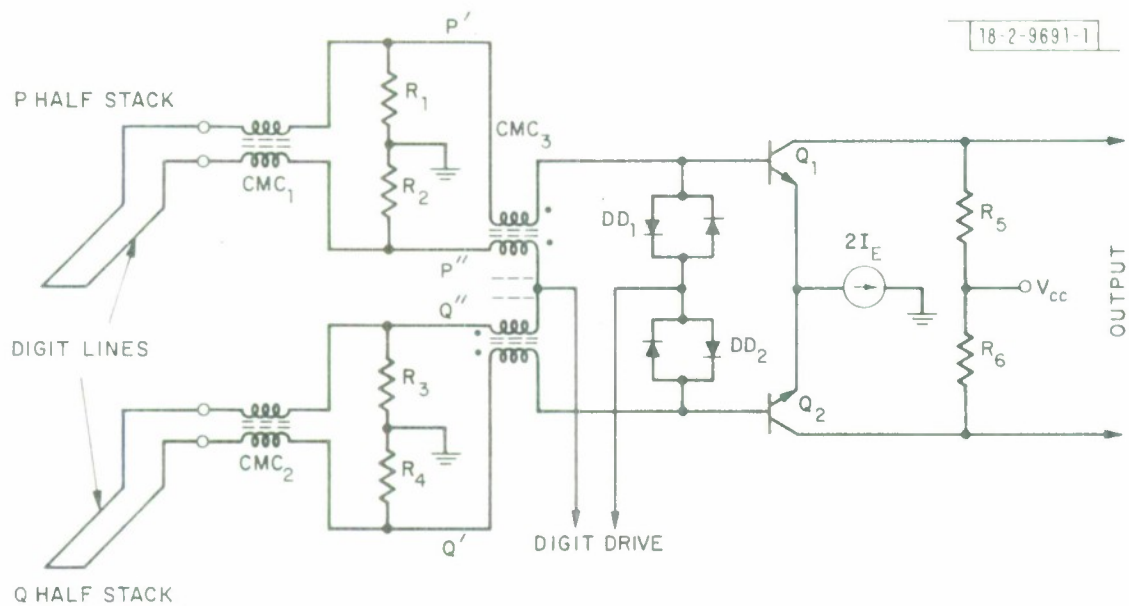


Fig. 15. "Single-differential" sense-system input stage.

complete rejection of any remaining common-mode voltage appearing at both P' , P'' and Q' , Q'' , but any voltage appearing on only one line pair would appear in difference mode and not be rejected. Transformer CMC_3 between the common-mode filters and the amplifier inputs accommodates differences in common-mode voltage. To first order, it operates as follows: if its P half-stack terminals (P' , P'') are at a voltage V , and its Q half-stack terminals (Q' , Q'') at 0 v, then the Q_1 base will be at $V - V/2 = V/2$ and the Q_2 base at $0 + V/2 = V/2$.

Transformer CMC_3 is less than desirable on two counts: first, it adds manufacturing complexity to the sense system; and second, though to first order it stores no energy from digit-drive pulses, in fact there are second-order effects that do involve it in digit recovery. Neither of these problems is really prohibitive: The transformer is less difficult to fabricate than might be supposed, for it is a unity-turns-ratio device that can be quadrifilar wound. Its effects on digit transient can be kept in a frequency range that will be rejected by high-pass filters in the post amplifier.

The "single-differential" amplifier, then, may be less desirable as the ultimate solution for an input stage than the "double-differential" amplifier fabricated as a custom monolithic circuit. However, it has the important advantage that it can be made from commercially available monolithic and discrete components.

Signal and random noise--Because of the low amplitude of the film signals, the input stage of the amplifier must be designed for optimum noise performance, that is, for the maximum obtainable ratio of peak signal to rms random noise at the amplifier output. In his analysis of random-noise considerations, Blatt⁹ considered the case in which the signal source and amplifier input circuits appear resistive over the frequency range of interest;

frequency filtering then occurs only in the amplifier after all noise sources. Under such an assumption, the noise problem can be neatly factored into two parts: (1) the maximization of first-stage noise figure and (2) optimization of postamplifier bandwidth. However, with long digit lines and a practical input amplifier the assumption is no longer completely valid. In particular, bandwidth effects in the first stage become important; the first stage must itself be optimized for signal/noise.

In a direct-coupled input stage, signal/noise optimization involves: (1) choice or design of the most suitable transistors; (2) choice of circuit configuration; and (3) choice of circuit parameters, especially emitter current. In a transformer-coupled input stage, such as in LCM I, the choice of a turns ratio is also involved. It would appear that one important degree of design freedom is lost with a direct-coupled input, but such is not the case: turns-ratio selection is really equivalent to proper choice of the input transistors, as the two following arguments show.

For purposes of noise analysis, the transistor input circuit can be regarded as a network of impedances and noise sources. At the primary of the sense transformer, the impedances and mean square source amplitudes are all scaled by the same factor: the square of the turns ratio (or its inverse). The scale factor is chosen for an optimum relationship between the source and the reflected network. But exactly the same scaling can be done without a transformer by connecting identical input networks in parallel. If the optimum turns ratio were n , one could simply connect n^2 identical transistors in parallel. In practice, this means that one would choose a large-area, multiple-stripe transistor for a direct-coupled input stage in a situation in which a small transistor and a step-up transformer would ordinarily be used.

The question of input-transistor optimization can also be approached more directly. Noise sources in a transistor are shot noises associated with

junction currents and Johnson noise associated with the base resistance, r_b' . Paralleling many base stripes results in a reduced r_b' . It might seem that the optimum transistor would have so many stripes as to make r_b' negligible in comparison with loss elements in the source. However, there is an upper limit: as transistor junction area is increased, the current density must decrease, and gain falls off, bringing into importance noise generated in the first-stage output and in subsequent stages. Bias currents cannot be increased to hold current density constant because this results in increased shot noise. In addition, lowered frequency response caused by decreased current density plus increased junction capacitances will further degrade input-stage signal/random noise. The optimum input transistor would then be a transistor with good high-frequency performance and large geometry consisting of many parallel stripes.

The input-transistor pair in the "single-differential" amplifier faces a source consisting of two digit lines in series; each input pair in the "double-differential" amplifier faces one line, just half the impedance. The transistors in the "double-differential" amplifier must therefore be larger, and be run at higher emitter currents; because there are twice as many of them, the difference in current and area is even more marked. The large area may be uneconomic in monolithic fabrication; the high current, in the many amplifiers required, may cause unacceptable dissipation.

In the absence of custom fabrication facilities, the input transistors for a "single-differential" amplifier were chosen from those commercially available. The choice was made empirically by varying first-stage emitter current and postamplifier bandwidth for an optimum for each input device. A typical comparison of random-noise performances is presented in Table 4, which is based on data for LCM I lines and signals, for which a good transformer-coupled sense amplifier produces a signal/noise of somewhat

TABLE 4

Signal-To-Random-Noise Ratios with Various Input Devices Connected in the "Single-Differential" Configuration to LCM I (Short) Digit Lines, Driven by LCM I (1/8 mv) Signals

<u>Input Device</u>	<u>Signal/Noise</u>	<u>Comments</u>
2N3424	11	"Low-noise," small-signal dual transistor.
NE 511	14	Two monolithic differential amplifiers connected in parallel.
2N2219*	14	Medium-speed switch.
2N5109*	26	High-frequency large-signal amplifier.
MD3725*	27	Medium-current high-speed switch.
SN75303	27	Eight-transistor monolithic medium-current driver array; connected with 4 transistors in parallel on each side.

*Note: Devices not matched by d-c input parameters.

over 30. It should be noted that the transistors with good signal/noise ratios are high-frequency devices intended for operation at currents substantially higher than those usually used in small-signal amplifiers. The best practical choice from the table is the Texas Instruments SN 75303, which is an 8-transistor monolithic array that can be connected as a differential input stage with 4 transistors in parallel for each side. The composite transistor has frequency response limited by emitter transition capacitance to $f_t \approx 150$ MHz at a typical operating current of $I_E = 15$ ma.

There is little choice in the optimum circuit configuration for the input stage. Given that it must be of the "single-differential" type, the only real option is negative feedback for improved, or at least more predictable, performance. However, it can be shown that any simple resistive-coupled feedback, series or shunt, will degrade the noise performance; therefore the input stage must be operated "wide open."

Finally, the transistor operating points must be chosen. Collector voltage has little effect on random noise, so only emitter current is important. Results from the tests, this time with LCM II digit lines and signals, are shown in Figure 16. It can be seen that for any given low-pass time constant there is a broad maximum in signal/noise as a function of emitter current. While the choice of emitter current is obviously not critical, it is a little more important than the plot might suggest, for the mean time between failure for a noise-limited system is such a steep function of A/σ that a change of a few units can change the failure rate by many orders of magnitude.

C. Series Gate

From the standpoint of recovery from the digit transient, the entire sense system through the strobe should be direct coupled. However, this is fundamentally impossible in a system with signal amplitudes as small as

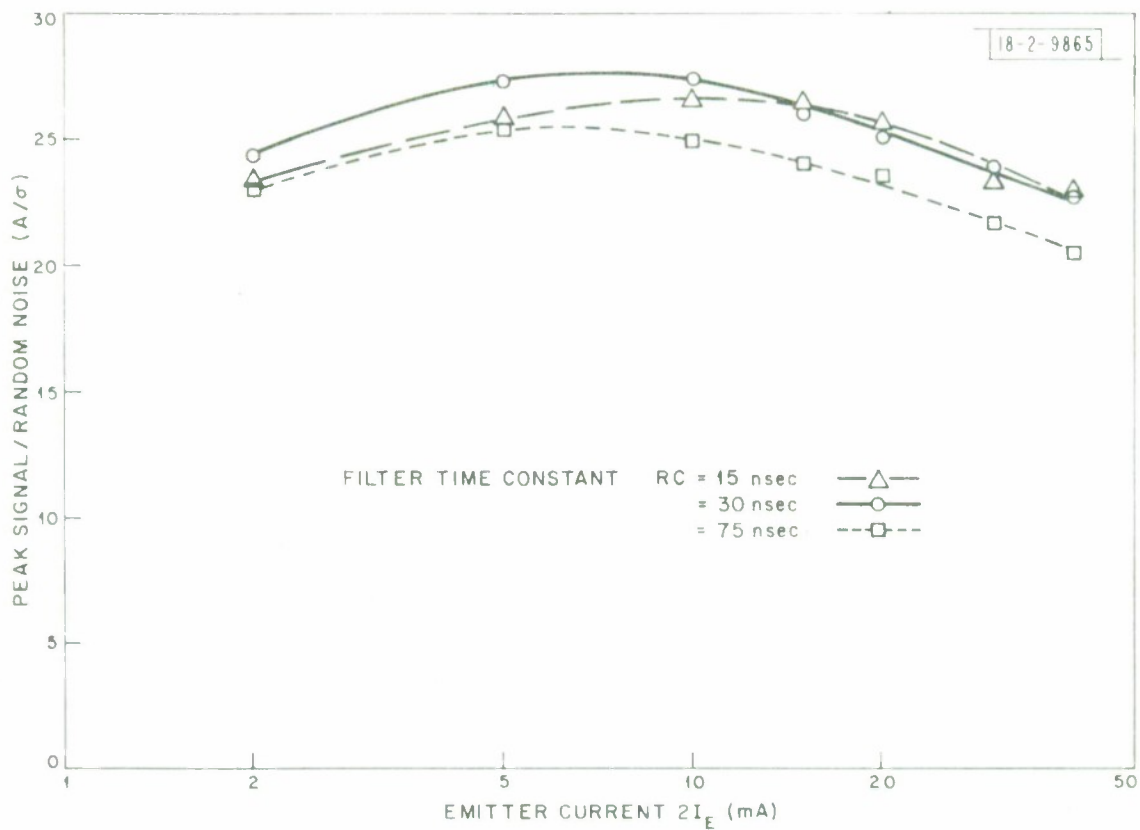


Fig. 16. Variation of signal-to-random-noise ratio with first-stage emitter current. Measurements on test jig with single-time-constant low-pass filter, with SN75303 in a "single-differential" configuration, LMC II digit lines, and "quarter-millivolt" signal.

those in LCM: any d-c offset in the input stage will subtract from one polarity of signal; to prevent an unacceptable reduction in the ratio of net signal to random noise, the subtractive offset from quarter-millivolt signals must be limited to about $50\text{ }\mu\text{V}$, a value unrealizable at present.

The sense system, then, must be a-c coupled. With a-c coupling the problem arises of keeping the digit-drive transient from causing energy storage in coupling capacitors, and so extending recovery time. One solution would be some sort of switch between the digit lines (and the digit drivers) and the bases of the input stage, to disconnect the amplifier during the digit-drive transient. However, signal levels are so low at this point that the switch transient would seriously slow operation. In addition, the on resistance of such a switch would degrade the signal-to-random-noise ratio. The solution actually chosen was a series switch after the first stage, just before the first coupling capacitor. Because the first stage is direct coupled, there are no major energy-storage elements there to extend the digit transient. Signal level is high enough at the output that the switching transient is tolerable.

A practical form of series switch consists of a matched pair of MOSFET's connected between the output of the first amplifier stage and the first pair of coupling capacitors. Because signal transmission is differential, there is a first-order cancellation of the common-mode switching transient capacitively coupled from the MOSFET gates to drains.

The analytical determination of the effect of a series switch on random noise is not trivial and was not attempted.¹⁰ Instead, noise immediately after switch closure was measured on an experimental sense system. If there was any noise enhancement, it was negligible; for practical purposes, the switch can be regarded as not affecting random noise.

D. Postamplifier

The postamplifier must raise the signal amplitude to a level compatible with the strobe and provide an optimum frequency response with respect to systematic and random noises. Because the series gate eliminates the large overloads usually associated with the digit transient, there are none of the usual stringent requirements on the speed with which the amplifier recovers from saturation.

The principal design problem in the postamplifier, then, is correct shaping of the frequency response. Consider first the response requirements for nonrandom noise. Word noise frequently has sharp spikes, requiring some sort of low-pass filter. Group-select noise, on the other hand, is frequently in the form of a step function; to reduce its amplitude as quickly as possible the amplifier must have short coupling time constants. The same requirement applies in recovery from digit transient.

The requirement for optimum frequency response with respect to random noise is more complicated, and in some ways conflicts with the other requirements. For the case of an amplifier first stage driven by a signal in the presence of white noise, the optimum postamplifier frequency response is that of a matched filter: a filter whose impulse response is the mirror image of the signal waveshape. The conditions for a matched filter are not met in an LCM sense amplifier: in particular, there is considerable frequency distortion in the digit lines and in the input to the first stage, so there is no point at which one can talk about signal in the presence of white noise. Nevertheless, it is instructive to consider a matched-filter system as at least a starting point for bandpass optimization.

It is not necessary to approximate the mirror-image impulse response very closely to get a signal-to-random-noise performance near the optimum.

For example, a one-pole filter will give a signal-to-noise voltage ratio of 90% of that of a matched filter, and a two-real-pole filter 94%.¹¹ It has been found in experimental sense amplifiers that a single R-C low-pass filter is very nearly the best one can do for optimizing response to the approximately Gaussian film signal. (Undoubtedly some implicit filtering by higher frequency poles in a practical amplifier enters into the response.)

When using matched filters, any attempt to differentiate the signal, that is, any limitation of the low-frequency response, must lower the signal-to-random-noise ratio. However, the extent of signal-to-noise degradation is not as great as has been reported. (See Appendix E.) Experimentally it has been found that reducing a coupling time constant in a sense amplifier to about 40 n sec, compared to a signal width (at the amplifier output) of over 150 n sec, reduced signal/random noise only about 20%.

The experimental technique in bandpass optimization has been to adjust the amplifier high-frequency response with a single low-pass filter, while simultaneously varying first-stage emitter current. Typical results are shown in Figure 17. Next, to improve digit recovery the low-frequency response is reduced with one or more series coupling capacitors made as small as possible, until limited by signal/noise degradation.

E. Strobe

The strobe or comparator must sample the output of the sense amplifier to determine the signal polarity, and then store the result. Because of noise considerations, the requirements on the strobe for LCM II are somewhat more rigorous than might be expected. First, any strobe circuit will have some threshold or offset level. In a system with negligible random noise the only requirement is that this threshold be less than the signal amplitude. In a random-noise-limited system, this threshold subtracts from one polarity

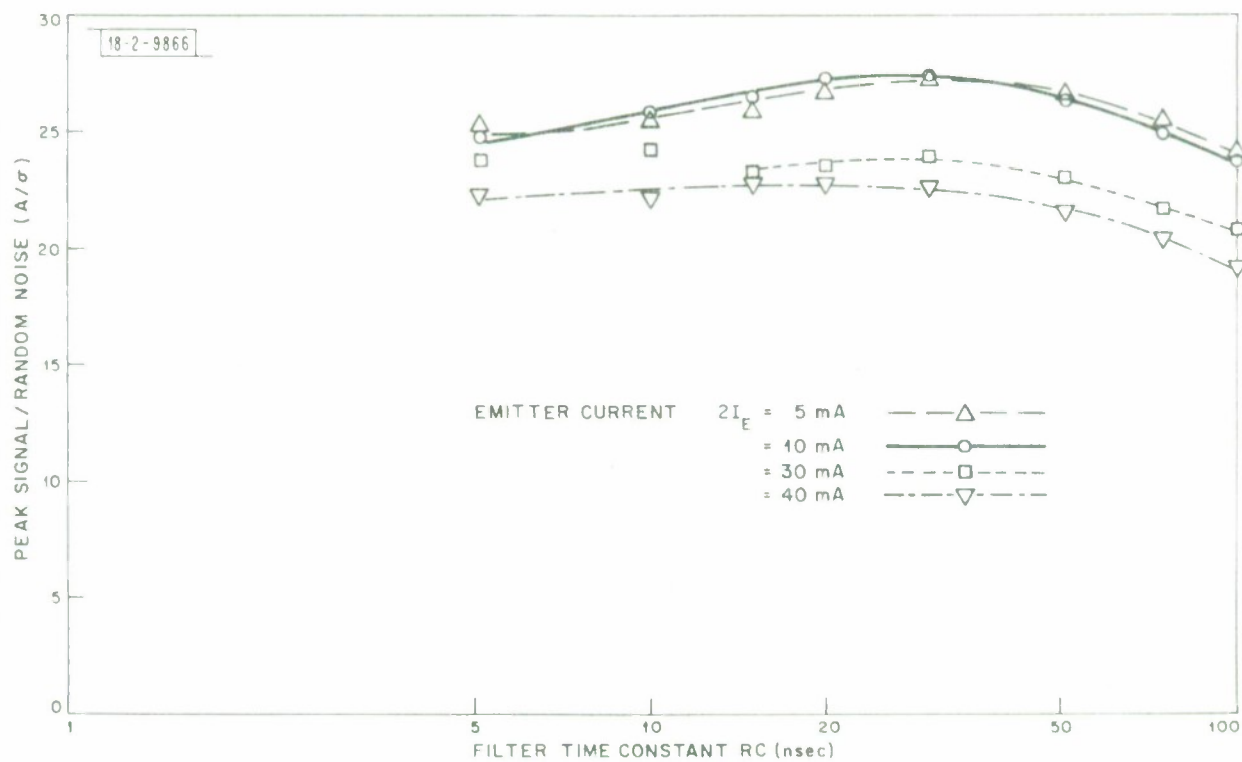


Fig. 17. Variation of signal-to-random-noise ratio with filter time constant. Measurements on test jig, with SN75303 in a "single-differential" configuration, LCM II digit lines, and "quarter millivolt" signal.

of the available signal, thus lowering effective signal/noise. Therefore, the threshold must be small with respect to signal amplitude.

Secondly, any strobe circuit will have some finite time in which it does its sampling: a "window." In LCM II this window should be narrow with respect to signal for two reasons: First, a wide window at the very least confuses the assumptions about the effect of random noise, which are based on infinitesimal sample time; and second, the film signal is invariably accompanied by transients of equal or greater amplitude only slightly separated in time, such as some types of word noise and stray coupling from the strobe pulse itself. A narrow window makes it possible to choose the best sample time.

One simple method of getting a low-threshold strobe with built-in storage is to connect the sense-amplifier output to a normally quiescent flip flop. If flip-flop power is turned on at strobe time, the eventual stored state will depend upon signal polarity.¹² A circuit of this type used in LCM I had a wide window, over 40 n sec at the 10% sensitivity points, because there was no provision to uncouple the flip flop from the sense amplifier after strobe time. However, much better performance can easily be obtained: the experimental circuit of Figure 18 had a threshold on the order of 5 mv and a window of 3 n sec.

If the sense-amplifier bandwidth remains as low as in the experimental system discussed in the following section, with output pulse widths over 100 n sec, commercially available integrated-circuit comparators with windows 20 n sec wide may also be satisfactory.

F. Experimental Sense System

A sense system used in experimental work on the LCM II prototype stack is shown in Figure 19. The basic configuration is that of Figure 12

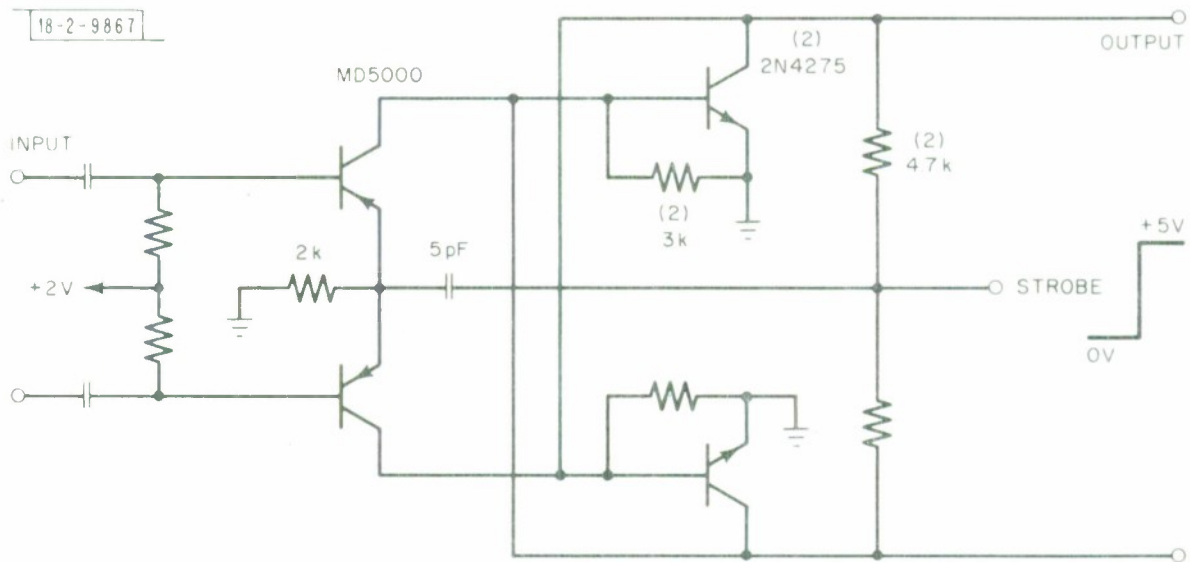


Fig. 18. Experimental flip-flop strobe.

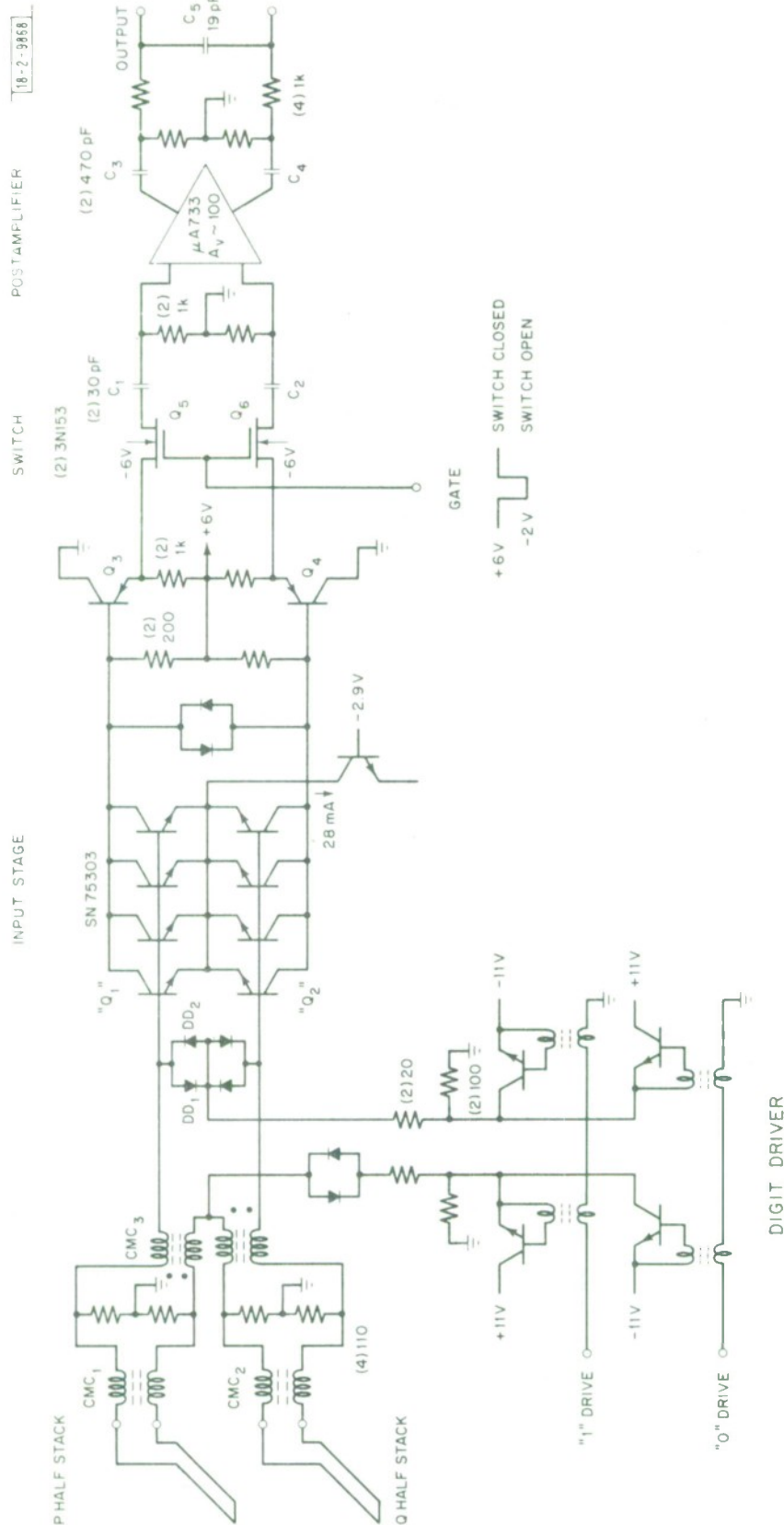


Fig. 19. Experimental sense system. CMC₁ and CMC₂ are wound as 20 bifilar turns on a Ferroxcube 213T050/3E2A core; CMC₃ as 20 quadrifilar turns on a 266T125/3E2A core.

but without a strobe. A "single-differential" input stage drives a MOSFET switch through a pair of emitter followers. The postamplifier is a commercial integrated circuit; frequency response is shaped by coupling capacitors and an output filter.

Amplifier response--With an input signal applied directly to " Q_1 " and " Q_2 " bases, large interstage coupling capacitors, and no output low-pass filter, the amplifier shows a voltage gain of about 6200 with a rise time (10 to 90%) of about 20 nsec. However, because of high first-stage emitter current, the input resistance is only about 180 ohms; input capacitance is a surprising 560 pf, mostly because of Miller effect on the high collector-base capacitance (~ 13 pf) with high voltage gain (~ 90). When the full "single-differential" input network is used and the source is placed in series with one of the two LCM II digit lines, the low-frequency voltage gain drops to about 5000, and the rise time increases to about 90 nsec, with a small overshoot.

With values for coupling and filter capacitors specified in Figure 19, the amplifier response is modified by high-pass time constants of approximately 50 and 550 nsec, and a low-pass time constant of about 33 nsec. Overall response is bandpass, with a peak gain of about 2100 at 3 MHz, and -3dB points at 1.5 and 5 MHz. Step response is shown in Figure 20.

Response of the sense system to an actual film signal on long digit lines is shown in Figure 21. The film signal, some 35 nsec in width, is smeared to about 150 nsec by digit-line and first-stage response. When short coupling time constants are used, the signal is differentiated, with the two lobes nearly equal in amplitude. Notice that high-frequency word noise is attenuated by the output low-pass filter.

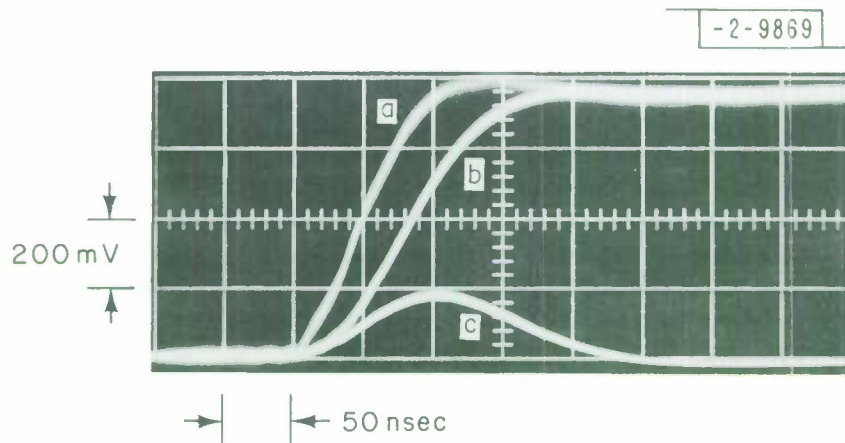


Fig. 20. Step response of experimental sense amplifier: (a) with no output low-pass filter and with large coupling capacitors; (b) Output low-pass filter inserted; (c) Output low-pass filter and small coupling capacitors inserted--circuit as shown in Figure 19. Amplifier was connected to 52 inch digit lines on aluminum substrate; $160 \mu\text{V}$ step applied in series with one line.

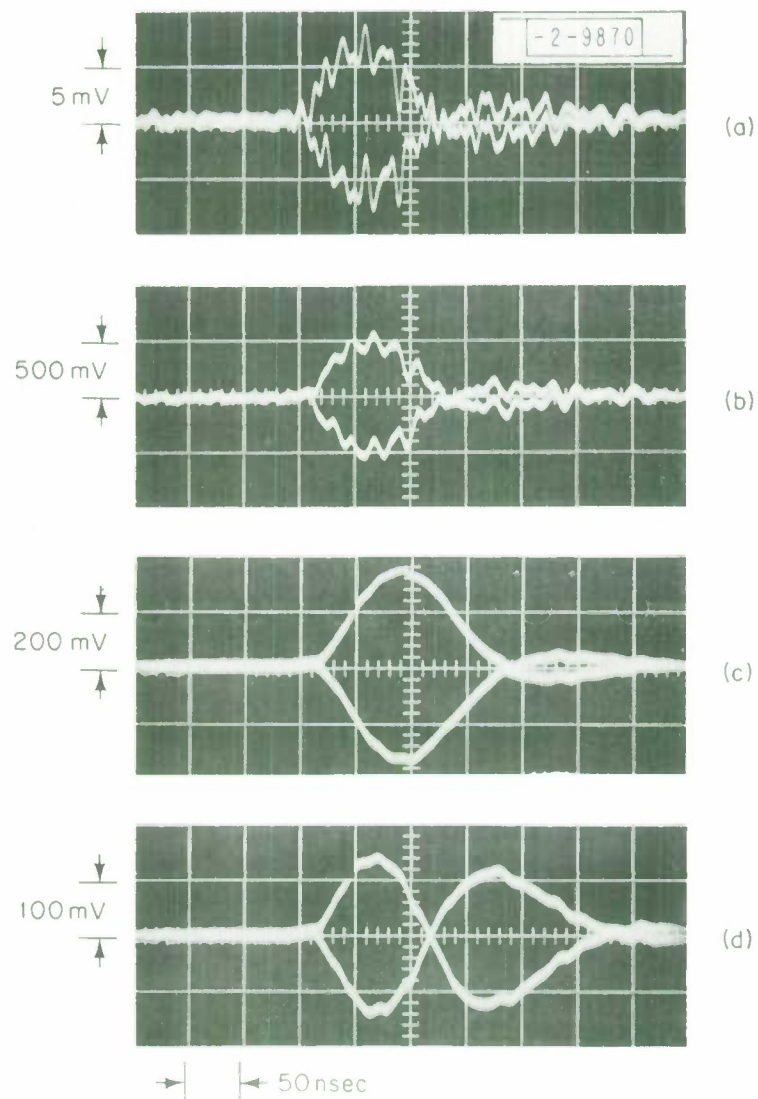


Fig. 21. Response of sense system of Figure 19 to "one" and "zero" film signals on long digit lines: (a) at first-stage collectors; (b) at μA 733 outputs; (c) and (d) at sense-amplifier output terminals. (b) and (c) were taken with very long coupling time constants, (d) with the short time constants of Figure 19.

Random noise--The amplifier of Figure 19 is in no way optimized for signal-to-random-noise ratio: The first-stage emitter current was an historical accident; the output low-pass-filter time constant was chosen to remove high-frequency ringing from word noise. Still, signal/noise is respectable: With amplifier low-frequency response extended by large capacitors for C_1 and C_2 , $A/\sigma = 26$ for a "quarter-millivolt" film signal (actually a simulated signal, a 35 n sec pulse of 5.6 mv-n sec integral). Because digit recovery is improved by short coupling time constants, C_1 and C_2 were reduced to the smallest values consistent with acceptable signal/random noise: 30 pf, for $A/\sigma = 21$.

Amplifier noise figure, referred to digit-line resistance, was about 6 dB.

Digit recovery--Waveforms pertinent to the digit-recovery performance of the sense system of Figure 19 are presented in Figure 22. First are shown drive and control waveforms: two closely spaced word pulses, the first to read, the second to write; "1" and "0" digit pulses, coincident with the trailing edge of the write word pulse; and the MOSFET gate pulse, which opens the series switch immediately before digit drive and leaves it open until the transient is well within the linear range of the amplifier. Figure 22d shows the resulting amplifier output: the digit transient decayed to negligibility some 0.8μ sec after the digit pulse. Figure 22e, taken with the word drive turned off to eliminate the signal, shows that part of the "digit transient" of Figure 22d is actually from the signal itself; charge from the signal stored on capacitors C_1 and C_2 cannot be removed when the MOSFET switch is open, and so produces a transient immediately after switch closure. The transient resulting from stray coupling of the MOSFET gate pulse is shown in Figure 22f;

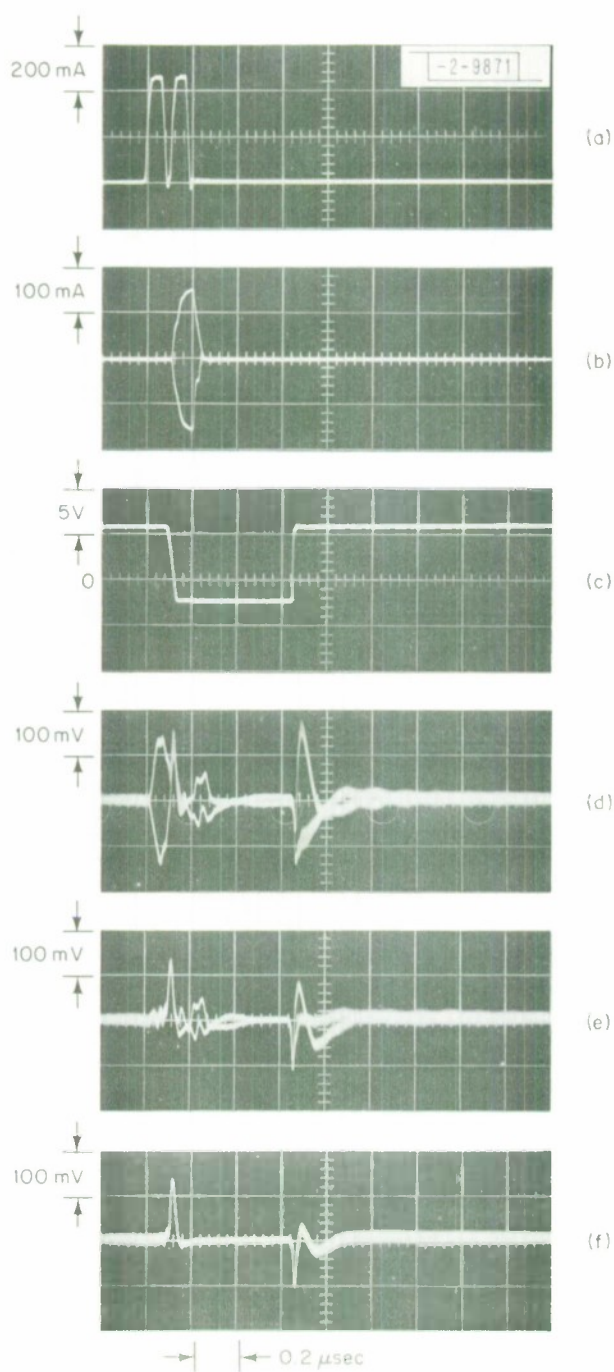


Fig. 22. Digit-recovery performance of test system: (a) word current; (b) digit current, (c) MOSFET gate voltage; (d) sense-amplifier output; (e) same, except word drive off to eliminate signal; (f) same, except digit drive off, leaving only gate transient.

because discrete, unmatched MOSFET's were used, this would have been much larger had not a small trimming capacitance been adjusted to minimize it.

The importance of the series gate is shown by Figure 23, which shows the sense-amplifier response to the digit transient if the switch is not opened. The gross extension of digit recovery is somewhat of an exaggeration, for the system was not designed to be operated without the gate.

The critical aspect of sense-amplifier digit recovery is not response to a single digit pulse, but rather response to a sequence of pulses in an unfavorable pattern in the execution of successive memory cycles. It is this response that fixes memory cycle time. The amplifier response in long bursts of memory cycles, with all "1's" and all "0's" in alternate bursts, is shown in Figure 24. The limiting recovery time happens to be that following the first digit pulse; it sets minimum cycle time at $0.9 \mu \text{ sec}$.

Two features of the digit driver of Figure 19 are essential to make possible the $0.9 \mu \text{ sec}$ cycle time. The first, and more important, is that the driver output is taken directly from the transistors, rather than through a transformer. The recovery of a drive transformer from a pulse inevitably is coupled into the sense-amplifier input and extends digit recovery time. The second feature is the symmetry about ground of the digit drive. It is tempting to use only half as many drive transistors, and let "1" drive be a positive pulse, "0" a negative one. This would have the additional advantage that the common point of DD_1 and DD_2 could be returned directly to ground, and the required common-mode compliance of the input stage would be reduced from the present plus or minus half the digit-line drop to plus or minus one diode drop. Unfortunately, such an arrangement results in a large common-mode voltage, half the digit-line drop, being applied to the common-mode chokes CMC_1 and CMC_2 . The tank circuit formed of choke series

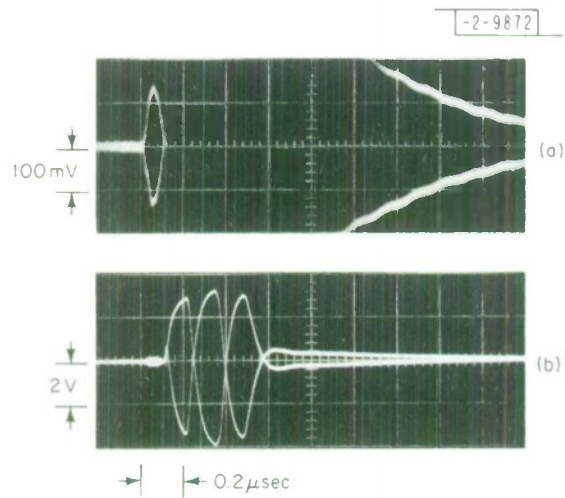


Fig. 23. Sense-amplifier digit recovery with gate disabled.

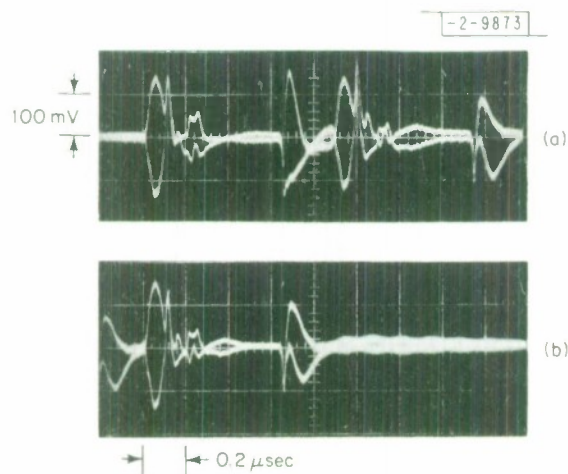


Fig. 24. Sense-amplifier digit-transient response for a burst of memory cycles. 0.9 μ sec cycle time. (a) First cycles of burst. (b) Last cycle of burst.

inductance and digit-line capacitance to ground then rings at a low (sub-MHz) frequency, and some of this common-mode ringing is converted back to a difference-mode signal at the sense-amplifier input, to appear as a low-frequency component of the digit transient.

Digit recovery is of course dependent upon balance of the input bridge, that is, upon matching of the diodes and digit lines. However, this dependence is not critical. The coupling diodes used in the system of Figure 19 happened to be matched monolithic arrays, but there was no perceptible change with discrete chips on a common header, or even with discretely packaged devices. For the digit-recovery performance of Figures 22 and 24, it was necessary that both the P and Q digit lines be faced by word pieces for matched transmission characteristics--an isolated dummy line for Q did extend recovery somewhat--but beyond that no particular care in matching was necessary.

The rather poor input-stage frequency response has some effect on digit recovery. If the SN75303 is replaced by a Signetics NE511B dual differential amplifier, with both sections in parallel, the effective input capacitance drops to 140 pf and response to an input step has a rise time of about 45 nsec. Digit recovery time of the sense amplifier drops about 0.1 μ sec, so 0.8 μ sec cycle times are possible. Unfortunately, the NE511B is not a practical input device because signal/random noise is only about 2/3 of that with the SN75303.

Still another conflict between noise requirements and digit recovery is illustrated by the low-pass output filter. While necessary from the standpoint of both word noise and random noise, it does slow digit recovery.

The system of Figure 19 was also tried with digit lines on aluminum substrates. Performance was substantially poorer: with well-matched digit lines (on the same substrate) the minimum cycle time went up to 1.1 μ sec;

with digit lines on different substrates it rose to $1.4 \mu\text{sec}$, reducible to $1.2 \mu\text{sec}$ with a doublet (rather than unipolar) digit pulse. Time was not available in which to establish the cause of the lengthened recovery.

Finally, the experimental system was also tried with 12-inch unkeep-ered (LCM I) digit lines. Digit recovery time was about $0.6 \mu\text{sec}$, making possible $0.7 \mu\text{sec}$ memory cycles. This is to be compared with the $1.2 \mu\text{sec}$ cycle times achieved with a transformer-coupled input in LCM I.

VII. Cross-Section-Stack Experiments

A. Stack Description

The performance potential of LCM II was evaluated on a cross-section stack that was a partially populated approximation to one half of a complete LCM II assembly. The test stack (Figures 25 and 26) had three 52×2.2 inch digit pieces face up over a heavy aluminum base plate. Crossing the digit pieces were 26 glass word pieces, each 10.76×1.6 inches, insulated by Kodak Thin Film Resist; a single sheet of aluminum foil above the word-piece array served as a ground plane. Most word pieces were 0.040 inch thick and backed by $1/4$ inch aluminum plates; some were 0.25 inch thick and unbacked. Digit and word pieces were held in close contact by pressure from an air bag beneath the digit pieces and a resilient material (expanded vinyl) between the word-piece backing plates and an upper aluminum structural member. The substrates were carefully cleaned and the stack was assembled in a clean room.

Two assemblies of the test stack were made. In the first, all three digit pieces were 0.25 inch thick glass substrates, and all word pieces were 0.040 inch thick glass. In the second, the two outer digit pieces were aluminum substrates, and a few of the word pieces were 0.25 inch thick.

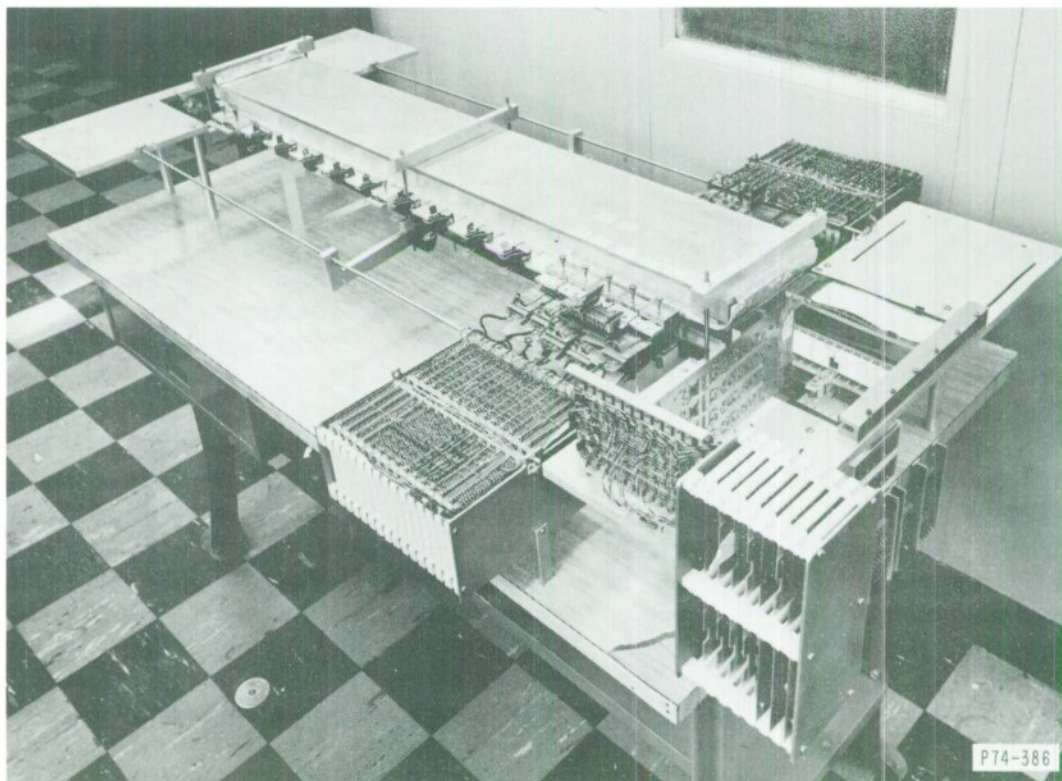


Fig. 25. Cross-section stack, shown with LCM I digit circuits. Word circuits are connected to word pieces at the open ends of the digit lines.

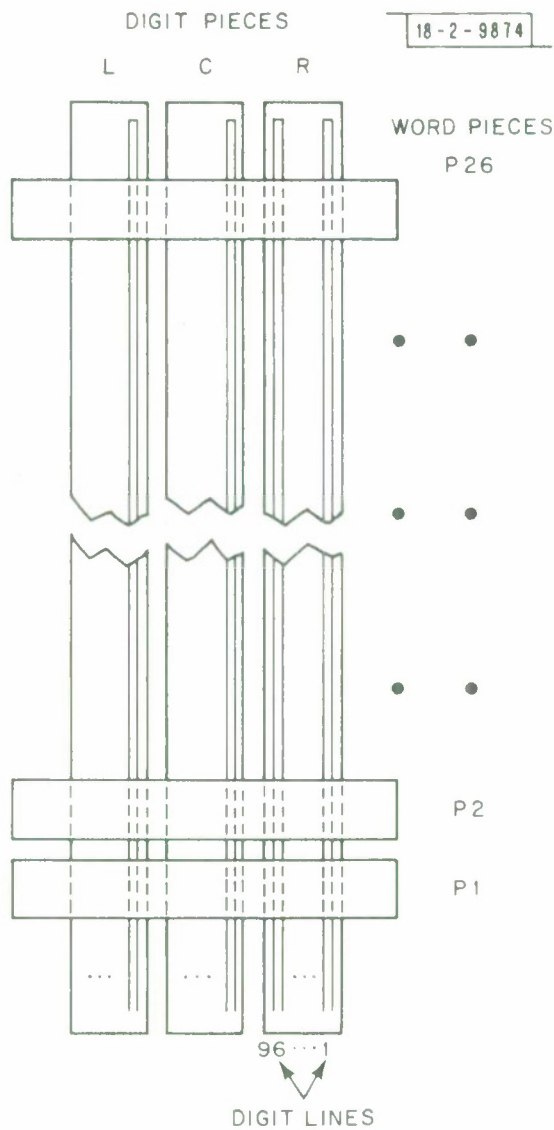


Fig. 26. Cross-section stack schematized.

Six word pieces, placed at the ends and center of the digit pieces, had word lines. Of these "active" word pieces, those on 0.040 inch substrates had 20 word groups, each of 18 1.2 mil word lines on 2 mil centers. The areas between these groups, amounting to half total surface area, were unscribed, unconnected copper strips. Active word pieces on 0.25 inch substrates were those used in LCM I; each of their 20 word groups consisted of 18 2 mil lines on 4 mil centers, with the entire area scribed.

Most of the remaining word pieces were "dummies": 0.040 inch pieces with copper coating scribed into 22 narrowly separated longitudinal strips to simulate word groups. Because of surface irregularities on these dummy groups, which caused word-to-digit shorts, 3 to 5 substrates had to be replaced with plain glass.

Each digit piece was scribed into 192 6 mil permalloy-keepered lines on 10 mil centers, connected as 96 hairpin-shaped digit lines. At some digit-piece edges an unscribed strip 0.1 to 0.15 inches wide was left; at others, the strip was removed.

Word groups on most word pieces in the test stack were connected to ground, either directly or through a resistor. Five word pieces, all adjacent, were connected to drive circuits of the LCM I type by means of spring-loaded connectors. Unselected groups on these substrates were held at +27 V bias potential; the selected group was brought to -0.8 v, a potential set by a group clamp diode mounted on the aluminum base plate under the digit pieces. A positive word pulse applied to the selected word-diode bus caused word current to flow down the selected line. The aluminum backing plates behind 0.040 inch word pieces were connected to the stack base plate by heavy straps, so that the return path for word current lay, at least in part, in the backing plate.

Connection to digit lines was by means of pressure-connected flexible extensions, all at the end of the stack adjacent to word piece P1. A fourth digit piece, without word pieces, located beneath the stack provided the necessary balance line for digit circuits. Only one digit channel was connected at any one time; the circuits were usually those of the sense system with single-differential input and differentiating interstage coupling shown in Figure 19.

Film signal amplitude varied widely over the stack because of the wide range in film characteristics on the word pieces used. Therefore, a simulated "quarter-millivolt" film signal, 35 nsec wide with 5.6 mv-nsec integral, was used as an amplitude reference. With a signal injected in series with one digit line, the sense amplifier of Figure 19 had a 120 mv peak output.

B. Group-Select Noise

1. Common-Mode-Voltage Variations

With thin glass word pieces, common-mode digit-line voltage resulting from group selection was found to vary widely (up to 5 to 1) as a function of the location of selected group and observed digit. Variation was particularly pronounced near the ends of the word pieces. There was strong evidence that this gross variation was a consequence of warping of the word pieces.

Although the common-mode voltage variation was large over extended distances, it was also gradual, never so abrupt that nonuniformity of charging currents could be expected to produce group-select noise comparable to that produced at digit-piece edges. However, in one limited region of steep change in common-mode voltage, up to 2 mv between lines, there was a correlation with group-select noise; the noise was probably a result of a difference in voltage coupled into the two sides of the line being sensed, rather than of any difference in currents on adjacent lines.

The regions of extremely low common-mode voltage must correspond to word-to-digit spacings of more than 1 mil; such spacing will degrade magnetic performance of the bits.

2. Group-Select Ringing

Glass digit pieces--In the stack with glass digit substrates, there was found to be a substantial amount of high-frequency (20 to 40 MHz) ringing for several tenths of a microsecond in the group-select noise, a consequence of multiple reflections of the common-mode transient on the digit-line array. Two remedies for this were applied. The first was to damp the ringing by making the common-mode transmission line lossy and dispersive. The shunt element of this transmission line is the capacitance from word groups to the digit-line array. If a resistor is inserted between each word group and a-c ground, the shunt element becomes lossy, the line dispersive, and ringing is damped. In the experimental setup this was approximated by inserting a 10 ohm resistor between ground and the parallel connection of all word groups on each unselected word piece, thus simulating approximately 200 ohms between each group and a-c ground. This reduced, but did not completely eliminate, high-frequency group-select-noise ringing.

The second remedy was the addition of common-mode terminations from digit lines to ground. A 200 ohm resistor was connected from the closed end of each digit hairpin to ground. (The effective parallel resistance of all resistors on a digit piece, ~ 2 ohms, was approximately the common-mode characteristic impedance of the line array.) This digit-line termination was effective in reducing ringing. It did, however, have the effect of increasing the amplitude of the first pulse of group-select noise, and changing it from a unipolar pulse about 0.1μ sec wide to a doublet about twice as wide. When a sense amplifier without a differentiator was used, there was also produced a substantial tail on the pulse, of several tenths microsecond duration, particularly on the first dozen or so digit lines from a stack edge.

Aluminum digit pieces.--A different kind of ringing was encountered with aluminum digit pieces. With the substrates connected to ground there was a strong 10 MHz component in group-select noise. This was found to be a consequence of common-mode ringing of the ground-strap inductance (small though it was) with the large substrate-to-line capacitance. The ringing was completely eliminated by isolating the digit substrates from ground. No other damping measures, such as group loss resistance or digit-line termination, were necessary.

3. Effect of Sense System on Noise

At group-select time the sense system is presented with a digit-line common-mode step on the order of 50 mv, more than two orders of magnitude larger than signal. In experiments with sense amplifiers with long coupling time constants it was found that the output group-select noise resulting from imperfect common-mode rejection by the sense-amplifier input circuits was typically on the order of 10% of signal amplitude.

Fortunately, the rather short coupling time constants introduced into the sense amplifier of Figure 19 for digit-recovery reasons also attenuate the transient resulting from poor common-mode rejection down to negligibility, and make the long tail observed with terminated digit lines much less important.

The limited high-frequency response is also helpful in reducing the high-frequency ringing found in group-select noise.

4. Systematic Measurement of Group-Select Noise

Test procedures.--Group select noise was measured over extensive areas on the stacks assembled with both glass and aluminum digit pieces. The one-channel sense system was moved from line to line, usually over all lines on the two outer digit pieces. For each digit line, group selection was cycled through the available group addresses while a threshold detector

checked for group-select noise above 30 mv (1/4 typical signal amplitude) in a 60-nsec window centered a specified delay time T_d after the start of group selection. Word drive was suppressed.

With glass digit substrates the selected groups were on the first three word pieces (P1 through P3) from the open ends of the digit lines, and the first two (P26 and P25) from the closed ends; with aluminum digit pieces only the first two from the open end were used. Digit lines on only one of the two outer digit pieces were used for closed-end, glass-substrate measurements.

With glass digit pieces, series resistors were inserted between dummy word pieces and ground to damp ringing. Measurements were taken both with common-mode-terminated and unterminated digit lines.

Access delay.--The delay T_d from group selection to the center of the detection window can be called "access delay", since, except, for logic delays, it corresponds to memory access time. T_d was adjusted for each experimental run to be just large enough to avoid an inconveniently high number of locations above the noise threshold. With the differentiating sense amplifier of Figure 19 in these tests, there was little difference in access delay between a glass-substrate system with terminated and unterminated digit lines: $T_d = 400$ and 380 nsec, respectively. However, aluminum digit pieces could be operated with a substantially reduced delay: $T_d = 310$ nsec.

Edge Effects.--Typical group-select noise waveforms in Figures 27 through 29 show the following: edge-effect noise is much smaller on aluminum digit pieces than on glass; on glass digit pieces it is smaller at the closed end of the digit line than at the open; and finally, it is smaller when the digit lines are unterminated than when they are terminated. Extensive measurements confirm these findings: it is possible to use the second digit line from an edge of an aluminum digit piece, while even at almost 100 nsec greater access delay the first useable digit line on an inner edge of a glass digit piece is the

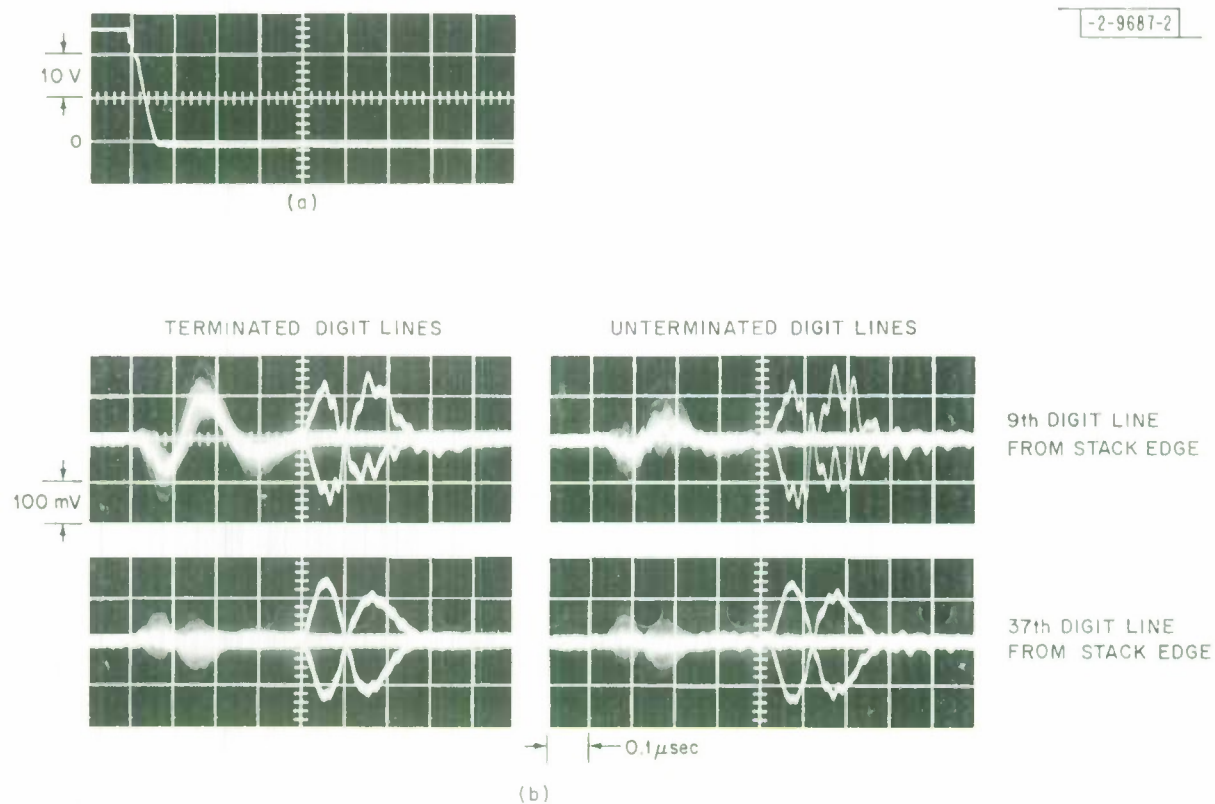


Fig. 27. Group selection with glass digit pieces. (a) Voltage on a typical selected word group. (b) Sense-amplifier outputs: group-select noise as all groups on 3 word pieces at open ends of digit lines are cycled through, with word drive suppressed. Superimposed is a signal from one word line only, a bit with nominal output, $T_d \approx 450$ nsec.

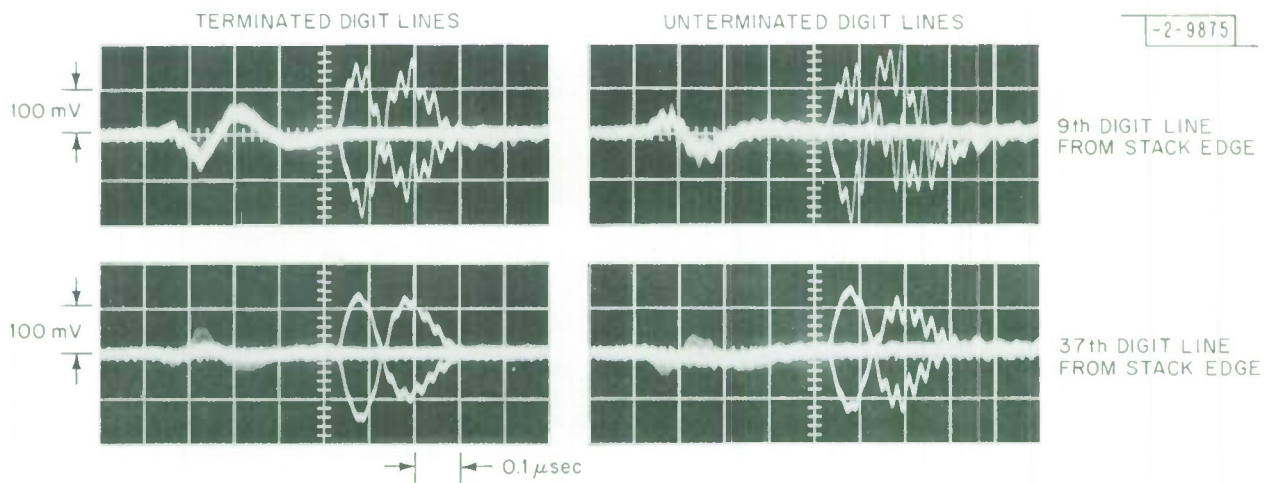


Fig. 28. Group selection with glass digit pieces. Sense-amplifier outputs as in 27b, except that the groups are on the last two word pieces at the closed ends of the digit lines.

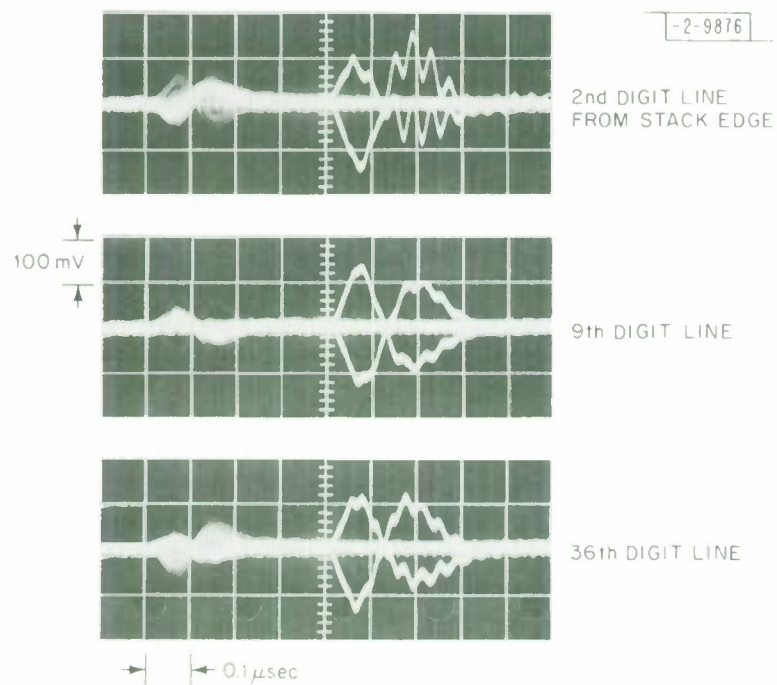


Fig. 29. Group selection with aluminum digit pieces. Sense-amplifier outputs as in 27b, for groups on the first two word pieces at the open ends of the digit lines.

3rd or 4th, and on the outer or stack edge is the 5th or 9th, for unterminated and terminated lines, respectively.

An unscribed strip at the edge of the digit piece does reduce the number of lines that are unusable. However, it tends to overcompensate for edge effects, and is less effective than a strip of equal width scribed into dummy digit lines.

Interior noise.--Glass digit substrates showed significant group-select noise at about 0.3% of interior locations at the open ends of the digit lines, and none at the closed ends (Table 5). In comparison, the aluminum digit pieces showed significant noise at only 0.1% of locations. The superiority of the aluminum substrates is even more striking in view of the smaller access delay used and also the fact that half the word groups in this assembly were 0.072 inches wide, while with the glass digit-pieces assembly all groups were 0.036 inches wide.

The fractional number of noisy locations may seem high for memory use. However, there are several ameliorating factors. First, noise amplitudes run low: noise on only 0.02 to 0.06% of all open-end locations is over $1/3$ standard signal amplitude (Table 6). Second, in the case of glass digit substrates most of the noisy locations are concentrated on the P2 word piece; they may well be a consequence of a severe warp of that particular word piece. And, finally, the noise can be reduced to negligibility at almost all the locations by simply increasing access delay by 50 nsec or so.

5. Conclusions

For best group-select-noise performance, the sense system must have not only a good common-mode rejection capability, but also a carefully limited frequency response: coupling time constants must be short, at least one on the order of 40 nsec, and high-frequency response must provide substantial attenuation above 10 MHz.

TABLE 5

Group-Select Noise at Interior Locations. Number of Group-Digit Intersections with Noise ≥ 30 mv. Note: The Total Number of Measured Intersections in Each of the Categories is ~ 3000 .

positions tested		glass digit pieces		aluminum digit pieces
		terminated lines	unterminated lines	
Groups at open end	word piece P1	3	1	6
	P2	25	30	0
	P3	2	2	—
Groups at closed end	P25 & P26	0	0	—

TABLE 6

Group-Select Noise, Distribution in Amplitude. Number of Group-Digit Intersections in Stack Interior with Noise in Specified Amplitude Ranges. Note: The Total Number of Measured Intersections at the Open End of Glass Digit Pieces is $\sim 10,000$; at the Closed End of Glass Digit Pieces $\sim 3,000$; and at the Open of Aluminum Digit Pieces $\sim 7,000$.

location	noise range	glass digit pieces		aluminum digit pieces
		terminated lines	unterminated lines	
Groups at open end	$V_n \cong 60 \text{ mv}$	0	1	0
	$60 > V_n \cong 50$	0	0	1
	$50 > V_n \cong 40$	2	6	2
	$40 > V_n \cong 30$	28	26	3
Groups at closed end	$V_n \cong 30$	0	0	—

The optimum configuration for low group-select noise would involve metal digit substrates and word pieces of controlled flatness. There should be no unscribed strips at the edges of the digit pieces, but rather dummy lines. Operation to within one line of the edge of the digit piece is possible. Access delay must be a little over 300 nsec; allowing some tens of nanoseconds for decoding and output logic operations, total access time will be less than 400 nsec.

If glass digit substrates are used, the word pieces should still have controlled flatness, and the digit pieces no unscribed strips. For minimum edge effects the digit lines should be unterminated; one can then expect to operate within about 5 lines of a stack edge, 3 of an inner edge of a digit piece. Word groups must be resistively terminated to reduce ringing. Access delay will have to be a little over 400 nsec; total access time less than 500 nsec.

C. Word Noise

1. Test Procedures

Word noise was measured in much the same systematic manner as group-select noise. The principal difference was that the 30 mv threshold detector had its 60 nsec window centered on the first lobe of the signal waveform; the signal itself was then removed by magnetically clamping the film, leaving only word noise.

Measurements were made on only one of the outside digit pieces. With glass digit pieces, the addressed words were all those on word piece P2 plus half those on pieces P1 and P3 at the "open end" of the stack, and all those on P25 plus a few on P26 at the "closed end." With aluminum digit pieces the addressed words were all those on word pieces P1 and P2.

2. Test Results

Edge effects.--Word-noise edge effects are minimal with aluminum digit pieces: it is possible to operate within one line of an edge,

provided there is no unscribed strip, which actually makes noise worse by overcompensation. Data on glass digit pieces were confused by the presence of unscribed strips, but it appears that operation to within a half-dozen to dozen lines of the digit-piece edges is possible, the lower figure applying to both edges with unterminated lines. Surprisingly, the edge effect was slightly more pronounced at the closed ends of the digit lines than at the open; it is believed that this is a spurious result caused by insufficient attention to word-current ground-return paths at the closed end.

Interior noise.--Data on noise on "interior" digit lines, i.e., lines excluding the edge ones, show what seems to be a rather bleak situation (Table 7): some 5 to 10% of all bits near the open ends of the digit lines have noise greater than 30 mv. However, things are actually not that bad. First of all, the noisy locations are concentrated on the first word piece, P1, which is vulnerable to noise inductively coupled from word-current ground-return paths; noisy bits fall to about 1% on P2 with glass digit pieces, 0.02% with aluminum ones. Furthermore, at least with glass digit pieces, the distribution in amplitude of noisy bits falls rapidly: only 25% of the noisy locations exceed 40 mv; 2%, 50 mv; and none, 60 mv (Table 8).

The rather large number of noisy locations on closed-end word pieces is also at least in part illusory. Those found with terminated digit lines are clustered along the edge—discarding three more edge lines will eliminate them all—and might more properly be called an edge effect. Those found with unterminated lines are almost exclusively in a "bad" region, involving two adjacent word groups and about a dozen essentially contiguous digit lines. One might suspect something like a severe warp of the 0.040 in. word piece in this region.

TABLE 7

Word Noise at Interior Locations. Number of Bits with Noise ≥ 30 mv. The Total Number of Measured Bits on Each Complete Word Piece is about 25,000.

positions tested		glass digit pieces		aluminum digit pieces
		terminated lines	unterminated lines	
Word lines at open end	word piece P1	1300 [*]	900 [*]	1900
	P2	240	270	5
	P3	6 [*]	0 [*]	—
Word lines at closed end	P25 & P26	380 ^{**}	480	—

* Note: Only half P1 and P3 words were connected.

** Note: All noisy bits at an edge—number reduces to zero if 3 more lines are not used.

TABLE 8

Word Noise, Distribution in Amplitude. Number of Bits in Stack Interior with Noise in Specified Ranges. Measured Bits at the Open End Total about 5×10^4 ; at the Closed End, about 2.5×10^4 .

location	noise range	glass digit pieces		aluminum digit pieces
		terminated lines	unterminated lines	
Word lines at open end	$V_n \geq 60$ mv	0*	0*	170
	60> $V_n \geq 50$	30	30	10
	50> $V_n \geq 40$	370	190	250
Word lines at closed end	50> $V_n \geq 40$	240	110	—

* Note: Incidence undoubtedly reduced by fact only half of P1 lines are used.

The P1 word piece with aluminum digit pieces is very noisy: there are many high-amplitude noisy bits. The problem evidently is not in the digit piece, for the P2 word piece is exceptionally "quiet," but rather in the fact that P1 was made of thick glass. The most probable way for this to have increased word noise was by the removal of the word-current ground-return path found in the 0.25 in. aluminum backing plate behind the thin-glass word pieces.

Noise waveforms.--Some typical waveforms of signal and word noise are shown in Figures 30 and 31. The signal in Figure 30a is of nominal LCM II amplitude; in the rest of Figure 30 it is of low amplitude, a consequence of poor magnetic film on the experimental word piece used, so the effect of word noise appears exaggerated. The defect producing the noise in Figure 31d evidently also affected the local magnetic characteristics.

Extremely noisy bits were almost always isolated. For example, the bit in Figure 31b had no neighbors above the detectable noise threshold; that in Figure 31d had one with the same noise amplitude and two more just at the 30 mv threshold.

Notice that the word noise on the glass digit pieces shows significant high-frequency (~ 40 MHz) ringing. In view of the limited high-frequency response of the sense amplifier this noise is surprising; it emphasizes the need for limited bandwidth.

3. Conclusions

The optimum configuration for low word noise would be aluminum digit substrates and thin, flat glass word pieces backed by a ground plane. There should be no unscribed strips at the edges of the digit pieces; operation to within a line or two of the edge is possible.

If glass substrates are used for digit pieces, again the word pieces should be thin and backed by a ground plane. There should be no

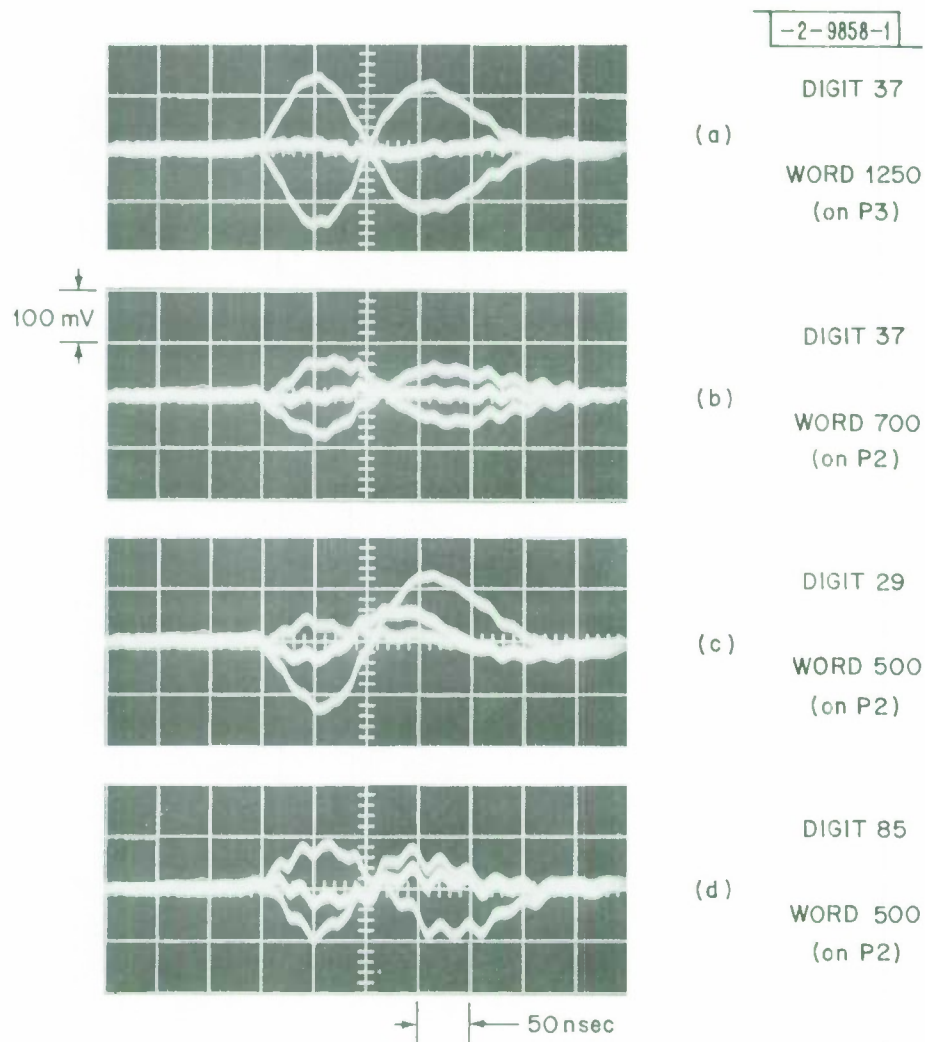


Fig. 30. Word noise at the open ends of terminated digit lines on glass substrates. Oscillograms taken with "1" and "0" signals and with films magnetically clamped. (a) - (b) Typical "quiet" bits. (c) - (d) Typical "noisy" bits.

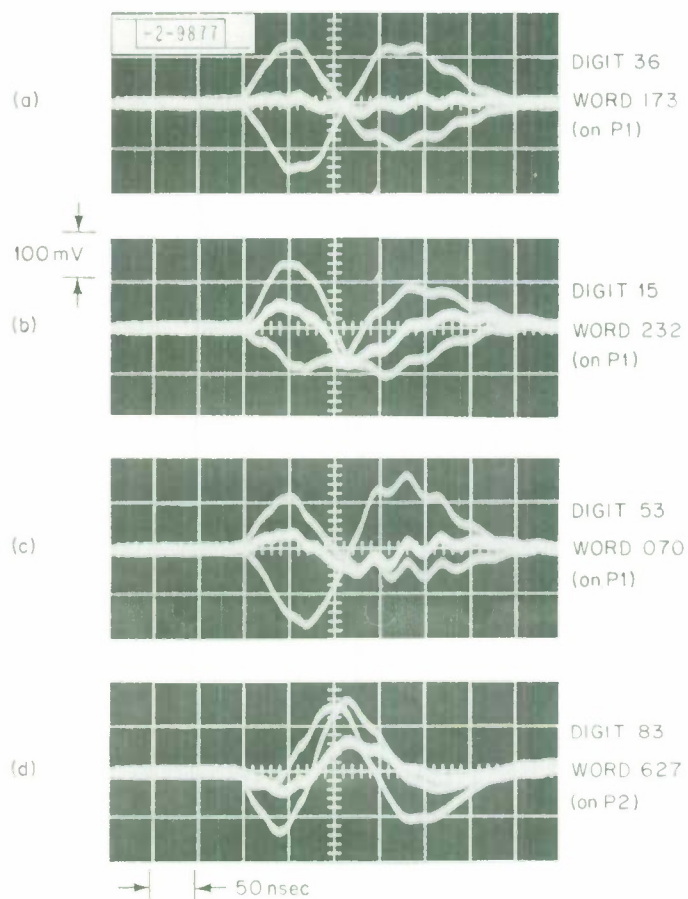


Fig. 31. Word noise with aluminum digit pieces, at the open ends of the digit lines. (a) Typical "quiet" bit. (b)-(d) Typical "noisy" bits.

unscribed strips at the digit-piece edges, but dummy lines if possible. Edge effects will render useless about half a dozen to a dozen lines at each digit-piece edge. There is a slight advantage to common-mode-terminated digit lines.

In the tests, a large number of bits on word pieces at the ends of the stack had unacceptably high noise; this may be greatly reduced by improvement of word-current ground return paths.

Sense-amplifier frequency response must be limited to provide substantial attenuation of the high-frequency components of word noise above 10 MHz.

D. Memory System

From the standpoint of both word and group-select noises, a memory of the LCM II type should use metal-substrate digit pieces. However, keeper films on metal substrates had an unacceptable sensitivity to digit disturb; even if that is overcome, metal substrates have also been shown to produce a digit-recovery time significantly longer than glass ones. Therefore, barring some substantial improvements, an LCM II memory would use glass-substrate digit pieces and word pieces of thin glass with carefully controlled flatness.

Word groups must be resistively terminated to reduce high-frequency ringing in both group-select and word noise. Requirements on common-mode termination of digit lines are contradictory: word noise at both the stack edge and interior is slightly lower with terminated lines, while group-select noise at digit piece edges is higher. Because word noise is the more critical parameter, the better choice may be terminated digit lines. In that case, one can expect to lose about six digit lines on an inner edge by word noise, and ten or so on a stack edge by group-select noise.

Because a signal-to-random-noise ratio of better than 20:1 can be obtained, it should be possible to tolerate word noise of up to about 40% of nominal signal amplitude. With this criterion, it may not be possible to use the word pieces at the extreme ends of the stack, because of too many noisy locations (barring improvement from ground-path relocation). However, at the next set of word pieces only about 0.02% of the bits should be lost, and substantially less than this farther into the interior; such losses should be easily absorbed by spare word lines.

A representative system performance is shown in the oscillograms of Figure 32, in bursts of $0.9\mu\text{sec}$ memory cycles at an access delay of $0.36\mu\text{sec}$.

VIII. Word Selection Matrix

LCM I diode-array connectors were used in the experiments described in Section VII. These removable connectors which used spring-loaded pins to connect a diode to each word line pad on the substrate were well suited to experimental work but their component cost and construction complexity precluded their use in a low-cost memory system.

A hybrid diode-chip array was being developed for LCM II. A diode chip was bonded with a gold-filled conductive epoxy to each word line pad on the substrate. Diodes were bussed together using the Kapton-conductor sheet shown in the cutaway drawing of Figure 33. A hole was etched in the Kapton at each chip position and the copper etched into bus lines with a tab at each chip. The tabs were conductive-epoxy bonded to the diode chips and the Kapton sheet bonded to the substrate. The tabs provided compliance to accommodate variations in diode chip height. Word line replacement would be done by cutting of the bus tab on the word line to be replaced and wire-bonding the replacement-line tab to the appropriate bus.

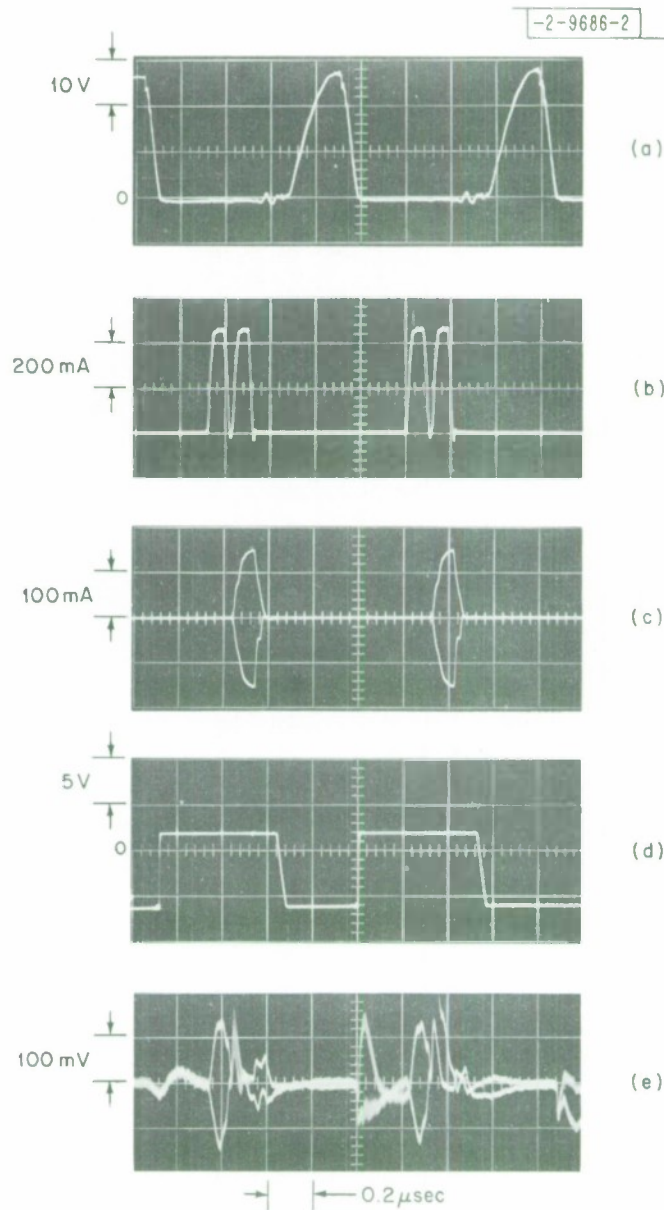


Fig. 32. Performance of test stack with terminated digit lines on glass substrates. (a) group voltage; (b) word current; (c) digit current; (d) MOSFET gate drive; (e) sense amplifier output.

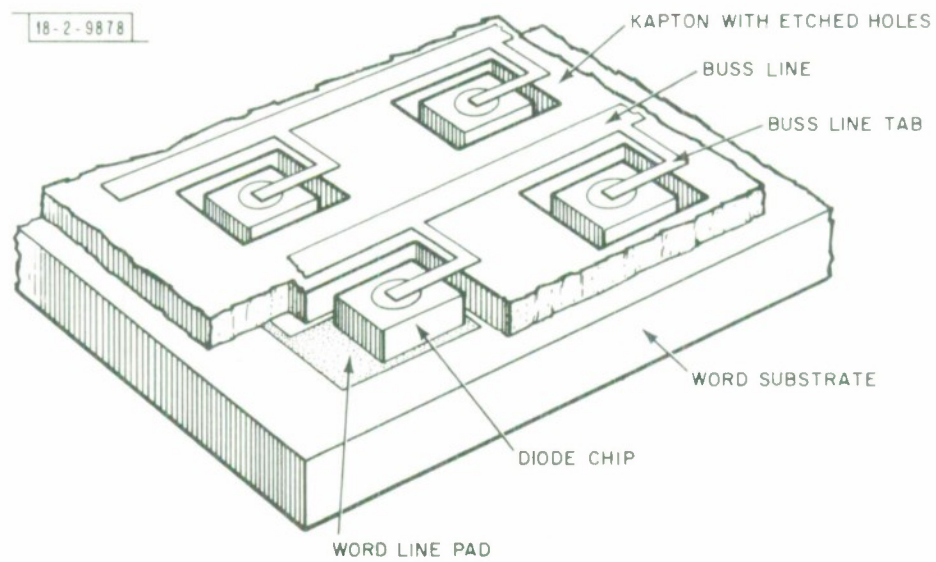


Fig. 33. Cutaway view of hybrid diode-chip assembly.

Substrate-to-substrate bus connections would be made using the spring-loaded connectors.

IX. Further Development

Throughout this report suggestions have been made for necessary further development. In summary they are:

1. Electroless plating—Improved control of H_c of the electroless closure-plating on the word substrate is required.
2. Yield verification—Complete testing of closure word substrates is required to establish yield data and determine optimum provision of spare lines.
3. Keeper on aluminum substrates—The advantages of aluminum digit substrates were well established for group and word noise reduction and the ability to use thicker word substrates. The keeper disturb effect would have to be solved, however, before they could be used in a memory.
4. Digit keeper—With either glass or aluminum digit substrates the best edge keeper configuration must be selected and complete testing done of finished substrates.
5. Sense system—Two portions of the sense system are open to significant improvement by integration: The first is the preamplifier, whose ultimate form is probably a monolithic "double-differential" stage, or, if that is not feasible, at least a performance-optimized "single-differential" one; enhanced signal/random noise and shortened digit recovery should be possible. The second is the series switch, where it is imperative that the MOSFET's be well matched to minimize the gate transient.

6. Stack fabrication—A stack must be designed with considerations of best ground paths and drive current distribution, uniform substrate spacing, and ease of assembly.

7. Word access circuitry—The word diode matrix is a critical component from cost and performance considerations and requires further development. The most economical partitioning of the access circuitry is undetermined.

X. A Feasible 10^7 Bit Memory

A specification of a finished LCM II based on the experience with LCM I, the experiments described in this report, assuming a somewhat wider word substrate with 1024 lines, and the use of fast digit-buffer circuitry would read as follows:

LCM II has a capacity of one million bytes in a single module. It is fabricated from a matrix of 32,768 word lines and 320 digit lines. The memory is formed from two half-stacks, each containing 16 word substrates and 4 digit substrates. A word substrate has 1152 (1024 + spares) lines 1.2 mil wide on 2 mil centers; each digit substrate has 80 pairs of 6 mil lines on 10 mil centers. The physical dimensions of the stack are approximately 44 x 12 x 6 inches.

Word access is accomplished through a diode matrix with diode chips bonded directly to the word substrate. For electrical and packaging reasons the matrix is subdivided into four 64 x 128 matrices. A complete digit channel (sense amplifier, buffer, and digit driver) is provided for each digit line.

The memory operates with 1.0 μ sec read-rewrite cycle time. The 320 megabits/sec data rate makes the memory a well-matched backup store for a high-speed semiconductor main memory, while the access time of 0.5 μ sec matches that of many smaller main memories.

The data buffer is organized as 32 bytes of eight or nine data bits each plus parity bits as required. For a data bus 4 bytes wide the buffer would be arranged as eight words, and words could be transferred to or from the memory at 75-nsec intervals during the appropriate time in the memory cycle.

Very high speed bursts of read-or-write-only cycles of 2048 bytes are possible at a rate of 16 bytes each 100 nsec.

XI. Conclusions

The feasibility of building a magnetic film memory with a capacity of 10 million bits and a high data rate has been demonstrated.

The principal accomplishments have been development of techniques for batch fabrication of word lines with closed magnetic structure, construction of keepered digit lines on large-area substrates, and the design of a simplified sense amplifier with adequate signal-to-noise ratio and good digit-transient recovery with long digit lines.

Unresolved questions were H_C variation of the electroless word-line magnetic-closure film and yield of the fabrication processes.

These fabrication processes should lead to low cost given further development and reasonably large production.

REFERENCES

1. J. I. Raffel, "Future Developments in Large Magnetic Film Memories," J. Appl. Physics, Vol. 35, no. 3, part 2, pp. 748-753, March 1964.
2. J. I. Raffel, et al, "A Progress Report on Large Capacity Magnetic Film Memory Development," AFIPS Conf. Proc. Vol. 32, pp. 259-265, 1968.
3. J. I. Raffel, et al, "A Million Bit Memory Module Using High-Density Batch-Fabricated Magnetic Film Arrays," (Summary only), IEEE Trans. on Magnetics, MAG-4, pp. 318-319, September 1968.
4. A. V. Pohm, et al, "An Efficient Small Thin Film Memory," Paper 11.4, Intermag Conference, 1965.
5. C. G. Ravi and G. G. Koerber, "Effects of a Keeper on Thin Film Magnetic Bits," I.B.M.J. Res. Develop. 10, pp. 130-134, 1966.
6. K. U. Stein and E. Feldtkeller, "Switching Properties on Multilayer Nickel-Iron Films with Ferrite Keeper," IEEE Trans. on Magnetics, MAG-2, pp. 184-188, 1966.
7. T. S. Crowther, "Specifications and Yields of Composite Magnetic Films for a High-Density Memory," IEEE Trans. on Magnetics, MAG-4, pp. 529-532, 1968.
8. M. Prutton, Nature 193, pp. 565-566, 1962.
9. H. Blatt, "Random Noise Considerations in the Design of Magnetic Film Sense Amplifiers," Group Report 1964-6, MIT Lincoln Laboratory, (17 August 1964), DDC AD-605 323.
10. S. O. Rice, Bell Syst. Tech. J. 49, p. 2221, 1970.
11. J. W. Craig, Jr., IRE Trans. Inf. Theory IT-6, p. 409, 1960.
12. W. C. Slemmer, IEEE J. Solid State Circuits SC-5, p. 215, 1970.

Appendix A. Word Line Fabrication

Each 0.040" x 1.6" x 10.7" glass word substrate has 20 interleaved groups of 36 lines 1.2 mils wide on 2 mil centers, with the lines terminating in pads on one end and shorting bars at the other (Figure A.1).

The stringent requirements for perfectly straight, nick-free word line edges preclude use of standard photoetching procedures mainly because of dust-caused imperfections. The technique used to generate excellent line edge definition on the 2 mil line 2 mil space geometry for LCM I was to diamond scribe slots in a photoresist coating and etch the metal layers. This approach does not work well when the space width is 1 mil or less because poor circulation of the etchant in the narrow slots leads to excessive, uneven undercut in the thick copper layer. In the new scribing procedure five thousand angstrom thick photoresist was applied by dip coating the substrate and the ends were exposed through a mask to produce the pad-shorting bar pattern. After selectively etching off the copper in the pad areas, the substrate was positioned in an automatic scribing machine, Figure A.2, with the pad pattern aligned with the diamond stylus. The stylus has a 0.7 mil wide cutting edge with a 45° included angle between sides and was operated with a negative rake angle of 7° at a cutting speed of 100"/minute in a commercial cutting fluid. In order to prevent cutting through the thin permalloy and into the glass under relatively high tool loadings, the cutting tip of the stylus was not "dead sharp." The bottom face that sits on the metal surface has a 0.3 mil wide flat which permits a load of 10 - 15 grams. Two passes per line were required to remove nearly all the copper down to the permalloy. Scribing time was 4 hours per substrate.

Following a degreasing step, the substrate was "flash etched" in a selective etchant for 1-2 seconds to remove any copper remaining at the bottom of the slot. Then selective permalloy and chrome etchants were used to remove

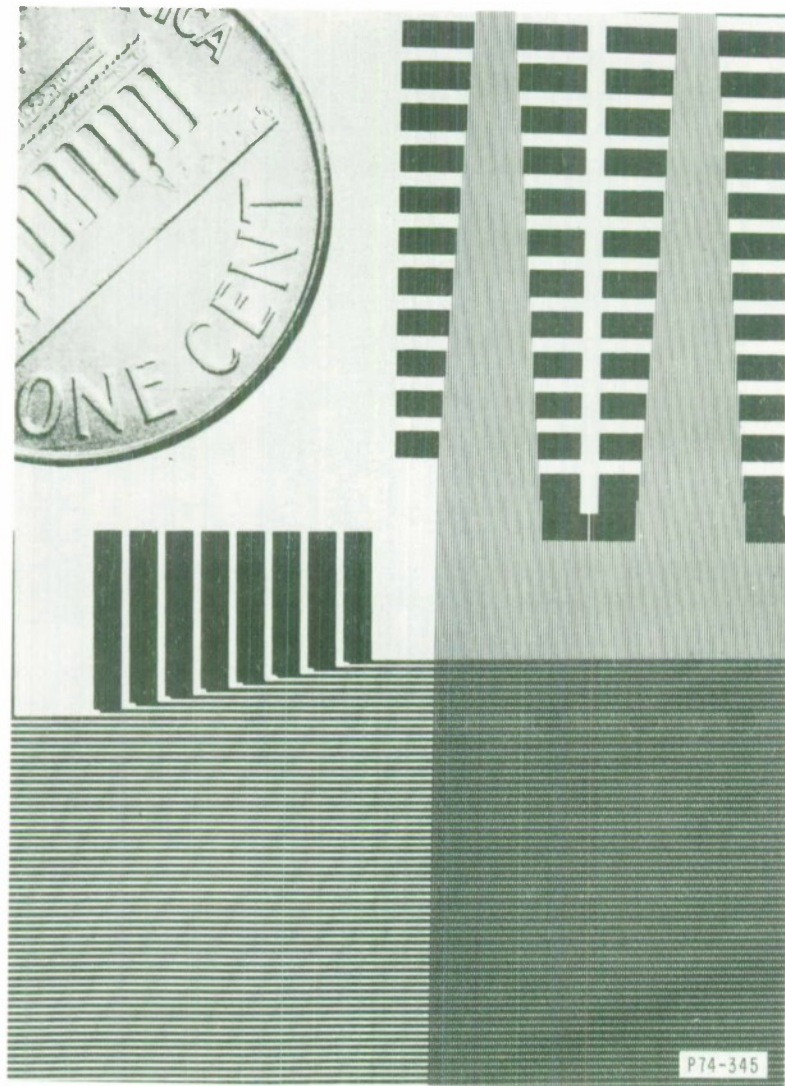


Fig. A-1. Word and digit lines and pads. At upper right are word pads and shorting bars (LCM I); at lower left are digit line pads.

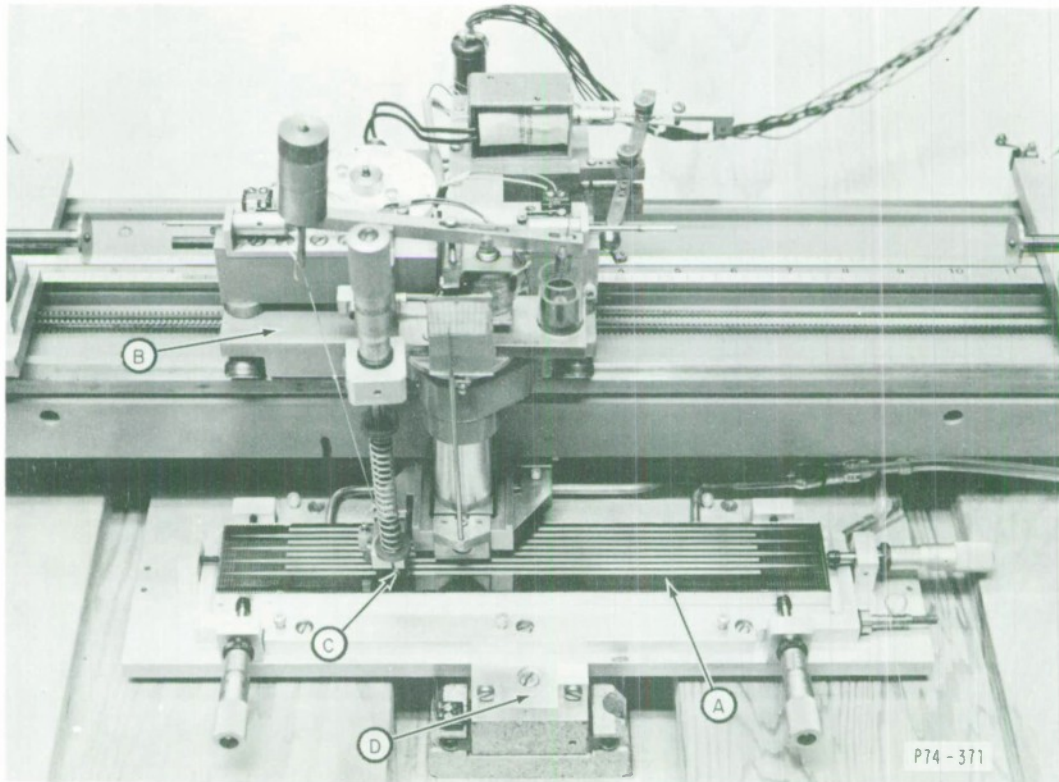


Fig. A-2. Closeup of substrate and carriage of automatic word-substrate scribing machine. (a) substrate, (b) carriage, (c) diamond tool, (d) table for line indexing.

those metal layers. After stripping the photoresist, the pads and shorting bars were gold plated. Following the electroless plating of the closure film an insulating layer of thick (0.3 - 0.5 mil) KTFR was applied to the lines by dip coating at a slow (.5 inches/minute) withdrawal rate. A number of half populated (360 lines) substrates were produced.

Appendix B. Electroless Plating of Magnetic Films

1. Introduction

The Lincoln Laboratory LCM II magnetic thin film memory was designed to use evaporated magnetic films on glass substrates as the memory elements. A layer of copper 5μ thick was evaporated on a 1500 \AA magnetic film,^{*} and then the metal was scribed into 1.2 mil lines on 2 mil centers to form the memory word lines parallel to the easy direction. Because of the very high demagnetizing field associated with such a structure, closure around the word line just by a superposed film is inadequate. Electroless plating, however, by providing uniform plating around the exposed scribed line regardless of the shape of the line cross section, should provide almost complete closure. The required magnetic properties are $H_k = 20$ to 30 oersteds and $H_c = 20$ to 30 oersteds for 1500 \AA thick films. This report deals with the preparation and magnetic parameters of the electroless platings.

2. Chemical Parameters

Magnetic electroless platings devolved from the hypophosphite reduced electroless nickel developed by Brenner.^{1,2,+} A number of authors have discussed methods of plating thin, magnetically soft films.³⁻¹¹

Electroless plating is an extremely simple task and controls are very easy: a typical process might require about 8 minutes of preparation and 4 minutes of plating, and the required tooling is so simple and inexpensive that samples may easily be processed in parallel. A typical plating rate vs. temperature curve illustrating both the ease of control within a reasonable range and the available range of control is shown in Figure B.1. Electroplating is comparably simple but has the following difficulties due to the

^{*} Magnetic film thicknesses are expressed in flux equivalents to 80-20 permalloy @ 10 Kgauss saturation flux density.

⁺References are listed at the end of this appendix.

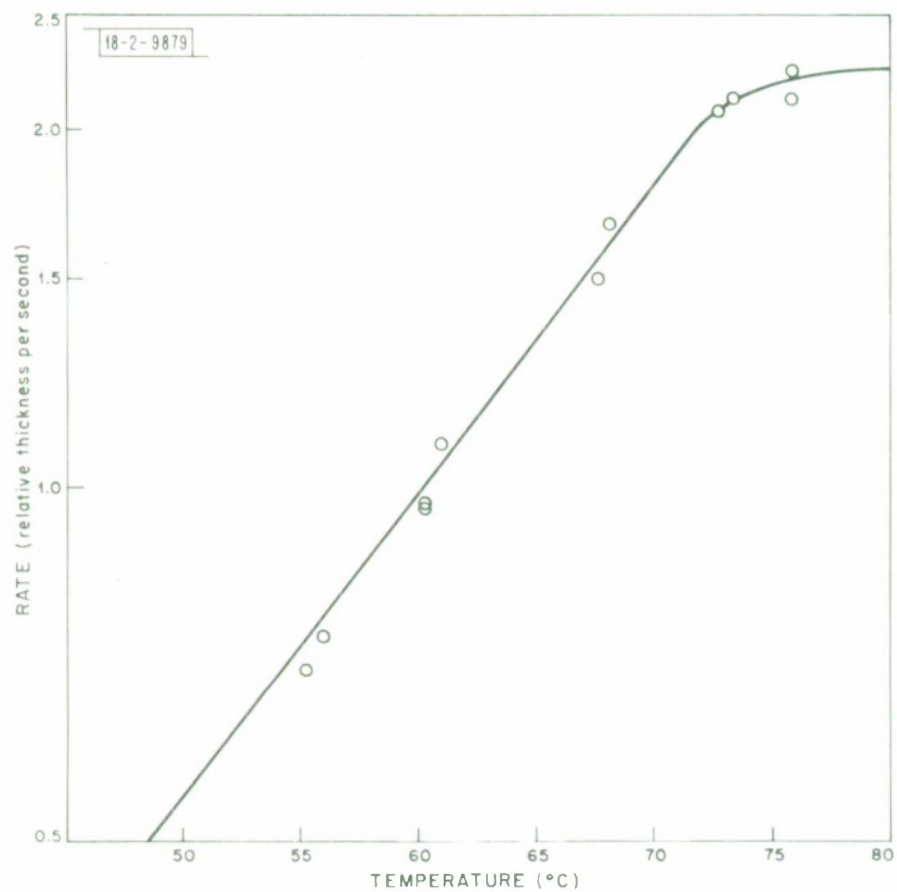


Fig. B-1. Plating rate as a function of temperature.

requirement that plating follow scribing and etching into lines: uniform contact to individual lines is difficult; voltage drop in the long, narrow lines leads to non-uniform plating or very long plating times; plating around the line periphery is non-uniform, building up at corners and not throwing into the recesses between lines; and prevention of shorts is extraordinarily difficult because of electrostatic attraction of solution particles to the narrow space between lines.

The electroless plating process consists of preparing the substrate by adequate cleaning and sensitizing and then immersing the substrate in a heated plating bath in an orienting magnetic field for a suitable time (Figure B.2). Sensitizing generally is done by touching with a sensitive material or covering the surface with an immersion plating of palladium or a preplate of electroless nickel or cobalt (another well known technique, pre-electroplating with nickel or from the magnetic plating solution leads to very high coercivity films). The bath contains nickelous, cobaltous, and/or ferrous salts; complexing agents to prevent their oxidation to their +3 states (which are generally insoluble) and to stabilize the plating rates; buffering agents; and a reducing agent, either a hypophosphite, hydrazine, or an amino-borane. Subsequent to plating, films may be given a stabilizing anneal, similar to that given electroplated magnetic films.¹²

The bath used here is derived from that of Ransom & Zentner.⁷ The composition of the basic bath is given in Table B.1. This bath is indefinitely stable at room and, if adequately prefiltered, operating temperatures.

Dimethylamine borane¹³⁻¹⁶ is used instead of sodium hypophosphite as the reducing agent for the following reasons:

- A) Amine-Borane baths give higher anisotropy.
- B) Amine-Borane baths plate at a lower potential, and will, for example plate directly on copper without presensitizing. Thus plating is more uniformly initiated and films are more uniform.

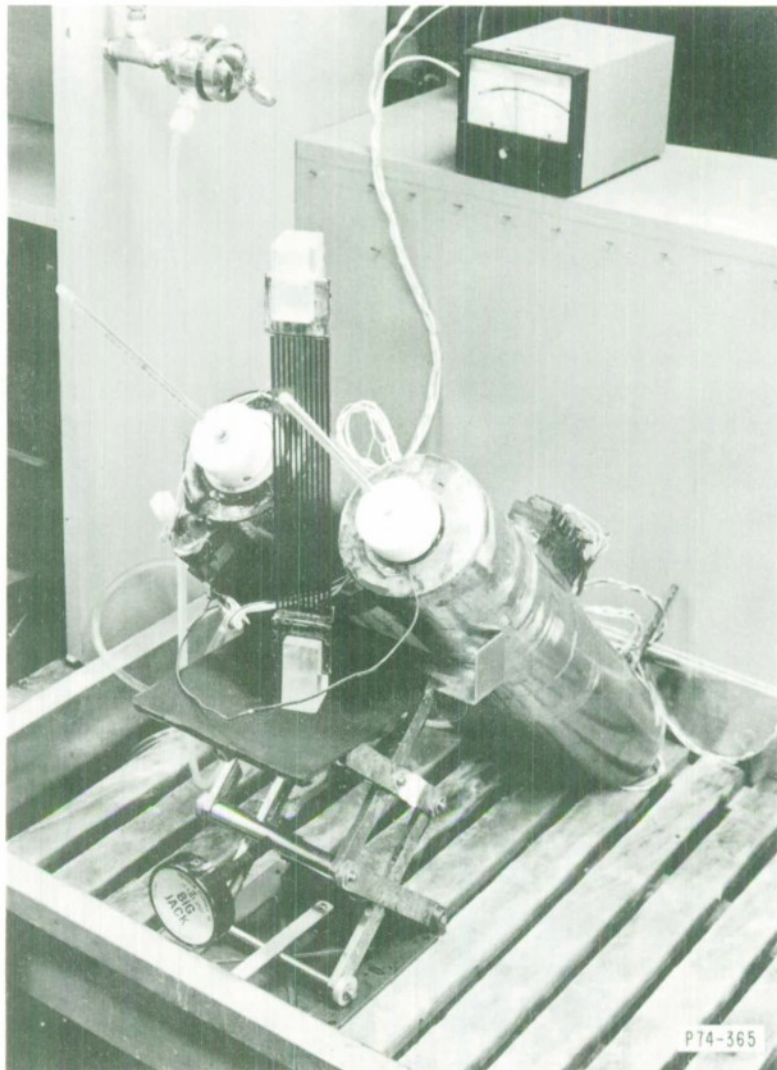


Fig. B-2. Electroless-plating tanks. The substrate is held in a holder with electroless Ni pads. One tank is for non-magnetic electroless nickel preplate, the other for the magnetic film.

TABLE B. 1

Plating Bath Composition

1.	Ammonium Sulfate $(\text{NH}_4)_2 \text{SO}_4$	800 gm
2.	Sodium Citrate $\text{Na}_3\text{C}_6\text{H}_5\text{O}_7 \cdot 2\text{H}_2\text{O}$	1600 gm
3.	Sodium Lauryl Sulfate	2.0 gm
4.	2-Mercaptobenzothiazole $\text{C}_6\text{H}_4\text{SCSH:N}$	5.0 mg
5.	Cobaltous Sulfate $\text{Co SO}_4 \cdot 7\text{H}_2\text{O}$	360 gm
6.	Nickelous Sulfate $\text{Ni SO}_4 \cdot 6\text{H}_2\text{O}$	18.8 gm
7.	Zinc Sulfate $\text{Zn SO}_4 \cdot 7\text{H}_2\text{O}$	1.8 gm
8.	Ammonium Hydroxide NH_4OH	260 ml
9.	Dimethyl Amine Borane $(\text{CH}_3)_2 \text{NH:BH}_3$	46.7 gm
10.	Water	to 20 L
	pH adjusted with NH_4OH electrometrically	$9.2 \pm .1$
	Temperature	70°C

C.P. Chemicals are used, and the bath is filtered through 0.2 micron absolute filters. Items 1, 2, and 8 are used for buffering, complexing, and pH adjustment. Item 3 is a wetting agent to aid the release of hydrogen bubbles from the surface. Item 4 is a stabilizer. The cobalt-nickel and cobalt-zinc ratios are adjusted for optimum coercivity and anisotropy while maintaining constant metal concentration. Item 9 is the reducing agent.

C) Amine-Borane baths operate at lower temperatures so operation and control are easier.

D) Amine-Borane baths are more stable.

E) Phosphorous containing platings are reported in some cases to be unstable. The precipitation of Ni_3P or Co_3P presumably would have serious magnetic consequences. The concentration of deposited boron is smaller than that of phosphorous from similar nickel baths, and boron is much more likely to remain interstitial.

The plating rate falls significantly below pH 8.9; consequently, the bath is operated with a great excess of ammonia and kept covered at all times.

3. Magnetic Parameters

The properties reported here were measured on 4 cm square glass substrates on which about 200 Å of chrome and 2000 Å or 10,000 Å of copper had been evaporated at 150°C before electroless deposition.

A. Anisotropy

Electroless plating offers very easy control of anisotropy over a very wide range. Co-Ni alloys may be deposited with H_k ranging from 5 oersteds³ to over 60 oersteds; presumably by incorporating iron,^{6,11,17} permalloy-like values could be reproduced. The easiest method for control of anisotropy is by controlling composition. Figure B.3* illustrates the range of anisotropy available in hypophosphite reduced films. Reduction with dimethyl amine borane instead of sodium hypophosphite yields similar results except the anisotropy is over twice as high: the higher anisotropy presumably results from replacement of phosphorous atoms with rarer and smaller boron atoms. Additions of small quantities of zinc lead to anisotropies of 70 oersteds, as shown in Figure B.4.

* The films discussed have had good hysteresis loops to $H_C = 1$ or 2 times H_k . The H_k values were measured by the Kobelev method.

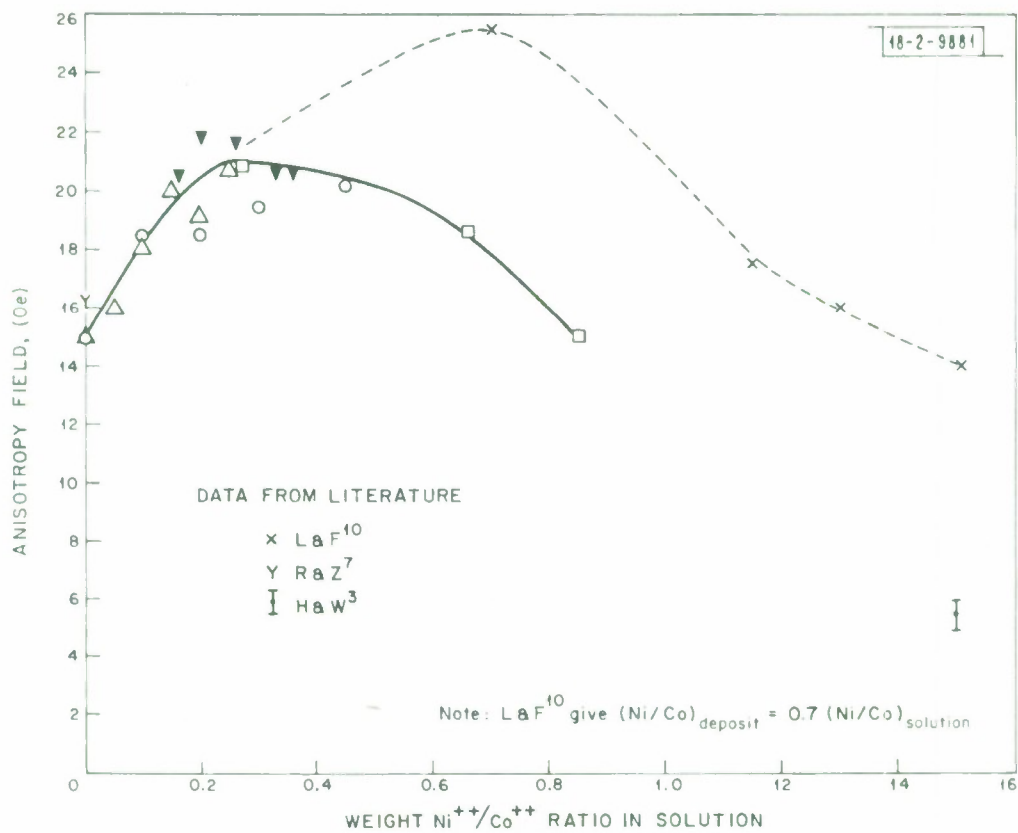


Fig. B-3. Anisotropy range of hypophosphite reduced films.

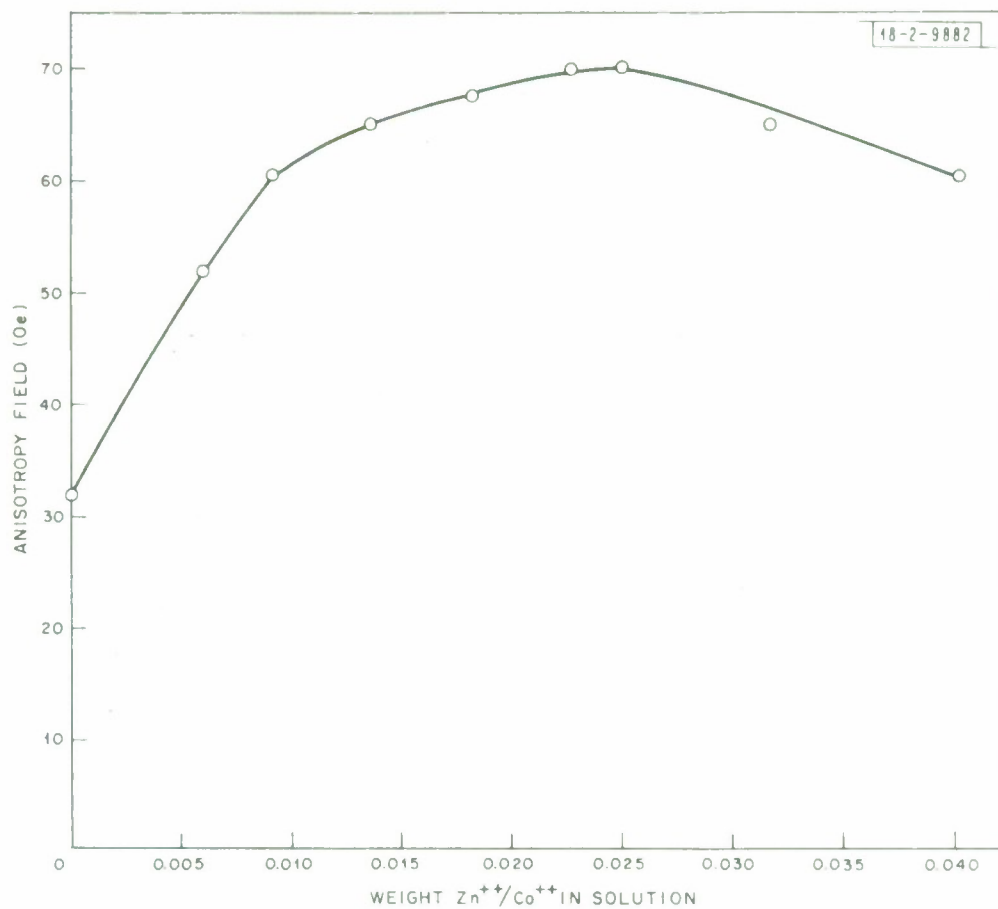


Fig. B-4. Anisotropy as a function of zinc content in amino-borane reduced films. Films annealed overnight in 75° C air, 100 oersted longitudinal field. Weight Ni:Co = .057 in solution; nominal film thickness = 1000 Å.

In general anisotropy is relatively independent of most plating parameters, changing very slowly with pH, temperature, surface condition, etc., although those factors which increase coercivity reduce anisotropy slightly. Anisotropy does vary slightly with film thickness, as shown in Figure B.5; increasing thickness from 1000 to 2000 Å leads to 10% reduction in anisotropy. This effect may be involved with non-uniform growth of the film.

The anisotropy field may also be adjusted by easy axis annealing. Figure B.6 illustrates the effect of annealing temperature in an easy axis field. Each sample was held at temperature for 1000 seconds: that the anisotropy becomes stable in this period is demonstrated by the independence of the value on the number of anneals the sample has received previously, as is also shown in Figure B.6. The data for Figure B.6 were terminated at 365° C because the films were becoming inverted: up to this temperature the coercivity had been stable. (Films annealed in air—especially moist air—tend to oxidize; oxidation is indicated by a rise in coercivity together with a color change. Hence, these annealings were done in nitrogen.) This stability was shown in another experiment where after an initial easy axis anneal at 167° C the anisotropy field did not change during a 700 hour anneal at 153° C. This is also shown in Figure B.7 at lower temperatures. The films do not become stable against annealing with fields in the hard direction however: this is illustrated in Figure B.7 wherein it can be seen that the anisotropy slowly decreases even at 55° C. If the perpendicular field is maintained, the easy and hard axes will eventually interchange. As shown in Figure B.7 the effect is reversible. It is not expected that memory operation would be impaired as hard axis fields are quite transitory and of relatively limited duty cycle.^{18,19} (No effect on skew was observed as long as films did not become very inverted.)

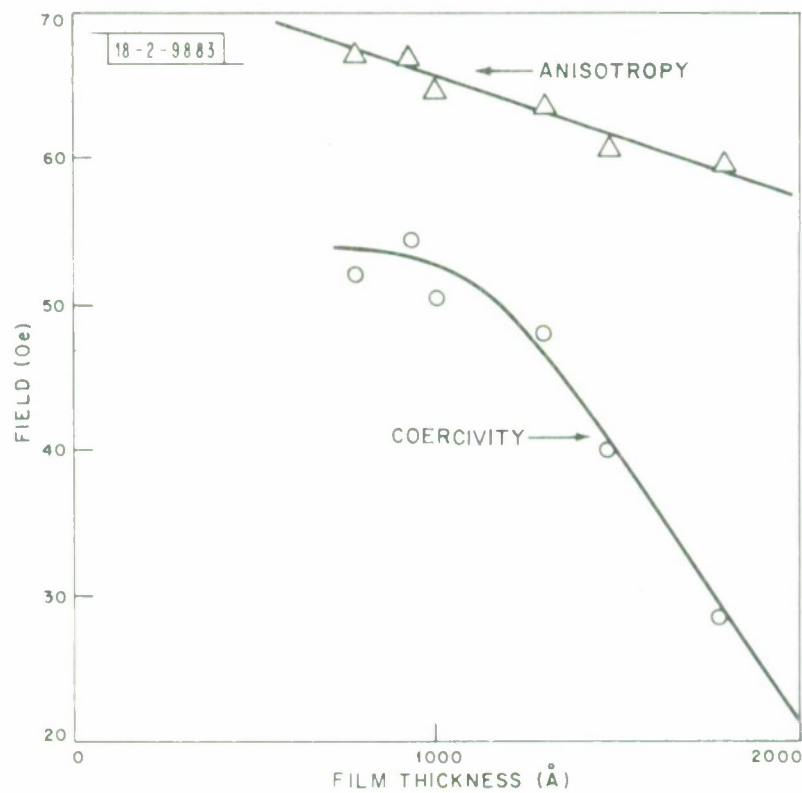


Fig. B-5. Anisotropy and coercivity as functions of film thickness. Annealed overnight @ 75° C. Weight Ni:Co = .057, Zn:Co = .0091 in solution.

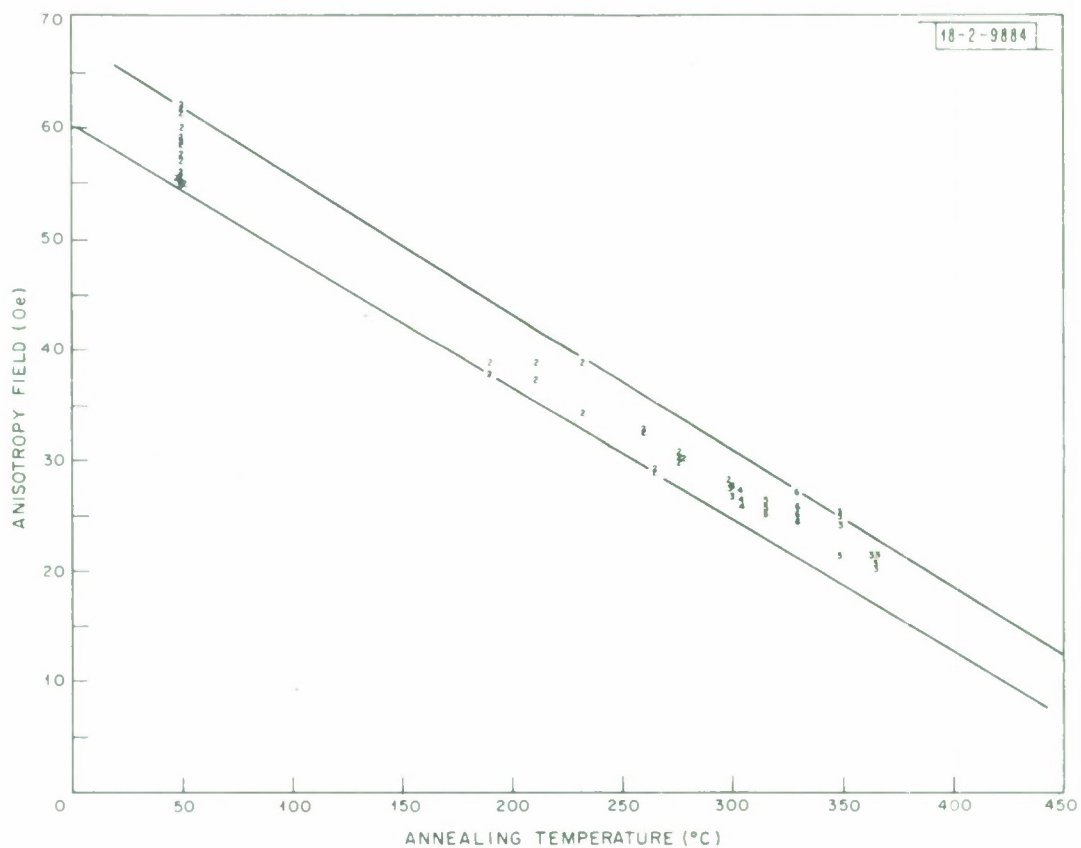


Fig. B-6. Effect of annealing in nitrogen on anisotropy. D. C. longitudinal field greater than 100 oersted. Annealing time 1000 sec. Weight Ni:Co = .057, Zn:Co = .008 in solution; film thicknesses 1600-2000 Å. Each film annealed several times, digit gives number of previous anneals for that datum.

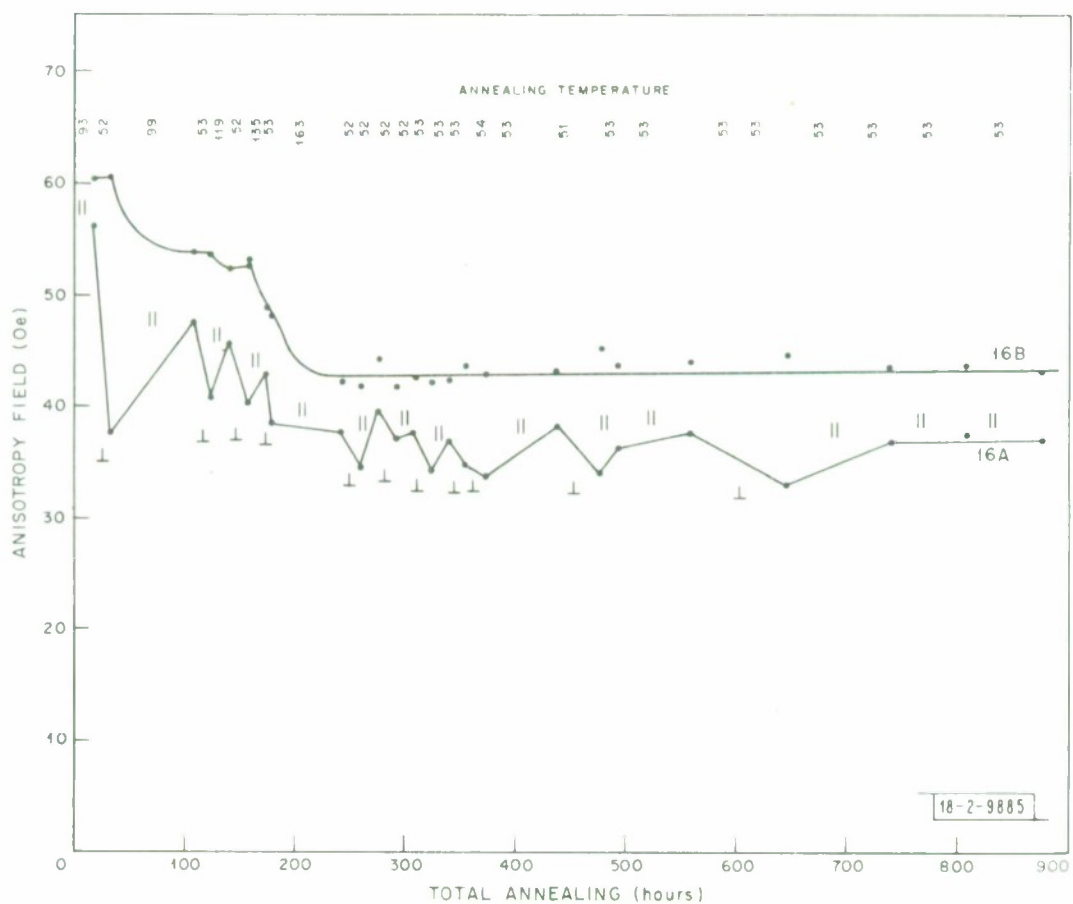


Fig. B-7. Effect of long-term annealing in air on anisotropy. D.C. longitudinal field greater than 100 oersteds. Weight Ni:Co = .057, Zn:Co = .0134 in solution. 16 B annealed parallel to easy axis; 16 A annealed parallel and perpendicular to easy axis as indicated.

B. Coercivity

Coercivity control is the most difficult task in making electroless magnetic films; no simple control means is available. Changing the anisotropy by altering the magnetic constituents as described above changes the coercivity about in proportion. Furthermore, modifications of the alloy, as by increasing the phosphorous content or the inclusion of tungsten,²⁰ increase coercivity at the expense of squareness and are therefore not suitable. Coercivity is extremely dependent on the surface on which the film is deposited and the film thickness, as shown in Figures B.5 and B.9 and Table B.2. Figure B.8 shows the variation for Co-Ni films and for a similar group of films for which the substrate copper had been overcoated with a thin layer of non-magnetic hypophosphite reduced electroless nickel.* The surface roughness of the evaporated copper as measured with a Tallysurf with 1.2 micron stylus was less than 100 Å^o; of the 2400 Å^o of electroless nickel, of the order of 100-200 Å^o. Similar films of amino-borane reduced electroless nickel,^o also non-magnetic and at least as rough, did not change the coercivity of superposed magnetic films. The illustrated variation of coercivity with thickness is similar to that given by Hendy⁹ and is probably involved with the Bloch-crosstie-Néel wall transitions; probably these films have higher saturation flux densities so the transitions occur for thinner films.

Table B.2 shows the effect of the temperature of the glass substrate during copper deposition on the coercivity of the electroless films deposited on the copper. The coercivity rises abruptly as the copper temperature is raised from 150^o C to 200^o C: this effect is so pronounced it has mainly served as an indication of the operability of the substrate temperature control; temperature control has not been good enough to evaluate this effect for

* Enthone Inc., Enplate 410.

^o Allied Research Products, NiKlad #754.

TABLE B. 2

Effects of Substrate Copper on Coercivity of Co-Ni-Zn Films

 H_K about 55 oersteds before annealing, about 25 oersteds after annealing. H_D is the field required to switch 0.5% of the total flux.

Substrate Temperature For Cu Deposition		10K $\overset{\circ}{A}$ CU Substrates		50K $\overset{\circ}{A}$ Cu Substrates	
		Before Annealing	After Annealing	Before Annealing	After Annealing
150 $^{\circ}$ C	$H_C - Oe$	43	30	49	38
	H_D/H_C	.77	.90	.84	.87
200 $^{\circ}$ C	$H_C - Oe$	61	50	54	44
	H_D/H_C	.61	.62	.85	.82
300 $^{\circ}$ C	$H_C - Oe$	41	27	48	40
	H_D/H_C	.85	.93	.90	.88
Two Layers of Substrate Copper:					
25K $\overset{\circ}{A}$ each, 150 $^{\circ}$ C then 150 $^{\circ}$ C	$H_C - Oe$			48	37
	H_D/H_C			.96	.95
25K $\overset{\circ}{A}$ each, 200 $^{\circ}$ C then 150 $^{\circ}$ C	$H_C - Oe$			47	33
	H_D/H_C			.83	.88
10K $\overset{\circ}{A}$ 150 $^{\circ}$ C then 40K $\overset{\circ}{A}$ electroplated	$H_C - Oe$			37	26
	H_D/H_C			.81	.95

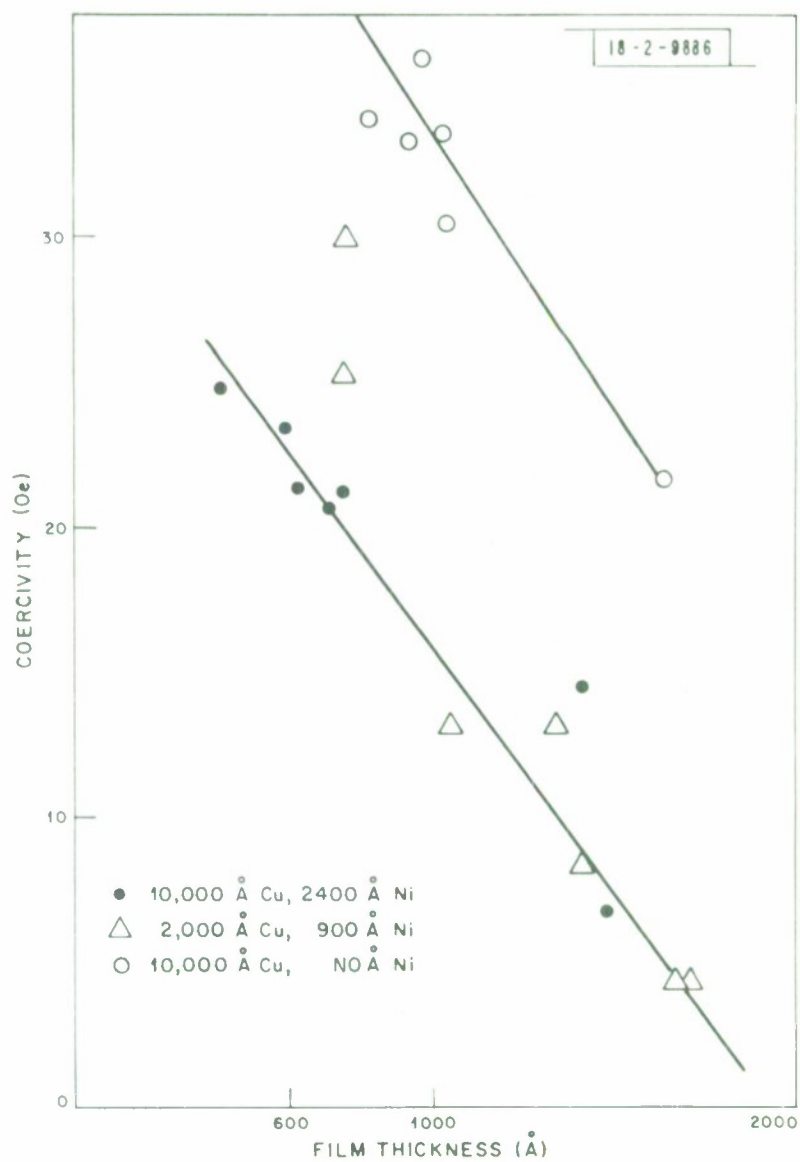


Fig. B-8. Coercivity as a function of film thickness: Co-Ni films on copper with and without Ni intermediate layer. Weight Ni:Co = .0545 in solution.

controlling coercivity. Surprisingly, the coercivity decreases again at higher temperatures. However, copper deposited at higher temperatures frequently has a milky appearance and is much less sensitive for initiation of plating. When substrates are first evaporated at 200°C and then covered with an equally thick layer at 150°C , the effect of 200°C copper is mostly erased. The last sample in Table B.2 was electroplated from an ordinary unagitated sulfuric acid-copper sulfate bath. Note that the films on plated copper are softer than those on evaporated; the coercivity was independent of current density up to the critical value for plating. The plated copper is noticeably less reflective—and thus rougher—than the evaporated copper. Proprietary additives lead to smoother copper and softer films.

The most severe problem in coercivity control is non-uniformity over the substrate. The second row of numbers for each temperature in Table B.2 gives H_d/H_c where H_d is the field at which 0.5% of the flux switches for the 4 cm square samples; this ratio is a measure of the lack of squareness in the hysteresis loops. Ideally of course H_d should equal H_c , the coercivity. When these films are examined in finer detail, they are revealed to consist of areas of varying coercivity, but with very square loops. An H_c map for a typical film is shown in Figure B.9: the 4 cm square substrate was sampled at .2 inch increments by an optical looper with a spot size as shown in the figure. The coercivity appears to be varying over distances of about this order.

Also shown in Table B.2 are the values of H_c and H_d/H_c after annealing in an easy axis field. As the anisotropy is reduced down near to the coercivity, the films begin switching by rotation. Since this affects the harder portions of the loops before the easier portions, the loops become squarer. This is reflected in increases of the ratios of H_d to H_c .

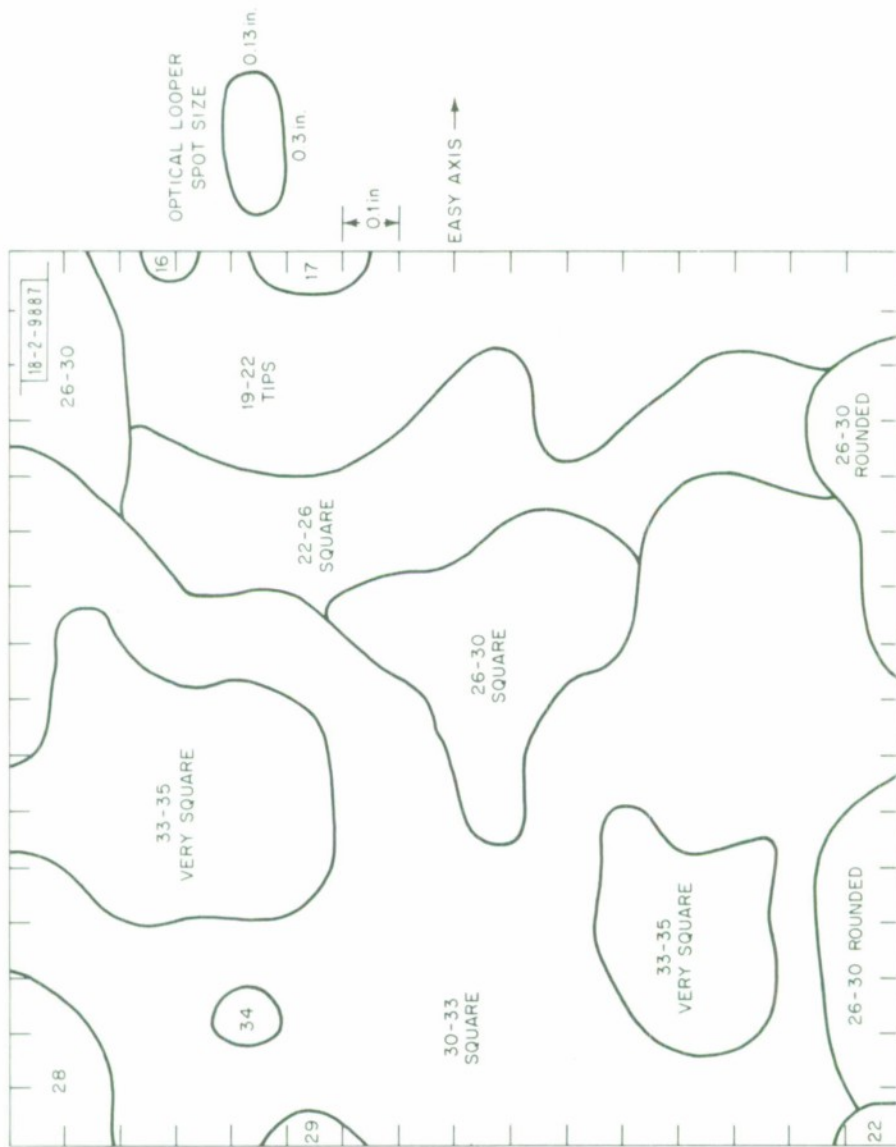


Fig. B-9. Coercivity map of 1.6 inch square substrate. Peak drive 40 oersteds. The anisotropy field is uniform over the surface. Loops with tips are non-square on the inside corners, showing presence of some higher coercivity material. Rounded loops are non-square on the outside corners, showing presence of some lower coercivity material.

C. Magnetostriction

Typical magnetostriction values are given in Table B.3. These values represent changes in anisotropy of about 6 down to 1/2 oersted and, being near the limit of sensitivity at the strain used (3×10^{-4}), may have large errors. The magnetostriction is negative, as expected, and appears to increase with zinc content. The addition of tungsten²⁰ leads to positive magnetostriction; however this much tungsten severely increases coercivity. No significant magnetostriction contribution to coercivity could be detected. The magnetostriction contribution to the magnetic properties is negligible for film performance.

D. Dispersion

Dispersion of typical films has been measured by both techniques given by Crowther.²³ By rotation α_{90} typically is of the order of 1° . Under easy axis guided fallback the films show behavior similar to that described as resilient by Kump:²⁴ after being switched to one easy direction the films return stably to that direction after saturation rotation to the hard direction. The films break up by slowly creeping with very small values of reverse dc longitudinal bias plus a.c. hard axis fields. A somewhat different cause of this behavior may be applicable for these films than that given by Kump. The very small size of crystallites of electroless films has been pointed out by several authors, including Goldstein ("Dense, Amorphous, Liquid-Like Structure"),²⁵ Graham ($<100 \text{ \AA}$),²⁶ and Marton ("Liquid-Like")²⁷ for Ni-P and Aspland ($<100 \text{ \AA}$)²⁸ for Co-P. According to a dispersion theory developed by Hoffman,^{29,30} the dispersion is proportional to the crystallite diameter. Hence, the small value of dispersion may be attributed to the small crystallite size. Both hypophosphite and amino-borane reduced films exhibit this behavior.

TABLE B. 3

Magnetostriction of Electroless Films

Film	Composition (Solution)		$\frac{H_k}{\Delta L/L}$		$\frac{H_c}{\Delta L/L}$	
	$\frac{Ni}{Co}$	$\frac{Zn}{Co}$	$\frac{W}{Co}$	Oe.	H _k Oe.	H _c Oe.
110868	.326			-1.6×10^3	40	—
110769	.0543	.0134		-21×10^3	60	-5.1×10^3
121569	.0543	.0134	.154	$+7.7 \times 10^3$	40	—
92970	.0543	.008		-2.7×10^3	58	0
92970	annealed @ 300° C			-3.0×10^3	27	0

* as .9 gm/Liter Na₂ WO₄ · 2H₂O

4. Summary

Magnetic films of a wide range of properties, including relatively high values of coercivity and anisotropy as are useful for high density memories, may be made by electroless plating. Problems remain in the control of the uniformity of coercivity, but these can be significantly ameliorated by plating high anisotropy films and then annealing in an easy axis field. Uniform coating around corners and even reentrant geometries are feasible.

REFERENCES

A general discussion of Electroless Nickel Plating with bibliography may be found in ASTM special Technical publication #265 "Symposium on Electroless Nickel Plating" 1959.

1. Abner Brenner & Grace Riddell, U. S. Patent 2532283, 1950.
2. A. Brenner & G. Riddell, Journal of Research, National Bureau of Standards, 39, p. 937, 1947.
3. R. J. Heritage & M. T. Walker, Journal of Electronics and Control, 7, p. 542, 1959.
4. J. Bagrowski & M. Lauriente, Journal of Electrochemical Society, 109, p. 987, 1962.
5. Thompson Ramo Wooldridge, Inc., British Patent #955,782; 1964.
6. Philip Eisenberg, U. S. Patent #2,827,399; 1958.
7. L. D. Ransom & V. Zentner, Journal of the Electrochemical Society, 111, p. 1423, 1964.
8. J. O. Holmen & J. S. Sallo, Proceedings of the Intermag Conference, Washington, D. C., 12-3-1, 1964.
9. J. Hendy, H. D. Richards, & A. W. Simpson, Journal of Materials Sciences, 1, pp. 127-141, 1966.
10. G. W. Lawless & R. D. Fisher, Plating, 1, June 1967.
11. A. F. Schmeckenbecher, Journal of the Electrochemical Society, 113, #8, p. 778, 1966.
12. J. P. McCallister & S. J. Strobl, IEEE Transactions on Magnetism, MAG-5, p. 495, 1969.
13. W. J. Cooper et al, Electroless Plating with Amine Boranes, Technical Bulletin CCC-AB-1, Callery Chemical Co., Callery, Pa. (1968).
14. H. G. McLeod, U. S. Patent 3,062,666; 1962.
15. E. I. DuPont deNemours & Co., British Patent #842, 826; 1960.
16. T. Berzins, Canadian Patent #715451, 1965.
17. H. Koretzky & A. Schmeckenbecker, U. S. Patent #3496014, 1970.

18. W. Doyle, R. Josephs, & A. Baltz, Journal of Applied Physics, 40, p. 1172, 1969.
19. J. Chang, U. Gianola, & M. Sogal, Journal of Applied Physics, 35, p. 830, 1964.
20. F. Pearlstein & R. Weightman, Plating, 1, 1967.
23. T. S. Crowther, "Techniques for Measuring the Angular Dispersion of the Easy Axis of Magnetic Films" MIT Lincoln Laboratory, Lexington, Mass., Group Report 51-2, (30 March 1959), DDC AD-255 697.
24. H. J. Kump, Proceedings of the 1964 Intermag Conference, Washington, D. C. , (9-2).
25. A. W. Goldstein, W. Rostoker, & F. Schossberger, J. Electrochem Society, 104, p. 104, 1957.
26. A. Graham, R. Lindsay, & H. Read, J. Electrochem Soc., 112, p. 401, 1965.
27. J. Marton & M. Schlesinger, J. Electrochem Soc., 115, p. 16, 1968.
28. M. Aspland, G. Jones, & B. Middleton, IEEE Trans. on Magnetics, MAG-5, p. 314, 1969.
29. H. Hoffman, IEEE Trans on Magnetics, MAG-4, p. 32, 1968.
30. T. Fujii, S. Uchiyama, S. Tsunashima, & Y. Sakaki, IEEE Trans on Magnetics, MAG-5, p. 223, 1969.

Appendix C. Digit Substrate Fabrication

The digit substrate was required to be rigid with a copper-line surface that was smooth and without unacceptable bumps or pinholes. One micron of anisotropic permalloy was needed for a magnetic keeper, and circuit considerations necessitated a copper thickness of at least 0.8 mil. The 52" long substrates were 2.2" wide and 1/4" glass was used for ease of handling and mechanical strength.

The first approach taken in making digit substrates was to vapor deposit 200 Å of chrome for adhesion, 10,000 Å of permalloy, and 0.1 - 0.2 mils of copper on the glass substrates. The required 1 mil copper thickness could not be vapor deposited due to high stress in the copper which led to spontaneous peeling of the metal layers from the glass. The remaining copper thickness was built up by electroplating. Several problems were encountered. Inadequate temperature and alignment field uniformity over the substrate during permalloy deposition produced unacceptable variations in the magnetic characteristics. Keeper-to-glass adhesion was erratic with thin (10,000 Å) vapor plated copper and copper-to-permalloy adhesion was also marginal. Even at low deposition rates tiny molten drops were emitted from the melt and adhered to the substrate producing unacceptably large bumps. In addition, dust caused pinholes and the problem of cleaning such a large substrate contributed to the complexity of this technique.

The successful fabrication technique involved laminating copper foil that had been previously electroplated on one side with permalloy to the digit substrate. This provided an essentially blemish free, minimum stress, metal layer requiring fewer assembly steps and simpler tooling.

Commercially available electrodeposited copper foil, 1.2 mils thick, was used because it had much better scribing characteristics than rolled foil which tended to tear during scribing. Prior to plating, the foil was inspected

for flaws, degreased, and then, in a clean bench, all dust was removed from both sides by wiping and blowing with filtered nitrogen. The vacuum chuck, consisting of a 1/4" x 2.5" x 60" plate glass insert in an aluminum frame, was also cleaned, the foil then placed smooth side down against the vacuum chuck and taped around the edges to assure a good seal. Vacuum (25" Hg) was applied to the chuck, pulling the foil tightly against the glass plate. After careful cleaning, a polished steel roller was used to roll the foil into intimate contact with the glass plate as shown in Figure C.1. Any slight dents in the copper, or small trapped air pockets between the glass and copper, were removed in this process.

The copper foil-vacuum chuck combination was placed in a commercial copper cleaner, to deoxidize the copper, followed by a dilute sulphuric acid rinse and a water rinse. It was then connected to the plastic anode holder and loaded into the plating tank, Figure C.2, keeping the vacuum on at all times. The plating bath is that given in Example 3 in U. S. Patent No. 3,354,059. This bath uses ascorbic acid and low pH to keep the iron ions in solution and is indefinitely stable. Too low pH leads to non-uniformity and streaking of the plating by hydrogen bubbles so the bath was operated somewhat more acidic than specified and with the substrate inclined as flat as convenient (about 58 degrees from the vertical). At the iron concentration specified in the reference RIS (rotatable initial susceptibility) films result so operation was at 2 times specified iron concentration and 20 ma per cm². Magnetostriction measurements show the plated films to be about 1% more iron rich than the zero-magnetostriction permalloy. An orienting field of 68 Oe was applied during plating. One micron of permalloy was plated in 600 sec. Typical hysteresis loops are shown in Figure C.3. The vacuum chuck-anode combination was removed from the bath, thoroughly rinsed with water, and the foil forced-air dried to preclude water spotting of the permalloy surface and baked under heat lamps for one hour.

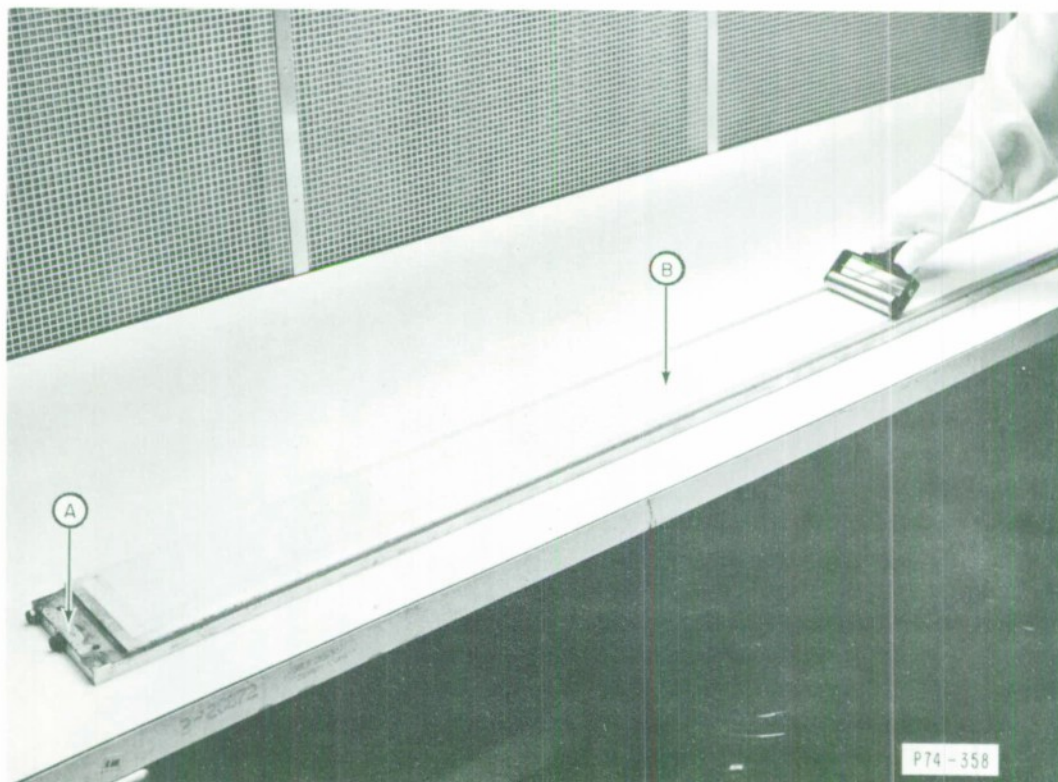


Fig. C-1. Copper foil on vacuum chuck being rolled to flatten out bumps and force out air bubbles. (a) Vacuum chuck, (b) Copper foil.

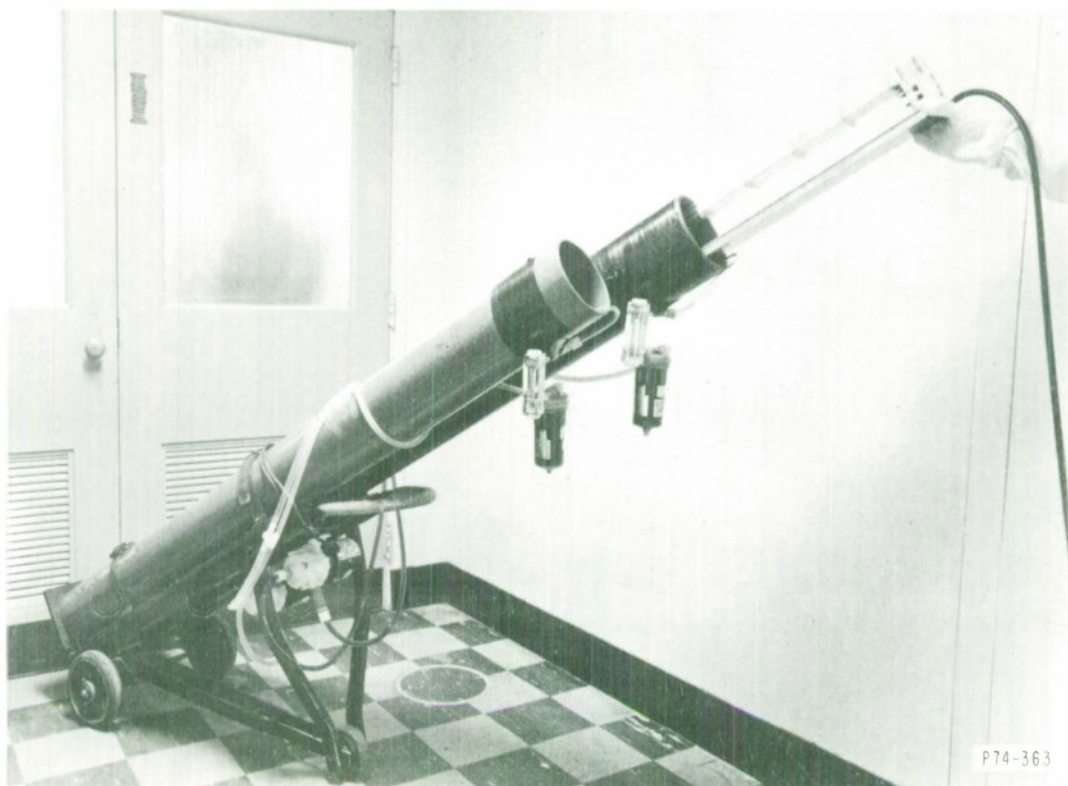


Fig. C-2. Vacuum chuck and anode assembly being inserted into the tank for electroplating of permalloy. The tank is wound with a coil to produce an orienting field. The second tank holds a copper deoxidant.

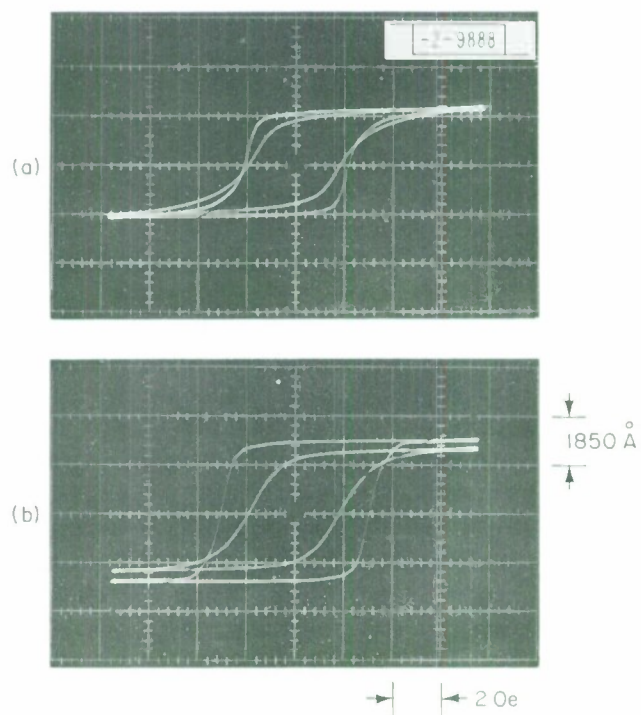


Fig . C-3. Hysteresis loops of permalloy plated simultaneously on copper substrate material (top) and glass (bottom). Inside loops = hard direction and outside loops = easy direction. Note degradation of amplitude and squareness due to surface finish of substrate copper.

Epoxy, having been previously centrifuged to remove air bubbles, was applied in a long bead down the center of the foil and spread evenly by a glass plate riding on 5 mil shims. The substrate was placed on one edge and slowly laid down in the epoxy thus "wedging out" most air bubbles. A mylar sheet was placed over the vacuum chuck, Figure C.4 (here with a metal substrate), and taped at the edges. A second vacuum, (20" HG max) was pulled between the mylar and foil which pressed the substrate into the epoxy and drew out any remaining entrained air bubbles. After approximately 30 seconds this vacuum was reduced to 5" Hg which produced a very consistent 0.8 - 1 mil glue thickness. The vacuum chuck-substrate assembly was baked at 160^o F for five hours to cure the adhesive. The substrate-foil laminate was then removed and the excess glue and metal trimmed off.

As a protective measure for subsequent etching steps, the substrate was degreased, deoxidized, and dip-coated with photoresist. This produced a 5000 Å thick resist layer that scribed very cleanly.

The 6 mil lines on 10 mil centers were generated by diamond scribing on the machine shown in Figure C.5. The substrate was mechanically clamped to the granite table and the scribing tool automatically indexed in 10 mil increments and pulled along the length of the substrate by carriage B. The vertically-sided stylus required two passes per slot to cut through the foil and into the adhesive layer. The "hairpin" geometry was produced by automatically lengthening and shortening the starting point of every other line. Scribing was done in a commercial cutting fluid at a tool speed of 70"/minute. Higher speeds caused tool chatter which produced shorts between lines or torn ling edges. Total scribing time was 6 hours/substrate.

If the "T" configuration was desired, after scribing, the substrate was degreased, deoxidized, and placed in a selective copper etchant. Approximately 0.4 mil of copper was removed from each side of the lines. Thus, the 3.2 mil

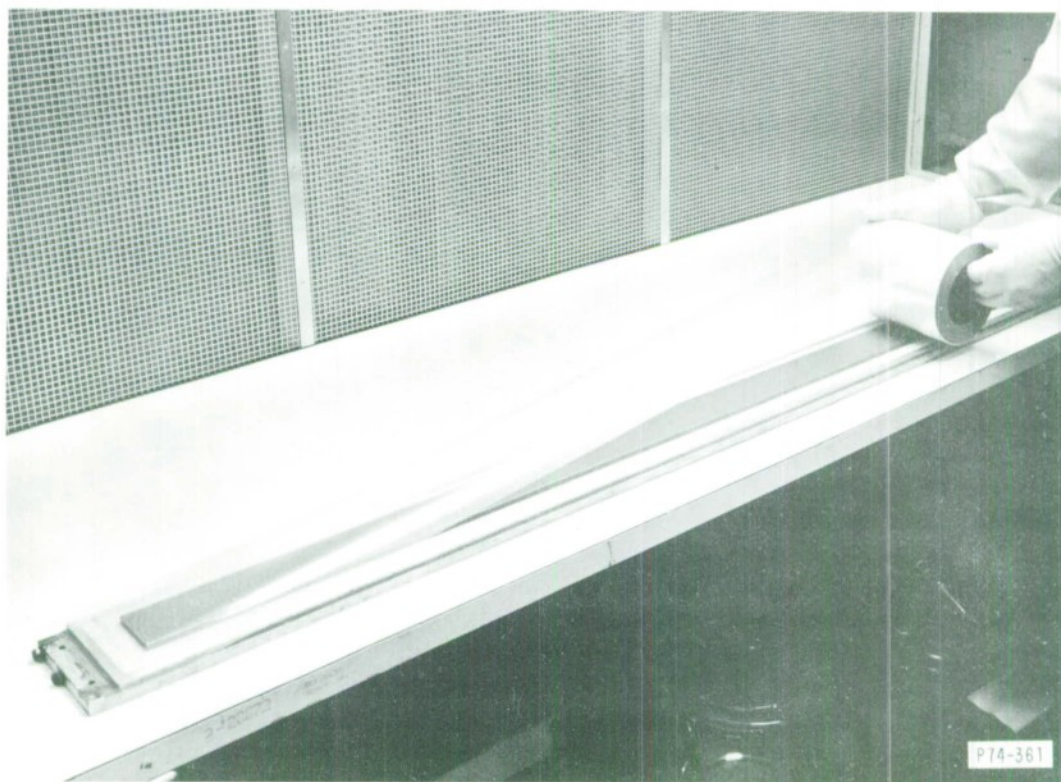


Fig. C-4. Metal digit substrate in place on electroplated copper foil with Mylar sheet being laid down for vacuum pull-down.

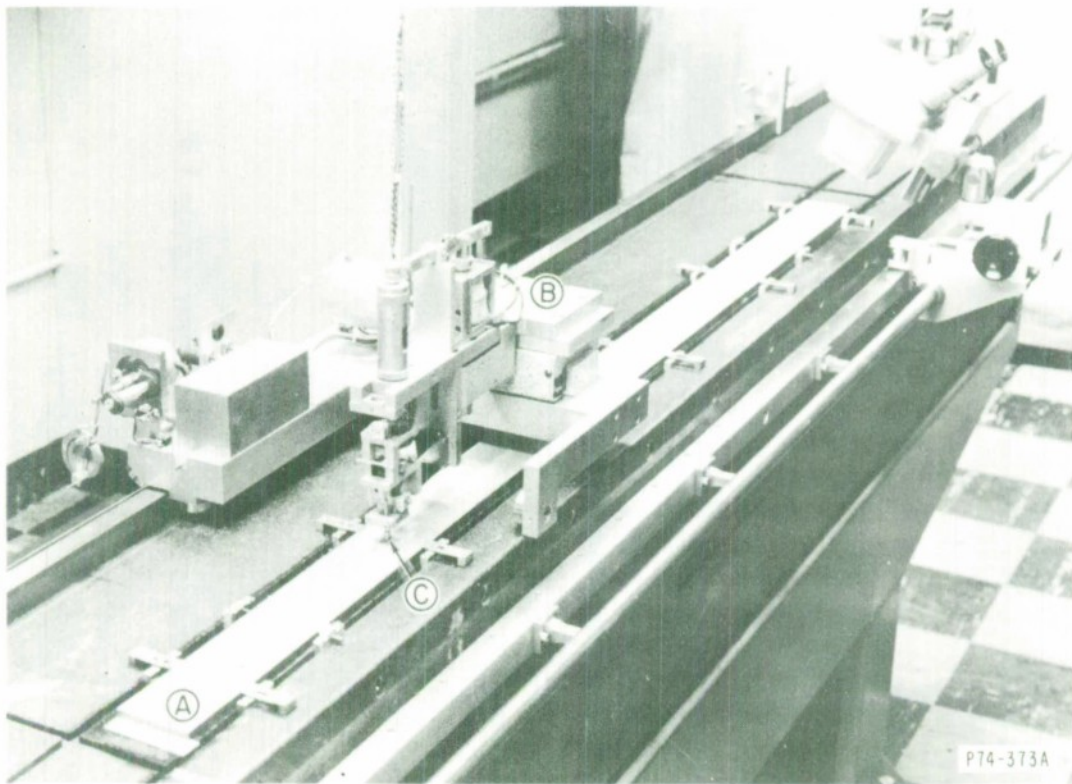


Fig. C-5. Digit scribing machine. (a) Digit substrate, (b) Carriage, (c) Diamond stylus.

wide scribed slot was increased to 4 mils in the copper and 0.4 mils of keeper was left sticking out on each side of the conductor to form the "T" configuration.

Application of permalloy keeper on the sides of the lines by electroplating involved the same steps of degreasing, deoxidizing and plating as were employed for plating keeper on the back of the foil. After plating, the photoresist on the tops of the lines was removed and the ends of the lines were opened by etching and then gold plated.

To fill between the lines ferrite-loaded epoxy was mixed to have the consistency of honey and doctor-bladed in several thin layers on the digit lines, scraping all excess off the tops of the conductors. After the ferrite keeper had been cured by baking, a second application of wet ferrite-epoxy was applied and cured to eliminate the effects of any shrinkage or small open holes in the thick first layer.

Lamination onto aluminum substrates having a 2-3 mil thick anodic aluminum oxide coating was done the same way except for an additional sealing step. If the foil was glued directly to the anodized surface, voids occurred in the epoxy layer either because of a chemical reaction between the glue and oxide or because the porous oxide "soaked up" some of the epoxy. A very thin (0.1 - 0.3 mil) layer of epoxy, applied and cured prior to laminating the foil, eliminated this problem. The anodic layer besides being an insulating coating provided a hard surface on which the scribing tool could ride. The resulting scribed line quality was as good as on glass substrates, and no other fabrication problems were encountered.

Three each of the long substrates were scribed with excellent line edge quality and very few defects. They were not "T" etched, edge plated, or filled with ferrite. A number of shorter substrates were etched back, plated, and filled. Some irregularity of etch back was observed and some etch pits on the top surface of the copper became filled with ferrite, which could be a problem.

Appendix D. Capacitive Imbalance Tester

For evaluation of capacitive imbalance on different types of digit lines a tester was built to measure the differential capacitance of neighboring intersections of crossed sets of lines. Excitation lines are 0.090" wide copper lines on 0.100" centers on a piece of 1/4" plate glass. The surface is coated with a 1/2-mil thick layer of resist for insulation. These lines are each terminated to ground with 51 ohms and driven through a reed-delay matrix by a pulse generator. The digit lines are pressed against the exciting-line substrate by an air bag. Since the transmission delay of the 10 inch long digit lines is short compared to the pulse rise-time, the voltage to ground on a digit line is equal to the excitation voltage times the ratio of the excitation line-to-digit line capacitance of the digit line-to-ground capacitance. With uniform spacing, in the absence of a close ground plane, this ratio is $1/(n-1)$ for n terminated excitation lines. This tester has 100 excitation lines. A measurement of common-mode voltage on a digit line as a function of position shows changes of spacing.

The measurement found most useful for flexible digit lines is the difference voltage between two adjacent digit-pairs. Instrumentation was built to detect difference voltages above a certain threshold; a typical threshold used was 5% of the expected common-mode voltage. The density of excitation lines on the tester was comparable to the density of word groups (10/in. vs 14/in.). The emphasis in these tests was on comparison of different digit lines under the same measurement conditions.

For rigid digit substrates the spacing variation is over such large distances that the useful measurements are common-mode voltage and total capacitance.

Appendix E. The Effect of a Differentiator on Signal-to-Random-Noise Ratio

1. Introduction

The optimum linear filter for detection of a signal of known waveform in white noise is a "matched" filter, one whose impulse response is the mirror image of the signal.¹ Now, by definition, any modification of the filter will result in a lower output peak-signal-to-rms-random-noise ratio. The question about the effect of a high-pass filter or differentiator on signal/noise is then reduced to: how severe will the degradation be? To answer this, two illustrative examples are solved. Both assume a rectangular input pulse; one assumes a matched filter followed by an R-C high-pass filter, and the other a cascade of R-C low-pass and high-pass filters.

2. Matched Filter with Differentiator

For a rectangular input pulse the matched filter will have a rectangular impulse response, and the output signal, the convolution of signal and filter response, will be triangular. These waveforms are shown in Figure E.1 with amplitudes adjusted for unit peak output. The typical effect of a single-pole or "R-C" high-pass filter is shown in Figure E.1d.

To determine signal/noise, the peak signal amplitude must first be found. Consider a high-pass filter with cutoff frequency ω_1 ; it is characterized by

$$H_2(s) = s/(s + \omega_1) \quad .$$

In the interval $0 < t \leq T$, the response of this filter to the triangular pulse of Figure E.1c is

$$p(t) = \frac{1}{\omega_1 T} \left[1 - e^{-\omega_1 t} \right] \quad .$$

The peak of the signal will always occur at time T :

$$A = p(T) = \frac{1}{\omega_1 T} \left(1 - e^{-\omega_1 T} \right) \quad (E.1)$$

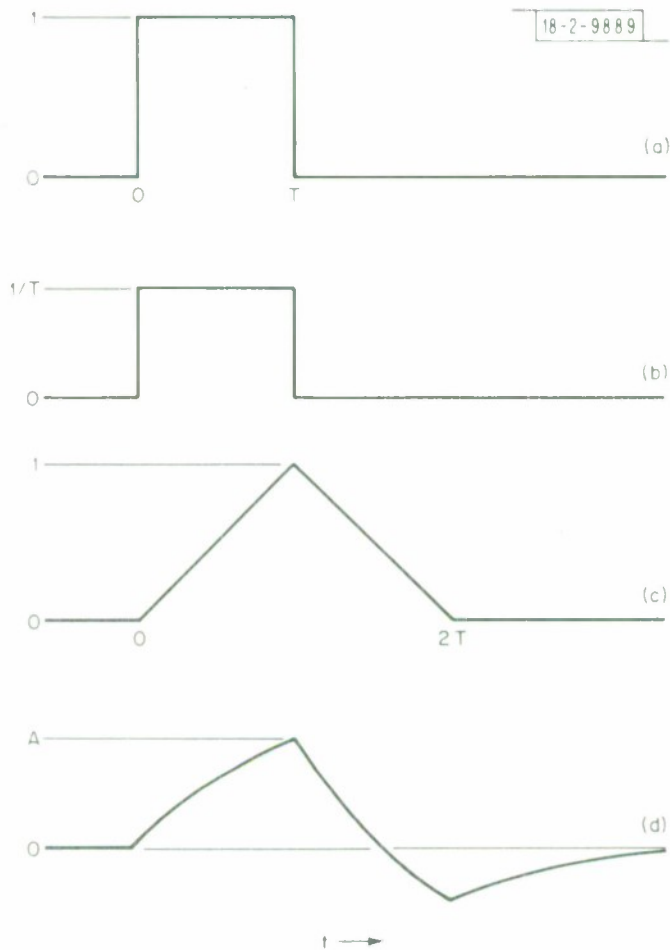


Fig. E-1. Filter waveforms: (a) rectangular input pulse; (b) matched-filter impulse response; (c) matched-filter output; (d) R-C high-pass filter output.

The mean square random noise at the output is determined by integrating the output power density function, which is just the input noise density multiplied by the system power transfer function, or squared magnitude of the system function. The matched filter alone has a system function

$$H_1(\omega) = \int_{-\infty}^{\infty} e^{-j\omega t} h(t) dt = \int_0^T \frac{e^{-j\omega t}}{T} dt = \frac{e^{-j\omega T} - 1}{-j\omega T}.$$

The power transfer function is

$$H_1 H_1^* = \frac{2(1 - \cos \omega T)}{(\omega T)^2}.$$

The power transfer function of the high-pass filter is

$$H_2 H_2^* = \frac{\omega^2}{\omega^2 + \omega_1^2}.$$

If the input white-noise power density is $N_o/2$, then the mean-square output noise is the integral of the product of that and the two power transfer functions:

$$\sigma^2 = \int_{-\infty}^{\infty} \frac{N_o}{2} \left[\frac{2(1 - \cos \omega T)}{(\omega T)^2} \right] \left[\frac{\omega^2}{\omega^2 + \omega_1^2} \right] \frac{d\omega}{2\pi}$$

$$= \frac{N_o}{\pi T^2} \int_0^{\infty} \frac{1 - \cos \omega T}{\omega^2 + \omega_1^2} d\omega$$

which reduces to

$$\sigma^2 = \frac{N_o}{2T} \left[\frac{1 - e^{-\omega_1 T}}{\omega_1 T} \right] \quad (E.2)$$

The output signal-to-noise ratio for a unit rectangular pulse driving a matched filter and R-C differentiator is then (from Equations E.1 and E.2):

$$\left(\frac{A}{\sigma}\right)^2 = \frac{2T}{N_o} \frac{1 - e^{-\omega_1 T}}{\omega_1 T} \quad . \quad (E.3)$$

Now the signal-to-noise ratio of a matched filter is just

$$(A/\sigma)^2 = 2E/N_o \quad ,$$

where E is the signal energy, that is, the integral square.² For the unit rectangular pulse this becomes

$$(A/\sigma)^2 = 2T/N_o \quad (E.4)$$

Filter efficiency η shall be defined as the squared signal-to-noise ratio normalized to that attainable by a matched filter. The efficiency of a matched filter followed by a high-pass filter is the ratio of Equation E.3 to E.4:

$$\eta = \frac{1 - e^{-\omega_1 T}}{\omega_1 T} \quad . \quad (E.5)$$

In terms of the filter time constant, $T_1 = 1/\omega_1$,

$$\eta = \frac{T_1}{T} \left(1 - e^{-T/T_1} \right) \quad (E.6)$$

The square root of the efficiency, which is the normalized voltage signal-to-random-noise ratio, is plotted as curve "a" in Figure E.2.

3. Cascaded High- and Low-Pass Filters

The system function of a cascaded high- and low-pass filter is

$$H(s) = \frac{\omega_2 s}{(s + \omega_2)(s + \omega_1)} \quad .$$

The response to a unit rectangular pulse of width T is

$$p(t) = \frac{\omega_2}{\omega_2 - \omega_1} \left(e^{-\omega_1 t} - e^{-\omega_2 t} \right) \quad , \quad 0 < t \leq T \quad ,$$

$$p(t) = \frac{\omega_2}{\omega_2 - \omega_1} \left[(1 - e^{-\omega_2 T}) e^{-\omega_2 T(t-T)} - (1 - e^{-\omega_1 T}) e^{-\omega_1 (t-T)} \right] \quad t > T \quad ,$$

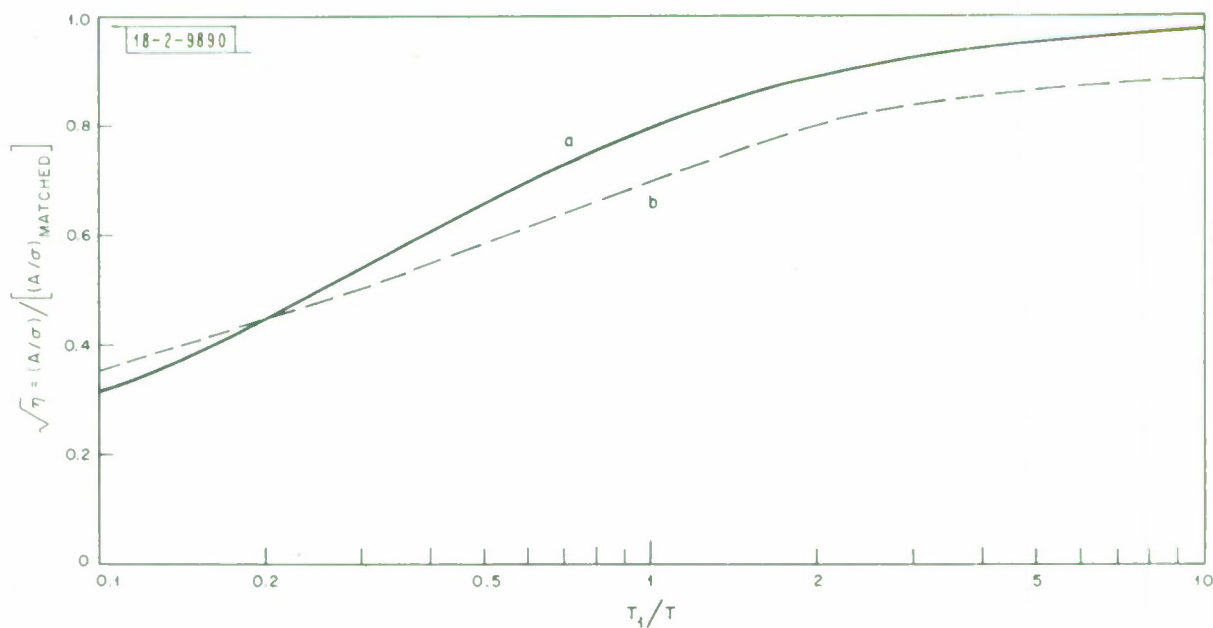


Fig. E-2. Effect of high-pass filter of time constant T_1 on signal-to-random-noise ratio, normalized to match filter: (a) with matched filter; (b) with single-pole low-pass filter, $\omega_2 T = 1.2564$.

provided $\omega_1 \neq \omega_2$. Differentiation shows that in the interval $0 < t \leq T$ there is either one extremum, a maximum, at

$$t = t_m = \frac{\ln \omega_2 / \omega_1}{\omega_2 - \omega_1}, \quad (E.7)$$

or that the function is monotonically increasing. There is always one extremum for $t > T$, but it is a minimum. Therefore the peak amplitude of the output signal is

$$A = p(\hat{t}) = \frac{\omega_2}{\omega_2 - \omega_1} \left[e^{-\omega_1 \hat{t}} - e^{-\omega_2 \hat{t}} \right], \quad \omega_2 \neq \omega_1, \quad (E.8)$$

where $\hat{t} = t_m$ or $\hat{t} = T$, whichever is smaller.

The system power transfer function is

$$HH^* = \frac{\omega_2^2 \omega^2}{(\omega_2^2 + \omega^2)(\omega_1^2 + \omega^2)},$$

and the output mean-square noise

$$\begin{aligned} \sigma^2 &= \frac{N_o}{2} \int_{-\infty}^{\infty} \frac{\omega_2^2 \omega^2}{(\omega_2^2 + \omega^2)(\omega_1^2 + \omega^2)} \frac{d\omega}{2\pi} \\ &= \frac{N_o \omega_2^2}{4(\omega_2^2 + \omega_1^2)}. \end{aligned} \quad (E.9)$$

The signal-to-noise ratio is given by

$$\left(\frac{A}{\sigma} \right)^2 = \frac{4(\omega_2 + \omega_1) \left(e^{-\omega_1 \hat{t}} - e^{-\omega_2 \hat{t}} \right)^2}{N_o (\omega_2 - \omega_1)^2}, \quad \omega_2 \neq \omega_1. \quad (E.10)$$

As in the previous calculation, the filter efficiency is obtained by dividing by the $(A/\sigma)^2$ of the matched filter, Equation E.4:

$$\eta = \frac{2(\omega_2 + \omega_1) \left(e^{-\omega_1 \hat{t}} - e^{-\omega_2 \hat{t}} \right)^2}{T(\omega_2 - \omega_1)^2}, \quad \omega_2 \neq \omega_1, \quad (\text{E.11})$$

where $\hat{t} = t_m$ or $\hat{t} = T$, whichever is smaller.

For computational convenience this expression can be treated differently for the two cases on \hat{t} . In the first case, algebraic reduction results in

$$\eta = \frac{2(\omega_2 + \omega_1)}{\omega_1^2 T} \left(\frac{\omega_1}{\omega_2} \right)^{\frac{2\omega_2}{\omega_2 - \omega_1}}, \quad \hat{t} = t_m \leq T, \quad \omega_2 \neq \omega_1; \quad (\text{E.12})$$

in the second case, the expression remains essentially unchanged:

$$\eta = \frac{2(\omega_2 + \omega_1) \left(e^{-\omega_1 T} - e^{-\omega_2 T} \right)^2}{T(\omega_2 - \omega_1)^2}, \quad \hat{t} = T, \quad \omega_2 \neq \omega_1. \quad (\text{E.13})$$

As an example, consider a filter with $\omega_2 T = 1.2564$; in the absence of a differentiator this is the optimum single-pole filter.³ The normalized voltage signal-to-random-noise ratio has been plotted in Figure E.2, curve "b", as a function of differentiating time constant $T_1 = 1/\omega_1$, where Equation E.12 is valid for $T_1 \leq 1.27T$, and Equation E.13 for $T_1 > 1.27T$. Performance is much like that of the matched filter followed by a differentiator, except that A/σ is somewhat lower.

The efficiency of the cascaded high- and low-pass filters calculated from Equations E.12 and E.13 is much higher than has been reported⁴; it is believed that the earlier work is in error.

REFERENCES

1. W. B. Davenport and W. L. Root, Random Signals and Noise, McGraw-Hill, New York, p. 244, 1958.
2. G. L. Turin, IRE Trans. Inf. Theory, IT-6, p. 311, 1960.
3. J. W. Craig, Jr. IRE Trans. Inf. Theory, IT-6, p. 409, 1960.
4. H. Blatt, "Random Noise Considerations in the Design of Magnetic Film Sense Amplifiers," Group Report 1964-6, MIT Lincoln Laboratory. (17 August 1964), DDC AD-605 323.

DOCUMENT CONTROL DATA - R&D			
(Security classification of title, body of abstract and indexing annotation must be entered when the overall report is classified)			
1. ORIGINATING ACTIVITY (Corporate author) Lincoln Laboratory, M. I. T.		2a. REPORT SECURITY CLASSIFICATION Unclassified	
		2b. GROUP None	
3. REPORT TITLE Final Report: Development of a 10 ⁷ Bit Magnetic Film Memory			
4. DESCRIPTIVE NOTES (Type of report and inclusive dates) Technical Note			
5. AUTHOR(S) (Last name, first name, initial) Raffel, Jack I. Crowther, Thomas S. Naiman, Mark L. Anderson, Allan H. Herndon, Terry O. Woodward, Charles E. Berger, Robert			
6. REPORT DATE 10 June 1971	7a. TOTAL NO. OF PAGES 140	7b. NO. OF REFS 44	
8a. CONTRACT OR GRANT NO. F19628-70-C-0230		9a. ORIGINATOR'S REPORT NUMBER(S) Technical Note 1971-15	
b. PROJECT NO. 649L		9b. OTHER REPORT NO(S) (Any other numbers that may be assigned this report)	
c.		ESD-TR-71-187	
d.			
10. AVAILABILITY/LIMITATION NOTICES Approved for public release; distribution unlimited.			
11. SUPPLEMENTARY NOTES None		12. SPONSORING MILITARY ACTIVITY Air Force Systems Command, USAF	
13. ABSTRACT Batch fabrication techniques for making 200,000 bit substrates with word lines integral with a closed magnetic film structure and keepered digit lines on large area substrates are described. A sense amplifier was designed which does not require a transformer for impedance matching to the digit lines. Cross-section-stack tests proved the feasibility of a 10 million bit memory with 1.0 μsec cycle time. All fabrication processes are consistent with the goal of low memory construction costs.			
14. KEY WORDS computer magnetic film magnetic film memory			keepered digit lines LCM I LCM II